UNIVERSIDADE FEDERAL DE VIÇOSA

ANA CAROLINA PEREIRA MARTINS

ECO-EFFICIENT STEEL SLAG CONCRETE FOR PRECAST INDUSTRY

VIÇOSA - MINAS GERAIS
2021

ANA CAROLINA PEREIRA MARTINS

ECO-EFFICIENT STEEL SLAG CONCRETE FOR PRECAST INDUSTRY

Dissertation submitted to the Graduate Program in Civil Engineering of the Universidade Federal de Viçosa in partial fulfillment of the requirements for the degree of *Magister Scientiae*.

Adviser: José Maria Franco de Carvalho

Co-adviser: Ricardo André Fiorotti Peixoto

VIÇOSA - MINAS GERAIS
2021

Ficha catalográfica elaborada pela Biblioteca Central da Universidade Federal de Viçosa - Campus Viçosa

T
M386e
2021

Martins, Ana Carolina Pereira, 1994-
Eco-efficient steel slag concrete for precast industry / Ana Carolina Pereira Martins. – Viçosa, MG, 2021.
129 f. : il. (algumas color.) ; 29 cm.

Orientador: José Maria Franco de Carvalho.
Dissertação (mestrado) - Universidade Federal de Viçosa.
Inclui bibliografia.

1. Aço - Indústria - Reaproveitamento. 2. Indústria de construção civil - Subprodutos. 3. Compósitos de cimento. I. Universidade Federal de Viçosa. Departamento de Engenharia Civil. Programa de Pós-Graduação em Engenharia Civil. II. Título.

CDD 22. ed. 624.1833

ANA CAROLINA PEREIRA MARTINS

ECO-EFFICIENT STEEL SLAG CONCRETE FOR PRECAST INDUSTRY

Dissertation submitted to the Graduate Program in Civil Engineering of the Universidade Federal de Viçosa in partial fulfillment of the requirements for the degree of *Magister Scientiae*.

APPROVED: March 1, 2021.

Assent:

Ana Carolina Pereira Martins
Author

José Maria Franco de Carvalho
Adviser

ACKNOWLEDGMENTS

Finishing this important stage of my life during a year so atypical as 2020 was very challenging, but it was also rewarding. A year in which we had to stop our activities and collect ourselves, look inside, deal with our greatest fears and afflictions in such a chaotic and disturbing scenario. Analyzing the whole trajectory during these two years of master's makes me remember all those who helped and supported me on this journey, which is often difficult and exhausting.

I thank God for all the faith, light, and strength. I finish this work proud of the result of all my efforts and happy for the people who crossed my path and helped me get here.

To my parents, Ana Maria and Geraldo, my sisters, Aline and Amanda, and my aunt, Neuza, for being a source of love, inspiration, courage, strength, and determination. For always supporting and encouraging me to study, dedicate myself and do my best.

To the Federal University of Viçosa and the Federal University of Ouro Preto, for the opportunity and the infrastructure necessary to develop serious and quality works.

To Prof. José Maria, for his confidence in my work, support, patience, motivation, for his friendship, and for sharing his knowledge with me.

To Prof. Ricardo Fiorotti, for accepting the invitation to co-supervise this work, for the suggestions and approaches that were of great importance.

To Prof. Leonardo Pedroti, Prof. José Carlos, and Prof. Maria Teresa, for their generosity in accepting the invitation to participate in the examining committee and honoring me with their contributions to improve this work.

To the friends and colleagues who were part of this journey. Especially to Matheus Duarte for the excellent partnership at work, support, and good mood; to Carolina for her friendship and company on walks, lunches, and at LABENGE; to André for his advice, endless laughs, and support. The girls from the Republic, Rafaela and Amanda, for the moments of relaxation, conversations, laughter, and for always listening to me.

To the technical team of the Laboratory of Construction Materials (DEC/UFV), Wellington, José Carlos and Nathália, for all the support and assistance whenever necessary. Thanks also go to the following laboratories and their teams for the use of the equipment and collaborations:

Laboratory of Materials for Civil Construction – UFOP; Laboratory of Composite Materials – UFV; and Laboratories of X-ray Diffraction, and Scattering and Scanning Electronic Microscopy - Department of Physics - UFV.

This work was carried out with the support of the Coordenação de Aperfeiçoamento de Pessoal do Nível Superior - Brazil (CAPES) - Funding Code 001.

ABSTRACT

MARTINS, Ana Carolina Pereira, M.Sc., Universidade Federal de Viçosa, March, 2021. **Eco-efficient steel slag concrete for precast industry.** Advisor: José Maria Franco de Carvalho. Co-advisor: Ricardo André Fiorotti Peixoto.

The construction industry is one of the greatest consumers of natural resources, besides being responsible for about 25% of the solid waste generated worldwide. Sustainability actions have been discussed since the 1990s to save increasingly scarce natural resources. The search for industrial by-products that can perform as binders and as recyclable aggregates, replacing Portland cement and natural aggregates in cement matrices, are important mitigation routes, providing a destination for environmental liabilities in a circular economy structure. Within this context, the steel industry represents a high generation of industrial waste and by-products, about 90% of which are slag. Thus, powder and aggregates from steel slag were produced, and these materials were incorporated into cement-based composites such as pastes, mortars, and no-slump concrete for the precast industry. A characterization program was conducted to evaluate hydration kinetics, mineralogical phase formation, physical, morphological and mechanical performance. It was verified the great potential for using these by-products, especially in no-slump concrete, improving the physical and mechanical properties and the eco-efficiency of the matrices with the incorporation of waste.

Keywords: Industrial by-products. Steel slag. Cement-based composites. Eco-efficiency. No-slump concrete.

RESUMO

MARTINS, Ana Carolina Pereira, M.Sc., Universidade Federal de Viçosa, março de 2021. **Concreto de escória de aciaria ecoeficiente para a indústria de pré-moldados.** Orientador: José Maria Franco de Carvalho. Coorientador: Ricardo André Fiorotti Peixoto.

A indústria da construção civil é uma das maiores consumidoras de recursos naturais, além de ser responsável por cerca de 25% do resíduo sólido gerado no mundo. Ações de sustentabilidade vêm sendo discutidas desde a década de 90 para economizar recursos naturais cada vez mais escassos. A busca por subprodutos industriais que possam atuar como ligantes e como agregados recicláveis, substituindo o cimento Portland e os agregados naturais nas matrizes de cimento, são importantes rotas de mitigação, proporcionando um destino para os passivos ambientais em uma estrutura de economia circular. Dentro desse contexto, a indústria do aço representa alta geração de resíduos e subprodutos industriais, sendo que cerca de 90% são escórias. Dessa forma, foram produzidos powder e agregados de escória de aciaria e esses materiais foram incorporados aos compósitos a base de cimento tais como pastas, argamassas e concreto sem slump para indústria de pré-fabricados. Um programa de caracterização foi conduzido para avaliar a cinética de hidratação, formação de fases mineralógicas, desempenho físico, morfológico e mecânico. Verificou-se o grande potencial de uso desses subprodutos, principalmente no concreto sem slump, melhorando as propriedades físicas, mecânicas e a ecoeficiência das matrizes com a incorporação de resíduos.

Palavras-chave: Subprodutos industriais. Escória de aciaria. Compósitos a base de cimento. Ecoeficiência. Concreto sem slump.

TABLE OF CONTENTS

CHAPTER 1

General introduction

Abstract

This chapter presents a general introduction to the work, including the general and specific objectives. The way this work is structured is also presented, with comments about its specificities, in order to facilitate its reading and understanding.

1.1 Introduction

The scarcity of natural resources and the need to conserve them put pressure on the productive sector to improve the efficiency of the production processes, reducing waste and reusing by-products generated as raw materials [1–3]. The construction industry consumes an enormous amount of natural resources, being responsible for more than 30% of the extraction of natural resources, in addition to being responsible for 25% of the solid waste generated in the world [4,5]. However, such resources have become scarce, especially in large urban centers, making raw materials more expensive since there are increased costs associated with transporting materials from other regions [6–8]

The steel industry generates residues and by-products in the steel production process [9,10], including steel slag, which is the molten material formed by chemical reactions, responsible for removing impurities and separating them from metal in the production process [10,11]. On average, the production of one ton of steel results in around 200 kg of by-products for the electric arc furnace (EAF) route and 400 kg for the basic oxygen furnace (BOF) route [9].

Steel slags have a chemical composition close to that of the Portland cement clinker, mainly constituted by calcium-silicates and calcium-ferrites, which makes this industrial waste potentially usable as a raw material for cement and concrete production [12,13]. However, the presence of free CaO and free MgO in the presence of water and the oxidation of the metallic iron fraction raise concerns about the use of steel slag, as these oxides become unstable and can cause problems with slag expansion and cracking in matrices [14–17]. Procedures sush as weathering and metallic separation are efficient in stabilizing these oxides before being applied as a building material [15–18].

Instead of being disposed of in landfills causing environmental problems, residues of the steel industry could be applied in the construction sector as raw materials. The benefits obtained through the reuse of these resources in the economy include saving non-renewable natural resources, reducing CO_2 emissions and add value to waste through the reincorporation in the productive chain [2,9,19,20]. Several studies have been developed with the proposal of using steelmaking slag in cement-based composites as aggregates and binder material [21–26], and its technical and economic viability has been demonstrated.

The formulation of more eco-efficient cement-based compounds becomes a promising strategy to reduce CO_2 emissions and improve cement use efficiency [27]. Some of the

alternatives are the combination of strategies as the use of dispersants (superplasticizers) and increasing packing density of the concrete particles aiming the increase in compressive strength (or reduction in cement consumption), leading to the production of “green concrete” [27,28]. In order to mitigate the negative effects of excessive use of Portland cement and natural resources, many researchers have been working with the design of experiments focused on particle packing methods [23,24,29–32].

In this sense, this work constituted a comprehensive research on the use of steel slag as supplementary cementitious materials and as aggregates on cement-based composites’ production. Chemical, mineralogical, physical and mechanical aspects of the slag were investigated in a vast literature review, as well as the technological properties and durability of cementitious matrices produced with this material. An analytical study aimed at applying steel slag powder (SSP) partially replacing cement was carried out using a biodegradable and low-cost admixture based on Linear Alkyl Benzene Sodium Sulfonate (LAS) to investigate the influence of these materials on the rheology and hydration of blends. Furthermore, an experimental study focused on particle packing method with no-slump concrete was performed to evaluate the physical and mechanical performance, as well as the ecoefficiency of no-slump concrete with total replacement of conventional aggregates by BOFS aggregates.

1.2 Objectives

This research's general objective was to assess the eco-efficiency improvement potential of cement-based composites by partially replacing cement with steel slag powder and replacing natural aggregates with steel slag aggregates.

Therefore, the following specific objectives have been proposed:

- Analysis of the influence of steel slag powder as supplementary cementitious material on the physical, mechanical, and mineralogical characteristics of blended cement pastes and mortars;
- Analysis of the influence of Linear Alkyl Benzene Sodium Sulfonate (LAS) admixture on the physical, mechanical, and mineralogical characteristics of blended cement pastes and mortars containing steel slag powder;
- Evaluation of physical and eco-efficiency performances of the proposed no-slump concretes.

1.3 Dissertation structure

This work has been structured in chapters, with one chapter containing the general introduction, three chapters being presented in the form of articles and one chapter of final conclusions. The chapters in article format, except the first one, have abstract; introduction; materials and methods; results and discussion; conclusions; and bibliographic reference. The first one is a literature review, so it has a differentiated structure.

All bibliographic references are presented at the end of each chapter, so that there is no specific section at the end of this work. It is important to emphasize that the subjects of the chapters are complementary, so that they share some bibliographic references and present elements with similar contents in their introductions. Likewise, methodological elements are also shared, as well as results and discussions.

1.4 References

[1] M. Zhang, Y. Wang, Y. Song, T. Zhang, J. Wang, Manifest system for management of non-hazardous industrial solid wastes: results from a Tianjin industrial park, J. Clean. Prod. 133 (2016) 252–261. https://doi.org/10.1016/j.jclepro.2016.05.102.

[2] A. Yousefloo, R. Babazadeh, Designing an integrated municipal solid waste management network: A case study, J. Clean. Prod. (in press) (2020). https://doi.org/10.1016/j.jclepro.2019.118824.

[3] T.D. Bui, F.M. Tsai, M.L. Tseng, M.D.H. Ali, Identifying sustainable solid waste management barriers in practice using the fuzzy Delphi method, Resour. Conserv. Recycl. 154 (2020) 104625. https://doi.org/10.1016/j.resconrec.2019.104625.

[4] G.L.F. Benachio, M. do C.D. Freitas, S.F. Tavares, Circular economy in the construction industry: A systematic literature review, J. Clean. Prod. 260 (2020) 121046. https://doi.org/10.1016/j.jclepro.2020.121046.

[5] M. Yeheyis, K. Hewage, M.S. Alam, C. Eskicioglu, R. Sadiq, An overview of construction and demolition waste management in Canada: A lifecycle analysis approach to sustainability, Clean Technol. Environ. Policy. 15 (2013) 81–91. https://doi.org/10.1007/s10098-012-0481-6.

[6] Y. Kulaif, SUMÁRIO MINERAL - Departamento Nacional de Produção Mineral, Sumário Miner. 35 (2015) 135.

[7] OECD, Material Resources, Productivity and the Environment, OECD Green, OECD Publishing, Paris, 2015. https://doi.org/10.1787/9789264190504-en.

[8] UNEP, Worldwide Extraction of Materials Triples in Four Decades, Intensifying Climate Change and Air Pollution, 20 July 2016. (2016). https://www.unenvironment.org/news-and-stories/press-release/worldwide-extraction-materials-triples-four-decades-intensifying (accessed November 8, 2019).

[9] WorldSteel, Steel industry co-products, World Steel Association, 2020. https://doi.org/10.1201/9781420003840.sec2.

[10] IAB, Aço e sustentabilidade, Instituto Aço Brasil, Rio de Janeiro, 2019.

[11] C.S. Neto, Agregados Naturais, Britados e Artificiais para Concreto, in: G.C. Isaia

(Ed.), Concreto Ciência e Tecnol., 1st ed., IBRACON, São Paulo, 2011: pp. 233–60.
[12] T. He, Z. Li, S. Zhao, Z. Zhao, X. Zhao, Effect of reductive component-conditioning materials on the composition, structure, and properties of reconstructed BOF slag, Constr. Build. Mater. 255 (2020) 119269. https://doi.org/10.1016/j.conbuildmat.2020.119269.
[13] J.M. Franco de Carvalho, Obtention of eco-efficient cement-based composites uing industrial waste, Federal University of Ouro Preto, Ouro Preto, 2019.
[14] M. Tafesse, H.K. Lee, A.S. Alemu, H.K. Kim, S. Pyo, On the expansive cracking of a cement matrix containing atomized basic oxygen furnace slag with a metallic iron, Constr. Build. Mater. 264 (2020) 119806. https://doi.org/10.1016/j.conbuildmat.2020.119806.
[15] D.H. Diniz, J.M.F. de Carvalho, J.C. Mendes, R.A.F. Peixoto, Blast oxygen furnace slag as chemical soil stabilizer for use in roads, J. Mater. Civ. Eng. 29 (2017) 3–9. https://doi.org/10.1061/(ASCE)MT.1943-5533.0001969.
[16] J.-M. Kim, S.-H. Cho, E.-G. Kwak, RETRACTED ARTICLE: Experimental evaluation of volume stability of rapidly-cooled steel slag [RCSS] as fine aggregate for concrete, KSCE J. Civ. Eng. 19 (2014) 1548–1548. https://doi.org/10.1007/s12205-014-0328-2.
[17] A.C.P. Martins, J.M. Franco de Carvalho, L.C.B. Costa, H.D. Andrade, T.V. Melo, J.C.L. Ribeiro, L.G. Pedroti, R.A.F. Peixoto, Steel slags in cement-based composites : An ultimate review on characterization , applications and performance, Constr. Build. Mater. 291 (2021) 123265. https://doi.org/10.1016/j.conbuildmat.2021.123265.
[18] M.J. Da Silva, B.P. De Souza, J.C. Mendes, G.J.S. Brigolini, S.N. Da Silva, R.A.F. Peixoto, Feasibility study of steel slag aggregates in precast concrete pavers, ACI Mater. J. 113 (2016) 439–446. https://doi.org/10.14359/51688986.
[19] CNI, A industria do aço no Brasil., Confederação Nacional da Indústria, Brasília, 2017.
[20] S.H. Ghaffar, M. Burman, N. Braimah, Pathways to circular construction: An integrated management of construction and demolition waste for resource recovery, J. Clean. Prod. 244 (2020) 118710. https://doi.org/10.1016/j.jclepro.2019.118710.
[21] E. Belhadj, C. Diliberto, A. Lecomte, Properties of hydraulic paste of basic oxygen furnace slag, Cem. Concr. Compos. 45 (2014) 15–21. https://doi.org/10.1016/j.cemconcomp.2013.09.016.
[22] Z. Pan, J. Zhou, X. Jiang, Y. Xu, R. Jin, J. Ma, Y. Zhuang, Z. Diao, S. Zhang, Q. Si, W. Chen, Investigating the effects of steel slag powder on the properties of self-compacting concrete with recycled aggregates, Constr. Build. Mater. 200 (2019) 570–577. https://doi.org/10.1016/j.conbuildmat.2018.12.150.
[23] J.M. Franco de Carvalho, W.C. Fontes, C.F. de Azevedo, G.J. Brigolini, W. Schmidt, R.A.F. Peixoto, Enhancing the eco-efficiency of concrete using engineered recycled mineral admixtures and recycled aggregates, J. Clean. Prod. 257 (2020). https://doi.org/10.1016/j.jclepro.2020.120530.
[24] J.M. Franco de Carvalho, T.V. de Melo, W.C. Fontes, J.O. dos S. Batista, G.J. Brigolini, R.A.F. Peixoto, More eco-efficient concrete: An approach on optimization in the production and use of waste-based supplementary cementing materials, Constr. Build. Mater. 206 (2019) 397–409. https://doi.org/10.1016/j.conbuildmat.2019.02.054.
[25] Y. Jiang, T.C. Ling, Production of artificial aggregates from steel-making slag: Influences of accelerated carbonation during granulation and/or post-curing, J. CO2 Util. 36 (2020) 135–144. https://doi.org/10.1016/j.jcou.2019.11.009.
[26] A. Abdelbary, A.R. Mohamed, Investigating abrasion resistance of interlocking blocks incorporating steel slag aggregate, ACI Mater. J. 115 (2018) 47–54. https://doi.org/10.14359/51700898.

[27] B.L. Damineli, F.M. Kemeid, P.S. Aguiar, V.M. John, Measuring the eco-efficiency of cement use, Cem. Concr. Compos. 32 (2010) 555–562. https://doi.org/10.1016/j.cemconcomp.2010.07.009.
[28] J.S. Damtoft, J. Lukasik, D. Herfort, D. Sorrentino, E.M. Gartner, Sustainable development and climate change initiatives, Cem. Concr. Res. 38 (2008) 115–127. https://doi.org/10.1016/j.cemconres.2007.09.008.
[29] G. Hüsken, H.J.H. Brouwers, On the early-age behavior of zero-slump concrete, Cem. Concr. Res. 42 (2012) 501–510. https://doi.org/10.1016/j.cemconres.2011.11.007.
[30] M. Najimi, J. Sobhani, A.R. Pourkhorshidi, A comprehensive study on no-slump concrete: From laboratory towards manufactory, Constr. Build. Mater. 30 (2012) 529–536. https://doi.org/10.1016/j.conbuildmat.2011.12.012.
[31] W. Zuo, J. Liu, Q. Tian, W. Xu, W. She, P. Feng, C. Miao, Optimum design of low-binder Self-Compacting Concrete based on particle packing theories, Constr. Build. Mater. 163 (2018) 938–948. https://doi.org/10.1016/j.conbuildmat.2017.12.167.
[32] O.A. Mayhoub, E.S.A.R. Nasr, Y.A. Ali, M. Kohail, The influence of ingredients on the properties of reactive powder concrete: A review, Ain Shams Eng. J. (2020). https://doi.org/10.1016/j.asej.2020.07.016.

CHAPTER 2

Steel slags in cement-based composites: an ultimate review on characterization, applications and performance

Abstract

Steel slags are by-products generated in high volumes in the steel industry. Their main constituents are calcium, silicon, ferric, aluminum, and magnesium oxides. Larnite, alite, brownmillerite, and ferrite are also found. The presence of expansive compounds cause concern when used in cement-based composites; however, mitigating routes have been proposed. Activation techniques improve the binding properties of steel slag powder, potentiating its use as a supplementary cementitious material (SCM). As an aggregate, steel slag presents good morphological and mechanical properties. Promising mechanical and durability performances in cement-based composites encourage further research to promote the use of steel slag.

Keywords: Steel slag; cement-based composites; basic oxygen furnace slag (BOFS); electric arc furnace slag (EAFS); recycled aggregates; supplementary cementitious material (SCM).

Construction and Building Materials, 2021, 291
This manuscript was submitted on November 10th, 2020; received in revised form in April 4th, 2021. Accepted April 7th, 2021.
DOI: 10.1016/j.conbuildmat.2021.123265.

2.1 Introduction

The construction industry is one of the greatest natural resources consumers [1–3]. At a global level, civil works and building construction consumes 60% of the raw materials extracted from the lithosphere representing 32% of the world's resources, including 12% of water and up to 40% of global consumed energy [4–7]. However, such resources have become scarce, especially in large urban centers, making raw materials more expensive since there are increased costs associated with transporting materials from other regions [8–10]. Additionally, the construction sector is also responsible for around 25% of the solid waste generated in the world [4,11]. Actions for sustainability in civil construction have been discussed since the 90s [12–14].

Aggregates make up 85% of cement-based products' mass [1,15,16], and these materials are derived from natural rocks and sand, submitted to low industrial processing. According to the Brazilian National Association of Aggregate Producers [17], in 2014, the aggregates production sector had a demand of 740 million tons of gravel and sand, representing a consumption per capita of 3.7 tons/inhabitant/year. In 2019, 970 million tons of sand and gravel were produced in the United States, representing US$ 9.0 billion [18]. The European demand for aggregates is 3 billion tons per year, representing 6.0 tons/inhabitant/year and an annual turnover estimated at €15-€20 billion [19]. General aggregates consumption in China was approximately 20 billion tons in 2018, according to the Chinese Aggregates Association (CAA) [20].

Another major sector of the world's economy is the steel industry. According to the World Steel Association [21], in 2019, the world production of crude steel was 1,869 million tons, with China being the largest producer accounting for 996.3 million tons. Brazil is the 9th largest steel producer in the world. According to the Brazilian Steel Institute [22], Brazilian crude steel production reached 32.6 million tons in 2019. Along with the production of steel, waste and by-products are generated as a result of the steelmaking process, including the blast furnace and steel slags (90% by mass), dust, and sludge coming from atmospheric control systems [23,24]. On average, the production of one ton of steel results in around 200 kg of by-products for the electric arc furnace (EAF) route and 400 kg for the basic oxygen furnace (BOF) route [23].

Instead of being disposed of in landfills causing environmental problems, residues of the steel industry could be applied in the construction sector as raw materials for road

pavements [25–27], cement production [28–31], soil stabilization [32–34], building materials [35–38], among other applications. The benefits obtained through the reuse of these resources in the economy include saving non-renewable natural resources, reducing CO_2 emissions and adding value to waste through the reincorporation in the productive chain [24,39–43].

The use of steel slag as construction materials in terms of supplementary cementitious materials, fine or coarse aggregates could be a promising solution considering the massive demand of the concrete industry and a relevant alternative in the industrial waste management process aimed at a circular economy [44,45]. Through comminution processes, the steel slag can achieve a granulometry similar to lower than cement [46] and can be applied as a powder [30,46–50]. Other investigations were performed for using steel slag as aggregate in cementitious matrices [51–54].

This review provides a broad description of steel slags' chemical characterization with studies over the past 20 years. The occurrence data of the slags' chemical composition have been grouped by year and types (BOFS and EAFS). The slag's morphological issue is discussed within the physical characteristics regarding its importance and influence on the cementitious matrices produced. A literature synthesis of the physical aspects of BOFS slags, such as particle size, specific mass, water absorption, Los Angeles abrasion and crushing value, is made. Regarding the technological properties of slag, there is a subtopic discussing the hardness and grindability of slag, which has not been addressed in other recent literature reviews. A summary of the studies that addressed the slag grindability is brought to show the process's characteristics, the grinding time applied, and the fineness parameters achieved. The environmental classification of slag is also addressed, showing the heavy metal contents found in slag. The economic feasibility of replacing conventional aggregates with recycled slag aggregates and the partial replacement of cement with steel slag powders is also addressed. An in-depth topic on the performance of cement-based composites produced with ground steel slag was also built, assessing workability, mechanical strength and durability, bringing several references of recent studies in the subject.

2.2 Production of steel and its by-products

Steel production requires a complex industrial structure [55]. A limited number of production processes are applied worldwide, which use energy resources and similar raw materials. However, the difference in terms of energy consumption and CO_2 emissions from

each country is related to the quality of the resources used and the energy costs, determining the production process's cost-benefit ratio [42,55]. The steel production is made in the steel mills basically by two technological routes: integrated plants and semi-integrated plants.

Integrated plants produce steel from iron ore, using charcoal as a reducing agent in the blast furnaces (BF) to obtain pig iron. The refining process is carried out in the basic oxygen furnace (BOF), where steel production is carried out using mostly pig iron and a small amount of scrap metal [24,56,57]. About 75% of the steel is produced using the BOF route [57]. The integrated plants also have three essential production stages: reduction, refining, and rolling [24]. Integrated steel mills recirculate all the gases generated in the production process to generate electricity, thus increasing the efficiency of the process and effectively reducing greenhouse gas emissions [42].

Semi-integrated plants operate only the refining phases (via electric arc furnace - EAF) and rolling [24]. In the semi-integrated mills, steel production is done through iron scrap, so they do not have the reduction stage [24,56]. Steel made in an EAF uses electricity to melt scrap, pig iron and ferroalloys to adjust the desired chemical composition [57].

2.2.1 Blast Furnace Slag (BFS)

The steel industry involves the production of different slags throughout the processes [24,41]. Blast Furnace Slag (BFS) is a by-product of the reduction stage, in which iron ore is converted into pig iron. About 300 kg of BFS is produced per ton of pig iron [16]. During the blast furnace process, limestone ($CaCO_3$) is added to removing impurities: silica (SiO_2), phosphorus pentoxide (P_2O_5), calcium sulfide (CaS), magnesium oxide (MgO) and alumina (Al_2O_3), and consequently form the slags [58]. BFS is widely used in cement production as a component of the so-called Portland blast furnace cement. SiO_2 (30 - 40%), CaO (29 - 50%), Al_2O_3 (7 - 19%), MgO (0 - 21%) are more than 90% in the composition of BFS [59–61], the same oxides that comprise Portland cement, but in different proportions [16,24,41,58,62].

2.2.2 Steel slags (SS)

Steel slag is also a by-product of steel production, generated in the refining stage, forming the Basic Oxygen Furnace Slag (BOFS) by the BOF route, and the Electric Arc Furnace Slag (EAFS) by EAF route [63,64]. The slag metallurgical function is to remove impurities and separate them from the metal [58,65].

In the steel production process via BOF in an LD oxygen converter (Linz-Donawitz), the raw materials are liquid pig iron, steel or cast-iron scraps, iron alloys, and a lance injecting gaseous oxygen is introduced at high speed. After melting the metal, lime ($CaO/Ca(OH)_2$) and dolomitic lime ($CaMg(CO_3)_2$) are added to the process [58,66,67]. Oxygen and quicklime are used to eliminate unwanted elements in the steel, such as carbon, silicon, and phosphorus. Dolomitic lime is used to protect the refractory lining [66,68].

In an electric arc furnace (EAF), the production process consists of melting steel scrap by an electric arc [68]. After this fusion, oxygen is injected through a spear to promote reactions of carbon, silicon, and phosphorus [66,68]. The addition of ($CaO/Ca(OH)_2$) and ($CaMg(CO_3)_2$) promotes refining reactions that lead to the formation of EAFS consisting of silicates and oxides [66–68].

The open-hearth furnace (OHF) is a kind of primary steelmaking method that uses the iron produced in a blast furnace. The OHF process has been in constant decline since the 1960s because it is a relatively energy-inefficient method [9]. Today, around 0.3% of primary steel worldwide is still made using OHF technology [21]

Stainless steel production generates two main slags: argon oxygen decarburization (AOD) slag and electric arc furnace (EAF) slag, depending on the manufacturing process [69,70]. More than 80% of stainless steel is currently manufactured using the AOD refining process, whose procedure consists of decarburization and desulphurization of the molten metal and reducing the slag [71]. It has been estimated that about 270 kg of slag is generated during the production process of 1 ton of stainless steel in the refining stage [70].

AOD slag is Characterized by the dominance of high contents of calcium and silicon in its composition and mineral constituents such as dicalcium silicate, fluorite, and magnetite, making it considerable for reuse in cement production or as a construction material [72,73]. However, the high content of chromium in AOD slag can be leached out under the long-term action of rainwater and enters into soil and water bodies, and mainly presents as trivalent Cr(III) or hexavalent chromium Cr(VI) in leachates, which limits its recovery and requires measures to reduce the toxicity of chromium leaching [73,74].

Baosteel Metal Company developed a new slag process called Baosteel Slag Short Flow (BSSF). This process allows the molten steel slag to be cooled and stabilized quickly with compressed air through an atomization process [75,76]. In this industrial process, molten converter slag is cooled down by water and steel balls in a rotating drum. The iron is separated simultaneously due to the higher density and the centrifugal force [77,78].

The ladle furnace (LF) slag, which is also known as basic slag, reducing slag, white slag, or secondary refining slag, is a by-product of the final stages of steelmaking, when the steel is desulfurized in the transport ladle, during what is generally known as the secondary metallurgy process [79,80]. Some applications of such by-products in construction include the use as supplementary cementitious material [81–84], binder [85]; soil stabilizer [32,33]; and asphalt mixture component [86].

Additionally, the steel production process generates other by-products, such as dust and sludge, chemicals, emulsion and oils, and process gases [23,87].

2.3 Steel slag characteristics

2.3.1 Chemical and mineralogical composition

The chemical and mineralogical characterization of slags is a complex issue due to the raw material itself and the different production processes, cooling, and curing, which result in distinct chemical and mineralogical compositions [88,89]. *Table 2.1* lists the chemical composition of different steel slags. Data were collected from studies reported by the literature and separated by slag type (BOFS and EAFS) and year of publication to compare the two types over time. The amount of each chemical component depends on several factors; however, the main chemical constituents in both steel slags are CaO, Fe, SiO_2, Al_2O_3, and MgO, as shown in *Table 2.1*. Although there are similarities in the steel slags' chemical composition, the predominance of higher contents of specific components can be analyzed since these slags are generated in different refining processes. In this way, the BOFS are slags with higher concentrations of calcium oxide, and the EAFS has higher concentrations of iron and silica. The chemical composition is an important parameter to determine the slag's hydraulic activity [90].

Steel slags have a chemical composition close to that of the Portland cement clinker, mainly constituted by calcium-silicates and calcium-ferrites, which makes this industrial waste potentially usable as a raw material for cement and concrete production [91]. The presence of steel slag in the clinker manufacturing process reduces the sintering temperature of raw meal and is also associated with reducing CO_2 emission [30,153].

Table 2.1 Chemical composition of steel slag from the researched literature.

Slag type	Year	CaO	Fe Total (Fe_2O_3/ FeO/ Fe)	SiO_2	Al_2O_3	MgO	MnO	Na_2O + K_2O	SO_3	Cr_2O_3	V_2O_5	TiO_2	P_2O_5	Other oxides	References
BOFS	2020	40.82-54.29	16.78-29.49	8.45-16.93	0.33-5.85	1.93-9.15	1.2-8.7	0.27-0.84	0.07-0.71	0.14-0.33	0.42-0.53	0.16-1.57	0.89-7.14	1.07-1.3	[91–99]
EAFS	2020	25.08-45.9	22.3-38.51	12.2-20.3	1.55-12.2	2.82-7.68	1.3-5.87	0.62-0.63	0.42-0.65	0.8-2.0	-	0.37-1.06	0.5-1.37	-	[94,100,101]
BOFS	2019	34.4-50.26	5.24-34.5	9.45-36.33	0.75-11.38	1.56-10.11	1.07-5.0	0.33-1.34	0.3-0.98	0.16-0.8	0.03-0.34	0.45-1.23	1.03-2.15	0.01-2.5	[36,46,47,63,64, 102–107]
EAFS	2019	16.9-37.96	27.65-43.4	14.56-26.4	3.2-11.57	1.86-7.62	2.45-6.1	0.15-0.29	0.69	0.54-2.67	0.37	0.04-0.81	1.1-1.83	-	[36,64,84,108,1 09]
BOFS	2018	34.21-46.8	18.01-29.56	10.8-20.38	1.01-7.46	2.7-9.95	0.42-5.17	0.13-0.41	0.01-0.3	0.7	0.1	0.45-0.68	1.12-2.78	1.73-1.98	[26,31,48,110–113]
EAFS	2018	27.4-32.9	22.3-35.4	16.3-20.3	6.5-12.2	2.8-5.6	4.0-5.6	-	0.42	1.3-2.0	0.1	-0.8	0.5-1.1	-	[113–115]
BOFS	2017	36.9-42.77	21.87-29.0	9.6-19.24	1.8-4.76	5.19-11.2	0.82-3.2	1.74-2.1	0.3	0.11	0.25	0.61	1.14	2.22	[86,116,117]
EAFS	2017	25.94-53.4	8.5-36.8	15.5-17.32	4.15-12.7	3.4-6.86	1.5-6.0	0.28-0.4	0.56	-	-	1.98	0.25	1.6	[118–120]
BOFS	2016	33.97-49.92	20.49-37.6	8.58-26.1	1.12-6.8	2.0-9.5	2.4-10.31	0.02-0.24	0.12-2.7	0.21-1.2	6.51	0.25-1.78	0.81-2.32	-	[28,35,121–124]
EAFS	2016	16.9-35.8	26.5-43.4	12.5-26.4	2.27-12.0	1.86-7.5	2.66-7.5	0.3	-0.24	1.3-2.67	-	0.41-0.5	0.58-1.38	0.06	[35,83,121,125, 126]
BOFS	2015	39.4-46.73	18.42-30.23	11.97-14.77	2.16-5.52	6.27-9.69	2.74-2.76	0.30	0.12	0.2	0.9	0.4-1.18	1.0-1.67	-	[52,127]
EAFS	2015	22.56-33.4	24.6-36.1	13.9-28.55	5.82-11.62	3.82-9.76	2.82-4.15	0.1-0.2	0.01-0.3	0.73	-	0.6-0.71	0.46-0.58	-	[128–130]
BOFS	2014	35.5-40.95	10.88-30.2	12.2-32.08	4.76-7.73	6.57-8.55	1.26-3.97	-	0.18-0.74	3.14	-	0.32	0.25	3.11	[131–133]
EAFS	2014	26.1-38.86	25.75-39.69	10.36-17.47	4.03-8.96	3.21-5.01	2.32	0.59	0.48	1.96-2.46	0.08-0.1	2.11	1.5	-	[134,135]
BOFS	2013	38.62-52.4	10.07-25.49	8.87-18.94	1.4-5.64	5.2-7.68	1.59-2.9	0.53	0.18-0.88	-	-	0.7	0.33-2.3	0.41-14.84	[50,136–139]
EAFS	2013	32.5-33.0	26.3-36.8	13.1-18.1	5.51-13.3	2.53-5.03	3.94-4.18	0.13	0.14-0.44	0.8-1.38	0.06	0.47-0.6	0.48-0.7	-	[140,141]

Slag type	Year	CaO	Fe Total (Fe_2O_3/ FeO/ Fe)	SiO_2	Al_2O_3	MgO	MnO	Na_2O + K_2O	SO_3	Cr_2O_3	V_2O_5	TiO_2	P_2O_5	Other oxides	References
BOFS	2012	40.1-57.44	17.47-32.0	8.6-15.84	1.7-4.86	4.5-8.41	1.77-3.7	0.10	0.4-1.2	-	-	0.5-0.81	1.4-2.4	-	[142–145]
EAFS	2012	35.6-45.12	17.73-54.72	15.7-18.42	1.05-6.22	4.4-10.48	0.4-1.2	-	-	-	-	-	-	-	[146,147]
BOFS	2011	38.85-44.07	8.64-28.48	14.03-18.94	2.91-5.53	5.36-9.86	0.92-2.11	-	0.14-0.36	-	-	-	1.07	3.06-5.9	[29,148]
EAFS	2011	26.91-53.31	1.07-2.87	22.97-39.76	2.07-18.98	7.79-18.95	-	-	0.44	-	-	-	0.05	-	[148,149]
BOFS	2010	40.46-47.71	23.86-24.36	13.25-17.09	3.04-4.53	6.37-10.46	2.64	0.42	-	-	-	0.67	1.47	-	[90,150]
EAFS	2010	21.77-29.6	32.84-37.6	12.95-18.28	8.32-9.3	3.62-6.14	4.43-5.15	0.54	0.23	1.83-4.07	-	0.35-0.64	0.21	-	[151,152]
Occurrence range		33.97-57.44	5.24-38.06	7.74-36.33	0.33-11.38	1.56-11.2	0.42-10.31	0.02-1.34	0.01-2.7	0.11-3.14	0.03-6.51	0.16-1.78	0.33-7.14	0.01-14.84	**BOFS**
		16.9-53.31	1.07-54.72	10.36-39.76	1.55-18.98	1.86-18.95	0.8-5.87	0.1-0.59	0.01-0.69	0.54-4.07	0.06-0.37	0.04-2.11	0.05-1.83	0.06-1.6	**EAFS**
Average values		42.17	23.80	14.77	3.53	6.80	3.02	0.31	0.47	0.63	0.90	0.78	1.76	2.95	**BOFS**
		31.95	29.34	17.79	7.56	5.63	4.18	0.26	0.36	1.83	0.14	0.72	0.79	0.65	**EAFS**

Several studies have been carried out based on this approach in the scientific field [30,153–156]; however, this is not the scope of the present review, focusing on the application of steel slag as aggregates and supplementary cementing material in cement-based composites.

Typically, steel slag is cooled slowly, influencing the high content of crystalline free CaO and crystalline iron oxide; therefore, the steel slag should be cooled quickly to reduce volumetrically unstable crystalline free CaO and crystalline iron oxide [157]. A striking feature of steel slag is the high CaO content (25 to 55% by weight) [158]. Free lime (CaO) and free periclase (MgO) when hydrated and oxidation of iron cause volumetric instability (expansion problems), requiring long periods of aging and quality control before being applied as a building material [103,139,157,159,160].

However, the presence of oxides such as Ca, Mg, and Mn can be a positive factor in the steelmaking process, replacing part of the limestone, dolomite and manganese ore, reducing the production costs of iron and steel [158,161]. Slag basicity evaluated by the CaO/SiO_2 ratio indicates the amount of free CaO. The amount of CaO in the slag tends to increase with the increase in its basicity, and this relationship is significantly improved by slow cooling [58,162]. Also, cementitious properties are directly linked to this parameter [89,163]. The presence of higher amounts of P_2O_5 and S becomes problematic, affecting the direct recycling of steel slags in the iron and steel production process [103,158].

Fe in the steel slag is usually found in the form of steel (Fe), iron oxides (FeO, Fe_2O_3, Fe_3O_4) and iron-bearing minerals, which can be separated from slag by applying mineral processing technologies and be recycled as raw materials for sintering, blast furnace, and steelmaking [158]. Typical iron recovery methods include crushing, grinding, screening, and magnetic separation [103,161]. Lan et al. [161] showed an efficiency of 93.20% in the recovery of the metallic fraction of the studied BOFS and improved the recycling process's efficiency by 9.58%. Guo et al. [110] performed a treatment of BOFS with an additive mixture containing kaolin and carbon powder to reduce iron oxides and recover the metal fraction with more than 95% efficiency. The iron content can represent a problem to apply steel slag in the clinker production in the cement industry since standard clinker generally contains 2 to 3% Fe2O3, while BOFS contains 14 to 30% by weight of iron [103,139,161].

Since the chemical composition of slags is highly variable, their mineralogical composition also varies. *Table 2.2* summarizes the mineralogical phases found in the BOFS according to the researched literature. These slags undergo a process with fewer impurities, as they do not reuse scrap in the process; and represent a larger volume generated in the steel

refining process (about 75%). Thus, in BOFS, Olivine [$(Mg, Fe)_2SiO_4$], merwinite ($Ca_3MgSi_2O_8$), larnite (C_2S), alite (C3S), brownmillerite (C4AF), rhombohedral to orthorhombic phase (RO phase) solutions CaO-FeO-MnO-MgO, and free CaO are common minerals [112,148,164,165]. The main compounds of EAFS, according to the scientific literature, are wüstite (FeO), gehlenite (Ca_2AlSiO_7), kirschsteinite ($CaFeSiO_4$), larnite (C_2S), chromite ($CrFeO_4$), and magnetite (Fe_3O_4) [100,114,115,126,128,146].

The contents of the CaO, $Ca(OH)_2$, and $CaCO_3$ phases depend on the sample age [166]. Weathering and aging cause the formation of portlandite [$Ca(OH)_2$] and calcite ($CaCO_3$) from the stabilization of CaO and contributes to the volumetric stability of the slags [45,167]. C_2S, C_3S, C_4AF, and C_3A provide the slag's hydraulic and cementing properties [90,136,168–170]. However, steel slag can be considered a latent hydraulic material (which does not manifest itself) since the content of reactive calcium silicate compounds (C_3S and β-C_2S) is much lower than that in Portland cement due to their large crystal size, and it has a relatively high content of inert phases, such as the RO phase [29,50,136,148,171,172].

The process of cooling the slag under different rates significantly changes the crystallization process. Under very fast cooling, the mineral may retain its composition and structure at high temperatures, as is the case with C_3S, which is stable at temperatures above 1250 ºC, which decomposes into CaO and C_2S at lower temperatures. Besides, the cementitious β-C_2S turns to non-cementitious γ-C_2S when the temperature drops below 500 ºC during slow cooling [172,173]. That explains why clinker is sharply cooled down to low temperature in cement clinker production, keeping cementitious compounds with active hydraulic properties, unlike slowly cooled steel slag, which loses hydraulic potential [172]. Thus, cement mixed with steel slag generally has a longer average hardening time, with less initial mechanical strength, and in some cases, it presents volume expansion due to the high levels of oxides comprised in its chemical composition [136,148].

Table 2.2 Mineralogical phases observed in the recent researched literature regarding BOF steel slag.

Slag type	Calcite ($CaCO_3$)	Portlandite ($Ca(OH)_2$)	Lime (CaO)	Periclase (MgO)	Wustite (FeO)	Brownmillerite (C_4AF)	Larnite (C_2S)	Alite (C_3S)	Ferrite (C_2F)	Aluminate (C_3A)	Quartzo (SiO_2)	RO Phase	References
BOFS			✓		✓	✓	✓		✓				[94]
BOFS			✓				✓	✓	✓			✓	[97]
BOFS						✓	✓	✓		✓	✓	✓	[98]
BOFS	✓			✓	✓	✓							[93]
BOFS							✓	✓	✓			✓	[95]
BOFS	✓	✓	✓				✓	✓	✓				[96]
BOFS		✓			✓								[103]
BOFS^{W}	✓	✓	✓	✓	✓	✓	✓						[46]
BOFS				✓			✓	✓	✓			✓	[105]
BOFS	✓	✓	✓		✓		✓						[106]
BOFS	✓	✓	✓	✓		✓	✓	✓				✓	[63]
BOFS	✓	✓			✓		✓	✓		✓	✓	✓	[64]
BOFS				✓			✓						[31]
BOFS^{W}	✓			✓	✓	✓	✓						[113]
BOFS		✓	✓				✓	✓	✓			✓	[110]
BOFS				✓			✓	✓				✓	[48]
BOFS			✓	✓		✓	✓	✓	✓			✓	[165]
BOFS		✓	✓	✓			✓	✓	✓			✓	[112]
BOFS		✓		✓	✓		✓						[117]
BOFS^{W}	✓	✓		✓	✓						✓		[35]
BOFS^{HS}		✓				✓	✓	✓				✓	[122]
BOFS	✓	✓	✓				✓	✓	✓			✓	[123]
BOFS		✓	✓	✓	✓		✓		✓				[54]
BOFS			✓			✓	✓					✓	[28]
BOFS	✓	✓					✓	✓				✓	[174]

Slag type	Calcite ($CaCO_3$)	Portlandite ($Ca(OH)_2$)	Lime (CaO)	Periclase (MgO)	Wustite (FeO)	Brownmillerite (C_4AF)	Larnite (C_2S)	Alite (C_3S)	Ferrite (C_2F)	Aluminate (C_3A)	Quartzo (SiO_2)	RO Phase	References
$BOFS^{W/F}$		✓	✓				✓		✓				[127]
BOFS				✓	✓		✓	✓				✓	[132]
BOFS					✓		✓	✓		✓			[137]
$BOFS^{IC}$			✓	✓	✓		✓		✓				[139]
$BOFS^{SC}$			✓	✓			✓		✓				
$BOFS^{RC}$			✓	✓				✓	✓				
$BOFS^{d}$					✓		✓	✓					[142]
$BOFS^{v}$			✓	✓	✓		✓	✓					
$BOFS^{f}$	✓	✓	✓		✓		✓		✓		✓		[143]
$BOFS^{w}$	✓	✓	✓		✓		✓		✓		✓		
$BOFS^{hl}$	✓	✓	✓		✓		✓		✓				
$BOFS^{ll}$	✓	✓	✓		✓		✓		✓		✓		
BOFS		✓			✓	✓	✓	✓				✓	[144]
BOFS			✓	✓		✓	✓	✓				✓	[90]
$BOFS^{F}$			✓		✓		✓		✓				[150]
$BOFS^{W}$		✓	✓			✓	✓	✓	✓			✓	[175]
BOFS			✓				✓		✓				[176]
BOFS	✓	✓	✓	✓	✓	✓	✓	✓			✓		[66]
Mohs Scale	**3.0**	**2.0**	**3.0**	**6.0**	**5.0 – 5.5**	**5.5**	**6.0**	**4.5**	**5.5**	**6.0**	**7.0**		

d - dense texture
v - vesicular texture
f - fresh production
w - weathered production
hl - high lime content
ll – low lime content
IC - Industrial cooling
SC - slow cooling
RC - rapid cooling
W - weathered slag
F- fresh slag
HS - hot stuffy steel slag

2.3.2 Physical characteristics

Some physical characteristics of BOFS differ significantly from conventional raw materials used for aggregates production. *Table 2.3* shows a collection of data from recent literature comprising physical characteristics of BOFS, including morphology, specific gravity, water absorption, and abrasion resistance.

2.3.2.1 Morphology

The particle morphology can be expressed by three independent properties: shape, angularity, and surface texture. This property plays an important role, affecting the properties of cement pastes, mortars, and concrete [16,145,177], and in the raw slag, the morphology is dependent on the cooling condition [93,178]. It is known that in concretes, the bond strength of the interfacial transition zone (ITZ) between the aggregate and the hardened cement paste is the weakest link in the matrix [15,159]. Conventional methods for improving this ITZ include the use of aggregates with rough surface texture or the addition of superfine chemically active mineral additives to consolidate the interface bond physically and chemically. Steel slag, in turn, has both physical and chemical advantages, has a rough surface, and can react with the hardened cement past to a certain extent [159].

Ye et al. [178] studied BOFS under different cooling and treatment processes, roller steel slag (RSS), hot braised steel slag (HBSS) and layer pouring steel slag (LPSS). The morphological tests performed indicated that all steel slags have a rough surface and numerous pores, which contributes to improving the bonding performance between aggregate and asphalt binder, resulting in the enhancement of asphalt concrete structural stability in the research. Yang et al. [179] conducted morphological tests on two BOFS samples from two differente Chinese steel mills, the steel slags were identified as S_a and S_b slag. It can be observed that the BOFS exhibits surface morphology with a rough and pitted texture *(Fig. 2.1)*. Many honeycomb pores have adhered to their internal and external surface, and further observation shows rthat th surface of BOFS has many small “dust”, which are the alkaline hydration products contained in slags [179].

Souza et al. [124] evaluated the morphology of the BOFS in the small and large particle-size ranges and concluded that the aggregates have a greater specific surface and opacity, which suggests greater roughness *(Fig. 2.2)*. Moreover, the slag had less angular and more volumetric

grains. Characteristics such as texture, roughness, and rounded grain shapes can positively contribute to cementitious matrices' performance [124,180,181].

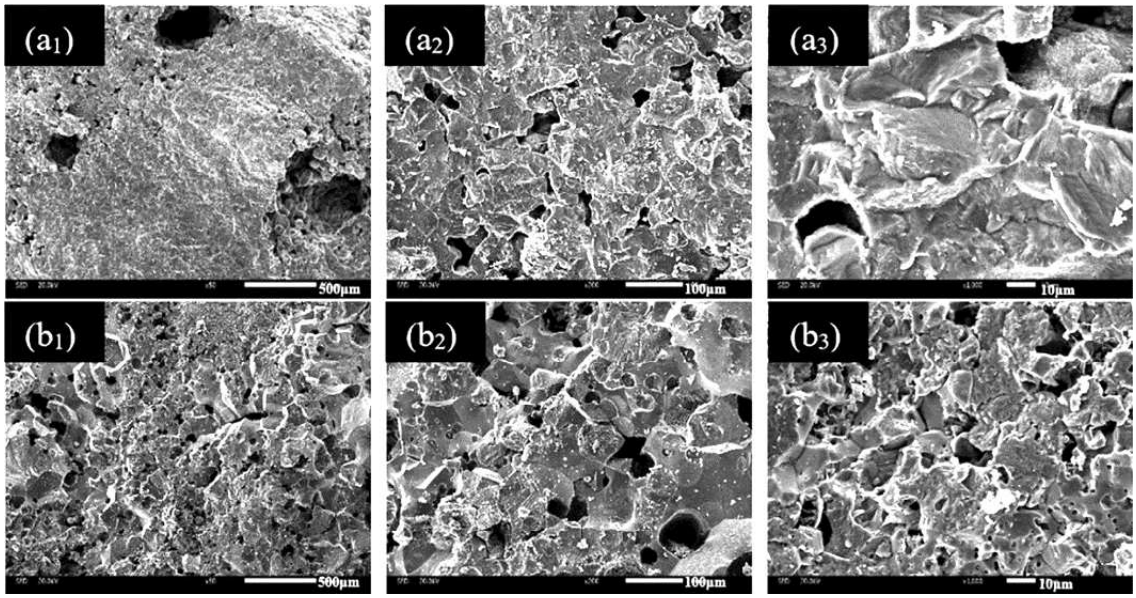

Fig. 2.1 Microscopic structure of two BOFS under SEM: (a) S_a slag; (b) S_b slag [179].

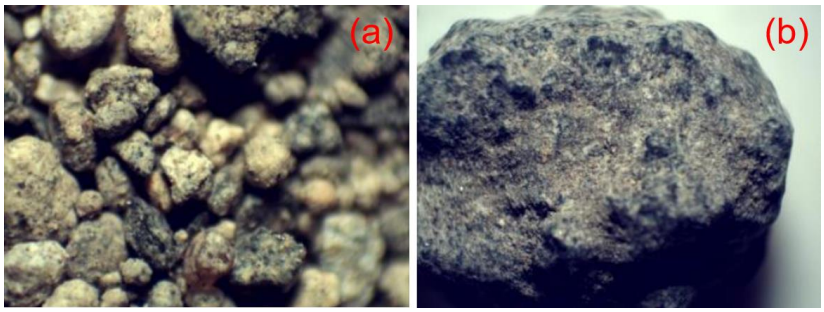

Fig. 2.2 (a) fine aggregate BOFS; (b) coarse aggregate BOFS [124].

Shen et al. [25] measured form factors and rounding indices and compared the results of conventional and slag aggregates. Slag aggregate showed high angularity and rough surface texture, and the shape of the particles provided high internal friction, with a good interlocking mechanism and increased skid resistance. The slag in the study showed a low percentage of flat and elongated particles that guarantee good quality to avoid breaking particles under traffic [25].

Kong et al. [104] carried out a study of the geometric characteristics of three samples of BOFS as coarse aggregate compared to the properties of conventional aggregates such as basalt and limestone. The experimental results show that the BOFS coarse aggregate has high sphericity, good angular performance and rough surface texture. The geometric characteristics of BOFS influenced the performance of asphalt mixture; the higher sphericity and angularity

of BOFS increase the air voids of asphalt mixture and improve the moisture damage resistance and rutting resistance of asphalt concrete [104].

Studies conducted by Franco de Carvalho et al. [46] reported that the particles that comprise powders produced from BOFS are predominantly equant, moderately rough, but with rounded edges. This morphology presented by the slag particles directly affected the rheological behavior of cement pastes, which showed good results, suggesting that the effect caused by the overall shape was predominant despite the large specific area.

2.3.2.2 Density

Values of specific gravity of steel slags are higher than those of natural aggregates, and this is due to the presence of high content of dense oxides - CaO, SiO_2, and FeO/Fe_2O_3 [35,36,143,175,182,183]. Values of apparent specific gravity (ASG) between 2.729 and 3.82 g/cm³, and bulk density (BD) between 1.945 and 3.37 g/cm³, have been reported in the literature (*Table 2.3*).

Ma et al. [105] compared the physical characteristics of BOFS with basalt and limestone. For the same granulometry, the specific gravity of the slag exceeded that of basalt by 20%. Kong et al. [104] analyzed three samples of BOFS with different particle sizes and showed higher specific gravity compared to standard aggregates; there was an increase of up to 31.7% in apparent specific gravity and 30.8% in bulk density [104]. The higher density of steel slag aggregates could lead to heavyweight concrete with high strength and durability [109,182–184].

2.3.2.3 Water absorption

The water absorption of the aggregates influences properties such as adhesion between it and the hydrated cement paste, the cementitious matrix's resistance to frost-defrost cycles, chemical stability abrasion resistance [16]. An aggregate's water absorption capacity can be used to determine its porosity and strength [15]. A range of water absorption of materials with different petrological classifications was proposed by Alexander and Mindess [185]. Average values of 1.8% for basalt aggregates, 1.6% for limestone aggregates, and 2.0-4.8% for blast furnace slag are presented.

Analysis of the slag morphology carried out in some studies [25,124] showed that the BOFS aggregates have higher surface moisture and greater water absorption. This is due to the slag grains' morphology, which has a rough texture, high angularity, and great surface area. The

increase in the steel slag's water absorption must be taken into account in the concrete mixture design [182].

Souza et al. [124] studied the steel slag as large and small aggregates compared to conventional aggregates. The water absorption presented by the coarse and fine BOFS aggregates was 2.05% and 7.71%, respectively, while for gravel and natural sand, the values were 1.2% and 0.72%, respectively. Ma et al. [105] performed BOFS water absorption tests (values between 1.79-2.63%), and the results showed values exceeding more than three times those presented by basalt (values between 0.71-0.82%) in different granulometric ranges.

Kong et al. [104] carried out water absorption tests of three different types of BOFS with distinct particle sizes and compared them with the natural aggregates of basalt and limestone. The results showed that water absorption increases with the decrease in the aggregate grain size since a smaller grain size is related to a larger specific surface area. Basalt and limestone showed similar water absorption in different granulometric ranges (values around 0.2-0.8%), and BOFS showed higher water absorption than natural aggregates in all grain size ranges (values around 0.5-2.2%) [104].

Higher than normal aggregate porosity and absorption do not necessarily imply reduced concrete strength or durability [185], as seen in several studies [52,124,182]. Furthermore, in high-strength concrete, aggregates with a higher than normal absorption can be used to provide a latent source of moisture to the hydrating matrix after initial hardening so that strength development is enhanced and autogenous shrinkage is reduced [185].

2.3.2.4 Abrasion resistance

Los Angeles abrasion test combines friction and abrasion of particles, and its results have a good correlation between the actual wear of aggregates in concrete and the compressive and flexural strengths of the concrete produced with them [16].

Shen et al. [25] compared conventional aggregate and BOFS slag and observed that the last presented low Los Angeles abrasion and low soundness. Greater resistance to the Los Angeles fragmentation of aggregate can lead to concrete with better mechanical behavior, as shown in the literature [53,182,186,187]. Qasrawi [188] also confirms that steel slag aggregates have a lower LA-value when compared to normal aggregate. The lower the LA-value, the higher the aggregates' strength and, consequently, concrete strength.

Ma et al. [105] showed that crushing and wear measurements for BOFS were between those observed for basalt and limestone, indicating that the steel slag's mechanical strength was worse than basalt but better compared to limestone.

2.4 Technological properties of steel slag

2.4.1 Hardness and grindability

The grinding process requires energy, and its efficiency depends directly on the hardness of the constituent phases of the materials. Therefore, for materials with higher hardness, like steel slags, the required grinding time will be longer, reducing the eco-efficiency of the process with high energy demand and high costs in the production of BOFS powders to be used as supplementary cementitious materials [44,54,192,193]. In this sense, the development of green energy sources, in addition to the use of blends containing lesser amounts of superfine powders, and higher amounts of thicker powders, are ways to mitigate the impacts caused and increase the eco-efficiency of the products [46]. *Table 2.4* shows information on grinding times and fineness indicators reported in the literature to produce different steel slag powders.

The mineralogical composition of steel slag can be divided into two parts: active components (e.g., C_3S, C_2S, C_4AF, and C_2F) and non-active components (e.g., RO-phase and Fe_3O_4) [136,144,194]. The grindability of the active components is similar to that of cement, but non-active elements that contain high metallic iron content are very difficult to grind [54,136,143,171]. Steel slag has poor grindability because of a large amount of iron oxides and continuous solid solution, fine particles of steel slag powders present high content of C_3S and C_2S phase since they were easy to grind, and there was a high content of RO phases in the coarse particles of steel slag powders since they were difficult to grind [48,193].

Currently, investigations aimed at improving the grinding efficiency of steel slag mainly aim to optimize the grinding equipment. Few studies aim to apply other measures, such as removing hard-to-grind phases (HGP) or using chemical admixtures to assist the process [193]. In studies of Zhao et al. [193], they provided a simple method for the determination of the hardly grinding phase (HGP) in steel slag by residues (i.e., oversize substance). After grinding and then screening steel slag powder, the oversize substance that passed a 0.9 mm square-hole screen can be considered hard-to-grind phases (HGP), and its proportion is about 1.5%.

Table 2.3 Physical characteristics of different BOFS.

Aspect of BOFS	Country of origin	Morphology	Particle size	ASG (g/cm^3)	BD (g/cm^3)	WA (%)	LA (%)	CV (%)	References
Granular	Colombia	Heterogenous morphology with irregular and angular shape	0,1 - 100 µm	3.51	3.43	0.68	-	-	[94]
Granular	China	-	9.5 - 16.0 4.75 - 9.5	3.584 3.551	1.982 1.923	1.78 1.31	-	10.6 9.8	[97]
Granular	China	Rough and pitted texture	9.5 - 16.0 mm 4.75 - 9.5 mm 2.36 - 4.75 mm 0 - 2.36 mm 9.5 - 16.0 mm 4.75 - 9.5 mm 2.36 - 4.75 mm 0 - 2.36 mm	3.386 3.426 3.465 3.127 3.365 3.407 3.389 3.235	- - - - - - - -	2.566 2.651 2.772 - 2.674 2.783 2.895 -	14.9 -	19.7 -	[179]
Granular	-	-	4.75 - 9.5 mm	3.55	1.78	-	-	6.8	[189]
Granular	Brazil	Volumetric, rough, rounded edges	4.8 - 12.5 mm	3.77	1.945	-	-	-	[46]
Granular	China	Pitted and vesicular texture and porous structure	13.2 - 16.0 mm 9.5 - 13.2 mm 4.75 - 9.5 mm 2.36 - 4.75 mm 13.2 - 16.0 mm 9.5 - 13.2 mm 4.75 - 9.5 mm 2.36 - 4.75 mm 13.2 - 16.0 mm 9.5 - 13.2 mm 4.75 - 9.5 mm 2.36 - 4.75 mm	3.306 3.293 3.302 3.308 3.293 3.302 3.263 3.275 3.582 3.563 3.587 3.543	3.153 3.125 3.102 3.092 3.186 3.179 3.124 3.098 3.517 3.453 3.426 3.379	1.49 1.60 1.90 2.10 1.0 1.2 1.4 1.7 0.50 0.90 1.35 1.40	16.5 15.6 15.6	14.3 15.2 13.9	[104]
Granular	China	Surface with macro and micro voids	13.2 - 19.0 mm 4.75 - 13.2 mm 2.36 - 4.75 mm	3.551 3.540 3.555	-	2.63 2.21 1.79	16.8	17.6	[105]
Granular	Brazil	-	<9.5 mm <4.8 mm	3.32 3.03	1.74 1.85	-	-	-	[36]
Granular	Japan	-	<5.0 mm	3.02	-	4.18	-	-	[106]

Aspect of BOFS	Country of origin	Morphology	Particle size	ASG (g/cm^3)	BD (g/cm^3)	WA (%)	LA (%)	CV (%)	References
Granular	Colombia	Rough texture and very irregular angularity	<19.0 mm	2.729	2.468	3.8	20.0	-	[26]
Powder	-	-	0.0001 - 0.1 mm	-	-	-	-	-	[112]
Granular		-	0.63 - 1.25 mm	-	-	-			
Powder	China	Irregular polygonal shapes	25.53 - 104.4 µm	-	-	-	-	-	[48]
Granular	-	-	5.0 - 12.5 mm 12.5 - 20.0 mm	3.82	-	1.68	13.5	-	[182]
Granular	China	Porous with rough surface texture	9.5 - 19 mm 4.75 - 9.5 mm 2.36 - 4.75 mm	3.342 3.381 3.319	- - -	1.7 1.6 2.0	16.8 14.8 17.6	-	[190]
Granular	India	Porous texture with angular shape	4.75 - 9.5 mm	3.35	-	2.0	18.0	21.0	[191]
Granular	China	Porous particle with cracks inside	2 - 8 mm	3.42	2.163	3.31	-	-	[52]
Powder			<0.6 mm	3.58	-	4.23	-		
Granular	-	-	-	3.19	1.94	0.8	17.0	-	[188]
Granular	China	Very variable surface texture, from very dense to vesicular with a lot of micro-pores	16.0 - 9.5 mm 9.5 - 4.75 mm	3.409 3.486	3.203 3.191	1.9 2.7	12.9 -	-	[142]
Granular	-	-	40 - 1250 µm	3.30	-	-	-	-	[175]
Granular	-	High angularity and rough surface texture	19 mm 12.5 mm 9.5 mm 4.75 mm	3.43 3.47 3.51 3.49	3.32 3.36 3.37 3.31	2.2	20.96	-	[25]
Range				2.729 - 3.82	1.74 - 3.517	0.55 - 4.23	12.9 - 20.96	9.8 - 19.7	

ASG - Apparent specific gravity
BD - Bulk density
WA - water absorption
LA – Los Angeles abrasion
CV - Crushing value index

Zong et al. [195] studied a component modification in-process solution to the difficult grinding of air quenching steel slag. The results show that the fly ash added into the steel slag before air quenching can more effectively improve the slag's grindability than mill tailings under the same conditions due to the reaction between fly ash and steel slag at high temperatures.

Franco de Carvalho et al. [30] produced BOFS powders to be used in cement production with low environmental impact. It was using a ball mill. The grinding times were adjusted to reach a volume of 80% of the material passing through the #200 sieve (0.75mm). BOFS required a high grinding time (180 min) in comparison to the other raw materials (60 min for limestone and 55 for quartzite). The presence of mineralogical phases with high hardness, such as larnite (hardness 6 on the Mohs scale), helvine (Mohs 6–6.5) and wustite (Mohs 5.5), contributes to the low grindability and makes the process more expensive [30]. The presence of metallic iron also increases the material's ductility, reducing grinding efficiency [171,196].

2.4.2 Expansive features

The presence of free CaO and free MgO in the presence of water and the oxidation of the metallic iron fraction raise concerns about the use of steel slag, as these oxides become unstable and can cause problems with slag expansion and cracking in matrices [32,58,93,106,127,157,199,200]. BOFS contain a certain amount of expansive components such as free CaO and free MgO, which have a low hydration activity and unstable crystalline iron oxide [157,201]. However, procedures such as weathering and metallic separation are efficient in stabilizing these oxides [29,32,35,58,106,127,175,200].

Oxygen and quicklime are used to eliminate unwanted elements in steel, such as carbon, silicon, and phosphorus. Dolomitic lime is used to protect the refractory lining [66,68,175]. Thus, the resulting slag contains free lime (f-CaO) and free MgO (periclase). Unhydrated free lime and free periclase in slag cause volumetric instability of the slag when hydrated, free CaO hydrates quickly in portlandite [$Ca(OH)_2$] and causes a large volume expansion, and free MgO hydrates slowly in brucite [$Mg(OH)_2$] and causes volume changes that continue for many years [25,89,127,202]. These are topochemical reactions in which hydroxide compounds involve outward, causing stress concentrations that can lead to microcracking in confined or bonded applications [203].

Table 2.4 Grindability of the BOFS.

Procedure / Equipment	Grinding times	Fineness parameters					References
		Range	D90 (µm)	D50 (µm)	D10 (µm)	Specific surface area (cm^2/g)	
Ball Mill	-	0.3 - 300 µm	-	-	-	-	[97]
Horizontal ball mill	180 min	80% by weight of the material passing through a #200 sieve (75 µm)	-	-	-	-	[30]
Horizontal ball mill	180 min	0.5 - 250 µm	118.0	27.23	1.704	2635[B]	[46]
Horizontal ball mill + High efficiency planetary ball mill	180/45 min	0.3 - 110 µm	39.59	8.550	1.109	5416[B]	
Small ball mill	40 min	-	-	14.9	-	9863[*]	[102]
Grinding	-	-	-	3.15 4.63 6.72 11.77 15.78	-	-	[197]
Small ball mill	40 min	25.53 - 104.4 µm	-	-	-	-	[48]
Grinding	10 min	0.15 - 60.0 µm	-	-	-	-	[198]
Ball mill	30 min	100% passing through a #30 sieve (600 µm)	-	-	-	5340[*]	[52]
Grinding	-	0.1 - 100 µm 0.1 - 400 µm	-	-	-	4420[*] 7860[*]	[136]
Grinding	-	0 - 125 µm	-	-	-	3800[B]	[143]
Grinding	-	-	71.45 37.03 19.82 7.72 2.17	60.25 30.79 15.17 5.74 1.43	51.72 25.84 11.59 4.07 0.81	-	[29]

B - Blaine
* - Uninformed

The metallic iron (Fe) represents approximately 70% of all iron oxides (Fe total) comprised in the unprocessed LD steelmaking slag and 35% in the unprocessed EAF slag [35]. Fe undergoes oxidation when exposed to mixing water in an alkaline environment and then to ambient air and can be found in its Fe^{+2} and Fe^{+3} forms. This oxidized fraction can generate a volumetric increase of up to 300% of its original form. The internal stresses from the oxidation of metallic iron generate microcracks in the cement matrix structure [35]. In the case of unstable crystalline iron oxide present in a solid system like concrete, the expansion will result in extensive cracking and loss of the concrete's structural integrity since oxidation starts on the interface zone between particles, and its rate of progress is naturally high in a crystalline structure that contains many interface zones [157].

Tafesse et al. [93] observed in their studies the formation of cracks in cement matrices containing atomized BOF slag, which contains metallic Fe and free MgO in its constitution *(Fig. 2.3)*. The cracks seem to have been initiated from the atomized BOF-slag particles due to metallic iron oxidation. At the cracked points, Fe oxide and brucite were formed, and portlandite was also found. The high hardness of BOF slag propitiates these cracks' propagation because that is a brittle material, which affects the matrix in which it is inside.

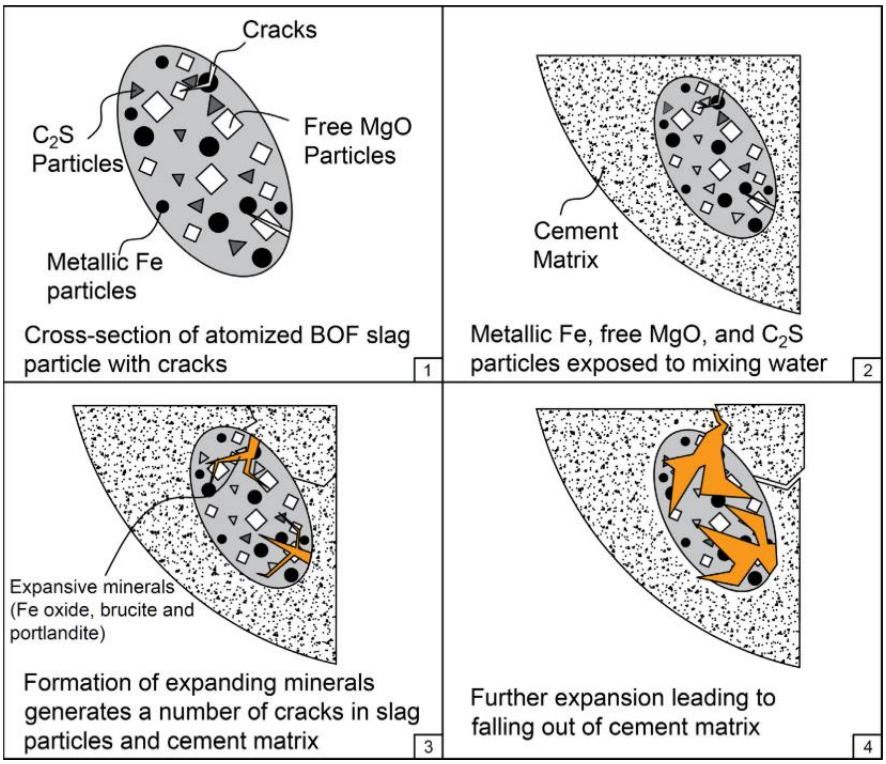

Fig. 2.3 Mechanism of cracking of BOF slag particles in the cement matrix [93].

Volume expansion of slag is a problem that must be controlled before it can be used in construction. The expansive potential of steel slag in confined cementitious matrices, such as Portland cement concrete, is a concern and requires special care [159,160]. The reaction between free lime (f-CaO) and water results in $Ca(OH)_2$ that has twice its original volume at normal temperatures. If this reaction occurs in a brittle solid material such as concrete, the expansion can easily destroy the material [157]. The free lime (f-CaO) content can fluctuate from less than 0.1% to more than 10% in the same type of slag. That highlights the importance of testing, evaluating, and establishing usability criteria [157,204].

The Rapid Cooled Steel Slag (RCSS) produced from the atomization process has a very low Free CaO content of about 0.15%, depending on the steel slag's cooling rate. Slow cooling allows the decomposition of CaO from calcium ferrite [C_2F, CF] and calcium silicate [β-C_2S], while a more rapid cooling rate prevents this decomposition. Furthermore, with RCSS, the slag does not require aging and is safe to be used as a building material [157].

The nonmetallic fraction of BOFS employed by Diniz et al. [32] went through an additional weathering process to neutralize undesirable expansive effects of calcium oxide (CaO) and magnesium oxide (MgO). Other studies have used the same weathering stabilization technique of expansive oxides present in the steel slag [30,36,46,128,175,191,205,206].
Palankar et al. [191] submitted the steel slag aggregates to a weathering process by exposing the aggregates outdoors and spraying water at regular intervals for nine months to reduce the free lime and magnesia contents in order to avoid volume deformation before use in concrete production. Visual examination of weathered steel slag aggregates displayed a formation of a calcite coating on the aggregates' surface *(Fig. 2.4)*. Proper weathering of steel slag aggregates resulted in a reduction of CaO and MgO, ensuring no further expansion or volume deformations [191].

Fig. 2.4 Image showing steel slag aggregates before and after weathering process. (a) Steel slag aggregates before weathering process. (b) Formation of a thin film of calcite on slag aggregates after undergoing weathering process. (c) Enlarged image of steel slag aggregate displaying the presence of calcite coating [191].

2.4.3 Environmental classification

Assessing the potential risks to human health and the environment associated with slag applications is necessary due to the high concentrations of heavy metals in their constitution [209–211]. BOFS could contain potentially toxic elements like Chromium (Cr), Nickel (Ni), and Vanadium (V), and they represent heavy metal leaching challenges and can be released [212–214]. Chromium can be leached out under the long-term action of rainwater and mainly presents as trivalent Cr(III) or hexavalent Cr(VI) chromium in leachates [74]. Cr(VI) is readily transported and can induce toxic and carcinogenic effects by a multifront mechanism of action [74,215]. According to the data presented in *Table 2.1*, chromium is present in some slags in proportions that vary between 0.11-4.07%; this value depends on the ore's composition and other primary materials used in steel production.

Vanadium is an important product used almost exclusively in ferrous and non-ferrous alloys due to its physical properties such as high tensile strength, hardness, and fatigue resistance [216]. It is expected that for use in the cement industry and road construction, the vanadium content in the slag should be lower than 0.1% by mass and 0.3% by mass,

respectively, according to Swedish conditions [217]. In *Table 2.1*, vanadium occurrence ranges from 0.03 to 6.51%.

According to Brazilian standard NBR 10004 (ABNT, 2004), leaching and solubilization tests show that steel slag can be classified as a non-inert non-hazardous material [32,35]. Based on the concentration levels of leachate in BOFS samples obtained from the analysis of the Toxicity Characteristic Leaching Procedure (TCLP) tests, the slag does not contain toxic materials, and it can be classified as type III solid waste, according to the Indiana waste criterion [117,218]. It is important to highlight that the incorporation of steel slag did not affect cement-based composites' environmental classification [35].

2.5 Performance of cement-based composites produced with steel slag

2.5.1 Workability and mechanical performance of steel slag powder (SSP)

The use of SSP as Supplementary Cementitious Materials (SCM) requires a detailed understanding of the slag properties due to their special production processes and chemistry [79,219]. Several studies have explored the potential use of steel slags as SCM by replacing the cement in cement-based composites [46,112,199] since steel slag has chemical and mineralogical composition similar to Portland cement clinker [220]. Researchers believe that it could improve the workability, decrease its hydration heat, fill the internal micropores and enhance its interfacial transition zone (ITZ) [49].

However, the hydraulic property of steel slag is poor, owing to its low contents of hydraulic components [44,45]. Thus, some techniques for activating steel slag have been analyzed to improve its cementing activity, such as mechanical activation [46], thermal activation [82,221] and chemical activation [122,137]. Incorporating mineral admixtures into the molten slag can increase cementitious materials' content, improving the hydraulic activity [137,148,198]. The powders' production derives from a mechanical activation, carried out by grinding, which can be done until reaching the desired particle size distribution. Some studies show that the addition of powder can improve the matrices' fluidity, which must be attributed to improving the particle size distribution of the alkaline constituents [48,102] or due to the improved shape of BOFS particles [46]. Also, the powder's addition can slightly increase the matrices' initial setting time since steel slag powders can decrease the hydration rate, with a significant reduction in the peak hydration temperature [48,102,192].

Wang et al. [136] investigated the cement properties of super-fine steel slag obtained by mechanical grinding with the results of ordinary steel slag, fly ash, and cement. The results indicated that the super-fine steel slag exhibits higher activity in the early and middle ages and lower in the late ages than usual steel slag. When comparing fly ash and cement, it was observed that the super-fine steel slag did not contribute to the increase in concretes' performance at late ages. Roslan et al. [83], on the other hand, observed that concretes produced with a 15% substitution of cement by steel slag had compressive strengths equivalent to those of the reference at the age of 28 days, but at 90 days, it surpassed the same by approximately 10%.

Yang et al. [48] reported that steel slag powders added to the Magnesium Potassium Phosphate Cement (MKPC) paste can significantly improve the samples' early mechanical strength. For a 10% steel slag powders addition, the compressive strengths of 5-h and 1-day were 17% and 32% higher than those of the reference sample, respectively. Similarly, for an addition of 20% steel slag powder, the compressive strengths of 5-h and 1-day were almost 5% and 30% higher than the reference paste, respectively, and at 60-day, it was 8% higher. The improvement in the particle size distribution, the filling and active effect obtained using steel slag powders, and a reduction in the water/cement ratio of MKPC paste for the same fluidity helped decrease the porosity and increase the compressive strength of the hardened paste. Meanwhile, the RO phases in the coarse particles of steel slag powders can be used as micro aggregates in hardened MKPC samples, increasing the compressive strength [48]. All of these factors contributed to the greater compressive strength of MKPC samples containing steel slag powder.

2.5.2 Mechanical performance of steel slag aggregates

Mechanical strength is considered the most important structural concrete property; thus, the relationship between concrete components and their compressive strength has been investigated in several studies [187,222–224]. Aggregates are materials of great importance and directly affect concretes and mortars' compressive strength [186,187,225].

Beshr et al. [186] compared the properties of concrete produced with four different types of aggregates: calcareous limestone, dolomitic limestone, quartzitic limestone, and steel slag. The highest compressive strength was measured in the concrete specimens prepared with the steel slag as coarse aggregates, while the lowest compressive strength was noted in concrete specimens prepared with calcareous limestone aggregates. After 28 days of curing, the compressive strength of concrete with steel slag was the highest, surpassing calcareous,

dolomitic, and quartzitic limestone in 25.5%, 20% and 15%, respectively. The strength and mineralogic composition of coarse aggregates can control the maximum concrete strength, especially in high-strength concrete [186].

Qasrawi [226] reported that the use of steel slag with a relatively high content of Fe_2O_3 as a coarse aggregate enhanced the compressive and flexural strength of concrete. He also showed that the steel slag concrete's strength development performed much better than conventional concrete, resulting in higher strength at later ages. In another study, Qasrawi [188] investigated the use of steel slag coarse aggregate as partial replacement of natural aggregate and observed increases in compressive strength depending on the substitution ratio used. The increase in strength can reach a value of about 20% from the conventional concrete when the steel slag aggregate replaces all the natural aggregate.

Pang et al. [52] researched concrete with carbonated slag aggregate (CSA). The untreated CSA was sieved into fractions from 2.36 to 18.0 mm sizes as coarse aggregates, carbonizes bricks produced with steel slag powder were crushed and sieved into fractions from 0.3 to 4.75 mm sizes as fine aggregates after carbonation. The results showed that the use of CSA completely replacing natural aggregates could increase the compressive strength of concrete by 20% at 28 days, and the concretes containing carbonated slag aggregate exceeded the strength of concretes containing slag aggregate without treatment at 60 days.

Franco de Carvalho et al. [46] obtained relevant results in concretes' performance containing fine slag aggregates that showed an increase in compressive strength of 16.4% compared to the reference concrete at 28 days. The higher strength of the concrete containing steel slag aggregates can be attributed to the higher angularity of BOFS aggregates, which enhances the interaction between the aggregate and the cementitious matrix [46,52,188].

Saxena and Tembhurkar [53] investigated the replaced of natural coarse aggregate with steel slag aggregate on the fresh and hardened properties of concrete, and it was found that 50% of replacement of basalt aggregate with steel slag aggregate resulted in improvements in compressive strength, flexural strength, and modulus of elasticity of concrete by 33%, 9.8% and 22% at the age of 28 days, respectively.

However, although most studies have reported increases in the mechanical strength of cement-based composites made with steel slag aggregates compared to conventional aggregates due to improvements in particle shape, better surface texture, phase composition, and stronger interfacial transition zone (ITZ), other studies have attested to a reduction in mechanical

strength, due to the physical and chemical properties of slag, a weak ITZ, or even the high substitution content of conventional aggregates [96,188,203,205,227–229].

In studies conducted by Brand and Roesler [203], the concrete's compressive strength with BOF slag aggregates was statistically lower than the control (crushed dolomite) compressive strength, while the concrete with EAF slag aggregates was statistically the same as the control sample. Both concretes with steel furnace slag aggregates had statistically lower split tensile strengths than the control. In this study, the EAF slag aggregates were more angular and had a rougher surface texture than the BOF slag aggregates, leading to better mechanical interlock with the cement paste, thus leading to the increased compressive strength for concrete with EAF slag aggregates.

In another study, Brand and Roesler [227] examined the microstructure of three different steel furnace slag (BOFS, EAFS, and EAF/LMF) aggregates and their influence on the interfacial transition zone (ITZ) in mortars. The ITZ was more porous for the BOFS and EAF/LMF slag mortars, while the EAFS mortar had similar porosity to the dolomite mortar. A more porous ITZ facilitates the crack initiation and propagation and may reduce hardened properties such as strength. The potential for the chemical reaction between SFS aggregate and cement paste can increase adhesion and improve mechanical performance. However, some SFS aggregates may result in a larger or more porous ITZ and negatively affect mechanical behavior.

2.5.3 Economic viability

The use of steel slag, both as an aggregate and supplementary cementitious material, has proven to be a viable alternative for managing solid waste and reducing the consumption of natural resources and CO_2 emissions. In studies by Zhang et al. [29], high-performance cement mixed with BOFS was prepared, comminuting the material with larger particle size, recovering part of the metallic fraction, and using the fine fraction to prepare the pastes next to the cement. A comparative study of cost/benefit analyzes was carried out, and it was concluded that a great economic benefit can be obtained from this approach. Besides, resources and energy conservation and the reduction of CO_2 emissions can also be achieved [29].

Gonçalves et al. [230] evaluated the economic viability of a steel slag processing plant. For this, they used simulation using the Monte Carlo method, in which it is possible to determine the risks and uncertainties inherent to the process. The simulation results indicated the economic viability of the slag processing project with 98% certainty and an estimated profit

of around 42%. Also, the use of recycled aggregates can significantly reduce construction costs by 40% to 50% when purchasing aggregates [230].

2.5.4 Durability

The durability of cement-based composites is an important parameter to ensure the applicability of recycled aggregates, such as steel slag. Thus, some authors in the literature studied the pore system and deleterious agents' effect in the steel slag matrices.

2.5.4.1 Chloride Attack

Chloride ions are found in the marine environment (atmosphere and seawater) and in chemical de-icing. These ions penetrate reinforced concrete structures, leading to concrete rebars' depassivation process and further corrosion [231,232]. In this regard, many articles evaluated the chloride ions permeability in composites produced with steel slag (as aggregates or powder). Usually, the authors use a rapid chloride permeability test (mostly ASTM C1202 [233]) since these procedures can afford information about the connection of pores being helpful to comprehend the effects of steel slag powders in the pore system of cement-based composites.

In general, the replacement of Portland cement with steel slag powder negatively affect the chloride permeability as higher contents of steel slag powder resulted in more permeable concretes [47,49,50,234]. The authors attribute this decrease in the chloride permeability resistance to the steel slag powder's low reactivity, which probably contributes to higher porosity and connectivity between the pores [50]. Concretes produced with steel slag powders demanded higher curing time to achieve similar results comparing to the Portland cement concretes. In fact, such concrete specimens tested with older ages (90 days) resulted in lower permeability, reducing the difference compared to the reference concrete [47,49]. Wang et al. [50] evaluated the resistance to chloride permeability in three different ages (28, 90 and 360 days) of concretes produced with steel slag powder (two different water contents, water-cement ratio: 0.35 and 0.50). The results showed that permeability was reduced with the age increment. At 28 days, the authors classified the concrete with higher water content (w/c = 0.5) as high permeability, while at 360 days, the classification changed to low permeability. This is a possible indication of the low hydration rate of the steel slag powder. Despite the influence of the low reactivity in this result, Han et al. [49] stand that the high content of Fe could also contribute to this negative effect since the rapid chloride permeability test involves a charge

passing through a saturated concrete, showing the importance of the fine metal recovery processes. Some authors propose using composite mineral admixtures to reduce the negative effect of steel slag (blends of steel slag powder with silica fume or ground granulated blast furnace slag) that lead to a faster supplementary cementitious activity that contributes to low permeabilities at earlier ages [45,198]. The effects of the steel slag powder in converting the ion chloride into stable forms, as Friedel salts, were not evaluated in any article.

Regarding the chloride permeability in cement-based composites fabricated with steel slag aggregates, the literature presents fewer results. Arribas et al. [235] and Biskri et al. [182] studied the performance of concretes produced with full replacement of coarse aggregate for steel slag and a partial one for the fine fraction. Biskri et al. [182] noticed higher values for the chloride ion diffusion coefficient in the steel slag concretes compared to the reference one and attributed this behavior to the higher porosity of the aggregates. The authors classified the steel slag concrete under chloride penetration test as moderate, not a bad performance analyzed isolated. Despite the corrosion effects of chloride ions penetrations, accelerated corrosion tests in steel slag concretes are rare. Arribas et al. [235] applied a wetting-dry methodology to simulate the tidal zone with a maximum exposure time of 230 cycles of 24 hours. The authors analyzed the chloride concentration in the section and the corrosion potential. The results indicated that the steel slag concrete presents a similar behavior compared to the reference one. Both had a chloride concentration higher than the threshold value at the 45 mm depth. Although the steel slag concrete was more susceptible to corrosion compared to the reference one when tested for the corrosion potential, the presence of metallic materials (as Fe) can negatively influence the resistivity of the concretes.

To the authors' knowledge, few articles evaluated steel slag powder or aggregates in real exposure conditions. Santamaria et al. [114] exposed concretes produced with electric arc furnace steel slag aggregates (replacement of 100% for the coarse fraction and 64% for the fine fraction) in a tidal zone for two periods: a small (1 year) and a long (5 years). For the analysis of small-time, the specimens' chloride concentration profile was tested and noticed that those produced with steel slag aggregate presented penetration rate similar to the reference one (35 mm), both under the usual cover thickness for the marine environment of 40-60 mm. Additionally, the incorporation of steel slag reduced the potential of rebar corrosion evaluated in the accelerated electrochemical corrosion test, a result contradictory to the study of Arribas et al. [235]. For the long-time analysis (five years), the penetration of chloride ions in steel slag

concrete was smaller than the reference one. Thus, despite the recognized contribution of steel slag aggregate in mechanical performance, its durability performance is still uncertain.

2.5.4.2 Carbonation

The carbonation of concretes is a durability parameter of increasing interest. The formation of calcium, sodium, and potassium carbonate due to the penetration of carbon dioxide present in the atmosphere in the concrete's pores causes detachment of the concrete, causing corrosion of the steel rebars.

Wang et al. [50] pointed out that concretes with partial replacement (45%) of cement by steel slag have good resistance to carbonation with three or more days of curing. As the initial curing period increases, the permeability of the concrete decreases, which reduces the diffusion of CO_2, in addition to the considerable reduction of calcium hydroxide from the replacement of conventional aggregates with steel slag aggregates [50].

Mo et al. [51] showed that concretes with up to 100% substitution cured in a carbonation chamber (98% humidity and 23ºC for 24 ± 2h) for (1, 3, and 14) days presented compressive strengths up to five-fold higher and smaller carbonation depths compared to the control sample. According to the authors, calcite was the main product found in steel slag concrete under CO_2 curing; this mineral is responsible for consuming many Ca-phases, such as brownmillerite and calcium silicates in Portland cement. Besides, the accelerated curing of CO_2 reduced the content of periclase; thus, the steel slag could potentially be used as fine and coarse aggregates in concrete [51].

When using steel slag as a powder to replace cement, the performance under carbonation was similar to the reference concrete, as observed by Liu and Wang [198]. These authors stated that a mixture containing steel slag powder had a lower calcium hydroxide content and was denser; thus, the diffusion of carbon dioxide in the concrete was more difficult.

Andrade [113] studied the carbonation of concretes with the full replacement of conventional aggregates by BOFS and EAFS aggregates. In addition to greater compressive strengths at 28 days, slag concretes showed decreases in carbonation depths of 59 - 83.3%, on average, when compared to concrete produced with conventional aggregate. This fact is attributed to the mixture's greater compactness in the hardened state, resulting in a less permeable matrix.

2.5.4.3. Other parameters

Several aspects influence the use of concrete and directly interfere in its performance, such as physical, chemical, and mineralogical features of the materials [50,182,236]. Also, mixing protocols and the mix design are essential to achieve satisfactory durability performance [46,191,205].

The presence of sulfates in steel slags implies the formation of expansible products (crystallization of ettringite), resulting from the hydration of free calcium and magnesium oxides and low resistance (plaster) [66]**.** Thus, it is important to evaluate the potential for the expansion of concrete containing steel slag aggregates.

Santamaría et al. [114] performed autoclave accelerated aging tests on concretes with EAFS, and their results were favorable to the use of this material. Franco de Carvalho et al. [196] also evaluated the expandability of concretes containing BOFS in partial replacement of Portland cement (25%), and they observed the potential for application of this material since its expansibility was less than 0.15%.

The concrete's pore structure and permeability determine its performance in terms of durability [50,237]. The research of Jiang et al. [45] indicates that the use of BOFS fines enhances the concrete porosity compared to a concrete that only uses cement, contributing to the increase of drying shrinkage as BOFS content increases in the mix. This factor may imply greater carbonation and penetration of chloride ions [45,50]. The porosity of EAFS is also an obstacle to making concrete resistant to freezing [205].

The powders and aggregates' grain size and distribution directly interfere with connectivity and pore structure [46,238]. Xialou et al. [239] observed that the presence of steel slag powder in the concrete studied reduced the shrinkage by drying and increasing the abrasion resistance compared to mixtures without the material. In contrast, Monosi et al. [125] addressed a study of durability through chemical and microstructural analysis that shows that the replacement of natural aggregates by EAFS aggregates does not affect the shrinkage due to the drying of cement mixtures. The use of BOFS as aggregates in concretes provides similar performance to the concrete with natural aggregates due to durability parameters, such as carbonation, electrical resistivity, and pore structure [238].

The study by Saxena e Tembhurkar [53] shows that the use of EAFS to replace natural aggregates improves the durability parameters and density of the microstructure. However, Palankar et al. [191] evaluated the resistance to acids and sulfates of alkali-activated concretes

and observed that concretes containing BOFS aggregates had lower resistances than those with natural aggregates.

2.6 Conclusions

The main constituents of steel slag are CaO (25.08-57.44%), Fe/Fe_2O_3 (0.48-38.5%), SiO_2 (7.75-36.33%), Al_2O_3 (0.33-12.2%), and MgO (1.93-10.46%). Due to the high content of dense oxides, the specific gravity of steel slag is higher than natural aggregates by around 30%. Slow cooling is directly related to the high amount of CaO in the slag and its basicity. Also, the high content of free CaO and iron oxide produces a material with high expansion potential. Fe in the steel slag is usually found as steel (Fe), iron oxides (FeO, Fe_2O_3, Fe_3O_4) and iron-bearing minerals, and the iron content can represent a problem in the production of clinker in the cement industry and durability of matrices. However, iron can be recovered by crushing, grinding, screening, and magnetic separation.

Typically, steel slag aggregates have a greater specific surface, with high angularity and rough surface texture, that can positively contribute to the performance of cementitious matrices, implying greater durability.

The grindability of the non-active components (e.g., RO-phase and Fe_3O_4) of steel slag is very difficult because of the high metallic iron. The presence of mineralogical phases with high Mohs values contributes to low grindability and makes the process more expensive. Also, the presence of metallic iron increases the ductility of the material, reducing the grinding process.

Despite the poor hydraulic properties due to low quantities of mineralogical phases such as alite, larnite, brownmillerite, and ferrite, some activation techniques (mechanical, thermal, and chemical) can improve their cementitious activity.

Steel slag powder can significantly improve the samples' mechanical strength because of their cementing properties, improvement in the particle size distribution obtained, and a reduction in the water/cement ratio for the same fluidity. Moreover, the RO phases in the coarse particles of steel slag powders can be used as micro aggregates and increase the compressive strength. As aggregate in cementitious matrices, the steel slag could increase the compressive strength up to 20% by replacing all-natural aggregates.

Partial replacement of Portland cement by steel slag powder reportedly increases the porosity in the short term, reducing in later ages. Thus, under chloride attack and carbonation

tests, the performance is worst to similar in the short term and similar to high in the long term. The higher porosity of the steel slag aggregates is related to the worst performance in the resistance to chloride attack, but lower carbonation depths have been reported; however, the contribution of steel slag aggregate in the durability performance of cement-based composites is still uncertain. Expansibility has been a great concern, but mitigating measures have brought the results of soundness tests within acceptable limits for usual replacement rates. Acting in the mix design is a promising measure to improve the durability performance of steel slag concretes.

Acknowledgments

This study was financed in part by the Coordenção de Aperfeiçoamento de Pessoal de Nível Superior – Brasil (CAPES) – Finance code 001. The authors also acknowledge the support provided by the Fundação de Amparo à Pesquisa do Estado de Minas Gerais (FAPEMIG), Conselho Nacional de Desenvolvimento Científico e Tecnológico (CNPq), Federal University of Viçosa (UFV) and Federal University of Ouro Preto (UFOP). Thanks are also due to the Brazilian research groups SICon-CNPq/ UFV and RECICLOS-CNPq/UFOP for the infrastructure and collaboration.

Conflict of Interest: The authors declare that they have no conflict of interest.

References

[1] V.M. John, Concreto Sustentável, in: G.C. Isaia (Ed.), Concreto Ciência e Tecnol., 1st ed., IBRACON, São Paulo, 2011: pp. 1842–69.

[2] X. Xu, Y. Wang, L. Tao, Comprehensive evaluation of sustainable development of regional construction industry in China, J. Clean. Prod. 211 (2019) 1078–1087. https://doi.org/10.1016/j.jclepro.2018.11.248.

[3] N.D. Oikonomou, Recycled concrete aggregates, Cem. Concr. Compos. 27 (2005) 315–318. https://doi.org/10.1016/j.cemconcomp.2004.02.020.

[4] M. Yeheyis, K. Hewage, M.S. Alam, C. Eskicioglu, R. Sadiq, An overview of construction and demolition waste management in Canada: A lifecycle analysis approach to sustainability, Clean Technol. Environ. Policy. 15 (2013) 81–91. https://doi.org/10.1007/s10098-012-0481-6.

[5] J. Xu, Y. Deng, Y. Shi, Y. Huang, A bi-level optimization approach for sustainable development and carbon emissions reduction towards construction materials industry: a case study from China, Sustain. Cities Soc. 53 (2020) 101828. https://doi.org/10.1016/j.scs.2019.101828.

[6] I. Zabalza Bribián, A. Valero Capilla, A. Aranda Usón, Life cycle assessment of building materials: Comparative analysis of energy and environmental impacts and evaluation of the eco-efficiency improvement potential, Build. Environ. 46 (2011) 1133–1140. https://doi.org/10.1016/j.buildenv.2010.12.002.
[7] M. Honic, I. Kovacic, H. Rechberger, Improving the recycling potential of buildings through Material Passports (MP): An Austrian case study, J. Clean. Prod. 217 (2019) 787–797. https://doi.org/10.1016/j.jclepro.2019.01.212.
[8] Y. Kulaif, SUMÁRIO MINERAL - Departamento Nacional de Produção Mineral, Sumário Miner. 35 (2015) 135.
[9] OECD, Material Resources, Productivity and the Environment, OECD Green, OECD Publishing, Paris, 2015. https://doi.org/10.1787/9789264190504-en.
[10] UNEP, Worldwide Extraction of Materials Triples in Four Decades, Intensifying Climate Change and Air Pollution, 20 July 2016. (2016). https://www.unenvironment.org/news-and-stories/press-release/worldwide-extraction-materials-triples-four-decades-intensifying (accessed November 8, 2019).
[11] G.L.F. Benachio, M. do C.D. Freitas, S.F. Tavares, Circular economy in the construction industry: A systematic literature review, J. Clean. Prod. 260 (2020) 121046. https://doi.org/10.1016/j.jclepro.2020.121046.
[12] Y. Miyatake, Technology development and sustainable construction, J. Manag. Eng. 12 (1996) 23–27.
[13] R. Duffell, Toward the environment and sustainability ethic in engineering education and practice, J. Prof. Issues Eng. Educ. Pract. 124 (1998) 78–90. https://doi.org/10.1061/(ASCE)1052-3928(1998)124:3(78).
[14] J. Bröchner, G.K.I. Ang, G. Fredriksson, Sustainability and the performance concept: Encouraging innovative environmental technology in construction, Build. Res. Inf. 27 (1999) 367–372. https://doi.org/10.1080/096132199369192.
[15] P.J.M. Mehta, P. K.; Monteiro, Concreto: Microestrutura, Propriedades e Materiais, 2nd ed., IBRACON, São Paulo, 2014.
[16] A.M. Neville, Propriedades do Concreto, 5th ed., Bookman, Porto Alegre, 2016.
[17] ANEPAC, O mercado de agregados no Brasil, Associação Nacional das Entidades de Produtores de Agregados para Construção, São Paulo, 2015. http://www.anepac.org.br/agregados/mercado/item/8-mercado-de-agregados-no-brasil.
[18] USGS, Construction sand and gravel data sheet, in: Miner. Commod. Summ. 2020, U.S. Geological Survey, 2020. https://doi.org/10.1130/REG1-p187.
[19] UEPG, European Aggregates Association: Annual Review 2019-2020, European Aggregates Association, 2020. https://doi.org/10.1111/anae.13788.
[20] Aggregates Business, China aggregates demand stays on a high, (2019). https://www.aggbusiness.com/feature/china-aggregates-demand-stays-high (accessed August 14, 2020).
[21] WorldSteel, 2020 World Steel in Figures, World Steel Association, 2020. http://www.worldsteel.org/wsif.php.
[22] IAB, Anuário Estatístico 2020, Instituto Aço Brasil, Rio de Janeiro, 2020.
[23] WorldSteel, Steel industry co-products, World Steel Association, 2020. https://doi.org/10.1201/9781420003840.sec2.
[24] CNI, A industria do aço no Brasil., Confederação Nacional da Indústria, Brasília, 2017.
[25] D.H. Shen, C.M. Wu, J.C. Du, Laboratory investigation of basic oxygen furnace slag for substitution of aggregate in porous asphalt mixture, Constr. Build. Mater. 23 (2009) 453–461. https://doi.org/10.1016/j.conbuildmat.2007.11.001.
[26] A. López-Díaz, R. Ochoa-Díaz, G.E. Grimaldo-León, Use of BOF slag and blast furnace dust in asphalt concrete: An alternative for the construction of pavements,

DYNA. 85 (2018) 24–30. https://doi.org/10.15446/dyna.v85n206.70404.
[27] S.H. Chen, D.F. Lin, H.L. Luo, Z.Y. Lin, Application of reclaimed basic oxygen furnace slag asphalt pavement in road base aggregate, Constr. Build. Mater. 157 (2017) 647–653. https://doi.org/10.1016/j.conbuildmat.2017.09.136.
[28] P. Xue, A. Xu, D. He, Q. Yang, G. Liu, F. Engström, B. Björkman, Research on the sintering process and characteristics of belite sulphoaluminate cement produced by BOF slag, Constr. Build. Mater. 122 (2016) 567–576. https://doi.org/10.1016/j.conbuildmat.2016.06.098.
[29] T. Zhang, Q. Yu, J. Wei, J. Li, P. Zhang, Preparation of high performance blended cements and reclamation of iron concentrate from basic oxygen furnace steel slag, Resour. Conserv. Recycl. 56 (2011) 48–55. https://doi.org/10.1016/j.resconrec.2011.09.003.
[30] J.M. Franco de Carvalho, P.A.M. Campos, K. Defáveri, G.J. Brigolini, L.G. Pedroti, R.A.F. Peixoto, Low environmental impact cement produced entirely from industrial and mining waste, J. Mater. Civ. Eng. 31 (2019). https://doi.org/10.1061/(ASCE)MT.1943-5533.0002617.
[31] S.Z. Carvalho, F. Vernilli, B. Almeida, M.D. Oliveira, S.N. Silva, Reducing environmental impacts: The use of basic oxygen furnace slag in portland cement, J. Clean. Prod. 172 (2018) 385–390. https://doi.org/10.1016/j.jclepro.2017.10.130.
[32] D.H. Diniz, J.M.F. de Carvalho, J.C. Mendes, R.A.F. Peixoto, Blast oxygen furnace slag as chemical soil stabilizer for use in roads, J. Mater. Civ. Eng. 29 (2017) 3–9. https://doi.org/10.1061/(ASCE)MT.1943-5533.0001969.
[33] V. Ortega-López, J.M. Manso, I.I. Cuesta, J.J. González, The long-term accelerated expansion of various ladle-furnace basic slags and their soil-stabilization applications, Constr. Build. Mater. 68 (2014) 455–464. https://doi.org/10.1016/j.conbuildmat.2014.07.023.
[34] I. Reijonen, H. Hartikainen, Risk assessment of the utilization of basic oxygen furnace slag (BOFS) as soil liming material: Oxidation risk and the chemical bioavailability of chromium species, Environ. Technol. Innov. 11 (2018) 358–370. https://doi.org/10.1016/j.eti.2018.05.004.
[35] M.J. Da Silva, B.P. De Souza, J.C. Mendes, G.J.S. Brigolini, S.N. Da Silva, R.A.F. Peixoto, Feasibility study of steel slag aggregates in precast concrete pavers, ACI Mater. J. 113 (2016) 439–446. https://doi.org/10.14359/51688986.
[36] L.C. Franco, J.C. Mendes, L.C.B. Costa, R.R. Pira, R.A.F. Peixoto, Design and thermal evaluation of a social housing model conceived with bioclimatic principles and recycled aggregates, Sustain. Cities Soc. 51 (2019) 101725. https://doi.org/10.1016/j.scs.2019.101725.
[37] A.C.P. Matias, H.D. Andrade, J.M.F. de Carvalho, G.J. Brigolini, R.A.F. Peixoto, Utilização de Escórias de Aciaria em Argamassas Sustentáveis para Assentamento e Revestimento de Alvenarias - Desempenho e Sustentabilidade, in: 23º CBECiMat - Congresso Brasileiro de Engenharia e Ciência dos Materiais, Foz do Iguaçu, 2018: p. 12.
[38] B. Tripathi, S. Chaudhary, Performance based evaluation of ISF slag as a substitute of natural sand in concrete, J. Clean. Prod. 112 (2016) 672–683. https://doi.org/10.1016/j.jclepro.2015.07.120.
[39] A. Yousefloo, R. Babazadeh, Designing an integrated municipal solid waste management network: A case study, J. Clean. Prod. (in press) (2020). https://doi.org/10.1016/j.jclepro.2019.118824.
[40] S.H. Ghaffar, M. Burman, N. Braimah, Pathways to circular construction: An integrated management of construction and demolition waste for resource recovery, J.

Clean. Prod. 244 (2020) 118710. https://doi.org/10.1016/j.jclepro.2019.118710.
[41] WorldSteel, Steel industry co-products: worldsteel position paper., (2018) 6. https://www.worldsteel.org/en/dam/jcr:2941f748-b906-4952-8b11-03ffee835b39/Co-products_position_paper_vfinal.pdf.
[42] WorldSteel, Fact Sheet: Climate change mitigation., Worldsteel Assoc. (2019). https://doi.org/10.4018/978-1-5225-0803-8.ch003.
[43] WorldSteel, Steel's contribution to a low carbon future and climate relisient societies - Worldsteel position paper, (2019) 6.
[44] L. Mo, S. Yang, B. Huang, L. Xu, S. Feng, M. Deng, Preparation, microstructure and property of carbonated artificial steel slag aggregate used in concrete, Cem. Concr. Compos. 113 (2020) 103715. https://doi.org/10.1016/j.cemconcomp.2020.103715.
[45] Y. Jiang, T.C. Ling, C. Shi, S.Y. Pan, Characteristics of steel slags and their use in cement and concrete—A review, Resour. Conserv. Recycl. 136 (2018) 187–197. https://doi.org/10.1016/j.resconrec.2018.04.023.
[46] J.M. Franco de Carvalho, T.V. de Melo, W.C. Fontes, J.O. dos S. Batista, G.J. Brigolini, R.A.F. Peixoto, More eco-efficient concrete: An approach on optimization in the production and use of waste-based supplementary cementing materials, Constr. Build. Mater. 206 (2019) 397–409. https://doi.org/10.1016/j.conbuildmat.2019.02.054.
[47] Z. Pan, J. Zhou, X. Jiang, Y. Xu, R. Jin, J. Ma, Y. Zhuang, Z. Diao, S. Zhang, Q. Si, W. Chen, Investigating the effects of steel slag powder on the properties of self-compacting concrete with recycled aggregates, Constr. Build. Mater. 200 (2019) 570–577. https://doi.org/10.1016/j.conbuildmat.2018.12.150.
[48] J. Yang, J. Lu, Q. Wu, M.F. Xia, X. Li, Influence of steel slag powders on the properties of MKPC paste, Constr. Build. Mater. 159 (2018) 137–146. https://doi.org/10.1016/j.conbuildmat.2017.10.081.
[49] X. Han, J. Feng, Y. Shao, R. Hong, Influence of a steel slag powder-ground fly ash composite supplementary cementitious material on the chloride and sulphate resistance of mass concrete, Powder Technol. 370 (2020) 176–183. https://doi.org/10.1016/j.powtec.2020.05.015.
[50] Q. Wang, P. Yan, J. Yang, B. Zhang, Influence of steel slag on mechanical properties and durability of concrete, Constr. Build. Mater. 47 (2013) 1414–1420. https://doi.org/10.1016/j.conbuildmat.2013.06.044.
[51] L. Mo, F. Zhang, M. Deng, F. Jin, A. Al-Tabbaa, A. Wang, Accelerated carbonation and performance of concrete made with steel slag as binding materials and aggregates, Cem. Concr. Compos. 83 (2017) 138–145. https://doi.org/10.1016/j.cemconcomp.2017.07.018.
[52] B. Pang, Z. Zhou, H. Xu, Utilization of carbonated and granulated steel slag aggregate in concrete, Constr. Build. Mater. 84 (2015) 454–467. https://doi.org/10.1016/j.conbuildmat.2015.03.008.
[53] S. Saxena, A.R. Tembhurkar, Impact of use of steel slag as coarse aggregate and wastewater on fresh and hardened properties of concrete, Constr. Build. Mater. 165 (2018) 126–137. https://doi.org/10.1016/j.conbuildmat.2018.01.030.
[54] M. Bodor, R.M. Santos, G. Cristea, M. Salman, Ö. Cizer, R.I. Iacobescu, Y.W. Chiang, K. Van Balen, M. Vlad, T. Van Gerven, Laboratory investigation of carbonated BOF slag used as partial replacement of natural aggregate in cement mortars, Cem. Concr. Compos. 65 (2016) 55–66. https://doi.org/10.1016/j.cemconcomp.2015.10.002.
[55] IEA, Tracking Industrial Energy Efficiency and CO2 Emissions, International Energy Agency, Paris, 2007. https://doi.org/10.1007/978-3-642-29446-4_14.
[56] L. de M. Ozorio, C. de L. Bastian-Pinto, T.K.N. Baidya, L.E.T. Brandão, Investment decision in integrated steel plants under uncertainty, Int. Rev. Financ. Anal. 27 (2013)

55–64. https://doi.org/10.1016/j.irfa.2012.06.003.
[57] WorldSteel, About Steel, (2019). https://www.worldsteel.org/about-steel.html (accessed November 8, 2019).
[58] L. V. Fisher, A.R. Barron, The recycling and reuse of steelmaking slags — A review, Resour. Conserv. Recycl. 146 (2019) 244–255. https://doi.org/10.1016/j.resconrec.2019.03.010.
[59] E. Özbay, M. Erdemir, H.I. Durmuş, Utilization and efficiency of ground granulated blast furnace slag on concrete properties - A review, Constr. Build. Mater. 105 (2016) 423–434. https://doi.org/10.1016/j.conbuildmat.2015.12.153.
[60] C. Kambole, P. Paige-Green, W.K. Kupolati, J.M. Ndambuki, A. Adeboje, Comparison of technical and short-term environmental characteristics of weathered and fresh blast furnace slag aggregates for road base applications in South Africa, Case Stud. Constr. Mater. 11 (2019) e00239. https://doi.org/10.1016/j.cscm.2019.e00239.
[61] R.K. Patra, B.B. Mukharjee, Influence of incorporation of granulated blast furnace slag as replacement of fine aggregate on properties of concrete, J. Clean. Prod. 165 (2017) 468–476. https://doi.org/10.1016/j.jclepro.2017.07.125.
[62] WBCSD, Total mineral components used to produce Portland cement, (2016). https://www.wbcsdcement.org/GNR-2016/world/GNR-Indicator_12TGW-world.html (accessed November 9, 2019).
[63] D. Wang, J. Chang, W.S. Ansari, The effects of carbonation and hydration on the mineralogy and microstructure of basic oxygen furnace slag products, J. CO2 Util. 34 (2019) 87–98. https://doi.org/10.1016/j.jcou.2019.06.001.
[64] N. Zhang, L. Wu, X. Liu, Y. Zhang, Structural characteristics and cementitious behavior of basic oxygen furnace slag mud and electric arc furnace slag, Constr. Build. Mater. 219 (2019) 11–18. https://doi.org/10.1016/j.conbuildmat.2019.05.156.
[65] C.S. Neto, Agregados Naturais, Britados e Artificiais para Concreto, in: G.C. Isaia (Ed.), Concreto Ciência e Tecnol., 1st ed., IBRACON, São Paulo, 2011: pp. 233–60.
[66] M. de O. Polese, G.L. Carreiro, M.G. da Silva, M.R. Silva, Caracterização microestrutural da escória de aciaria, Matéria (Rio Janeiro). 11 (2006) 442–452. https://doi.org/10.1590/s1517-70762006000400011.
[67] A.C.C. Giocondo, Uso do resíduo de escória de aciaria em sistema construtivo de alvenaria estrutural, University of São Paulo (in Portuguese), São Carlos, 2014.
[68] D.R.R. Gonçalves, Análise da viabilidade econômica via simulação Monte Carlo para utilização da escória de aciaria como agregado na fabricação de pré-fabricados para a construção civil - ecoblocos, University of Ouro Preto (in Portuguese), 2015.
[69] B. Park, E.J. Moon, Y.C. Choi, Investigation of microstructure and mechanical performance of carbon-capture binder using AOD stainless steel slag, Constr. Build. Mater. 242 (2020) 118174. https://doi.org/10.1016/j.conbuildmat.2020.118174.
[70] T. Gupta, S.N. Sachdeva, Laboratory investigation and modeling of concrete pavements containing AOD steel slag, Cem. Concr. Res. 124 (2019) 105808. https://doi.org/10.1016/j.cemconres.2019.105808.
[71] M. Salman, Ö. Cizer, Y. Pontikes, R. Snellings, J. Dijkman, B. Sels, L. Vandewalle, B. Blanpain, K. Van Balen, Alkali Activation of AOD Stainless Steel Slag Under Steam Curing Conditions €, 3074 (2015) 3062–3074. https://doi.org/10.1111/jace.13776.
[72] Y.J. Wang, Y.N. Zeng, J.G. Li, Y.Z. Zhang, Y.J. Zhang, Q.Z. Zhao, Carbonation of argon oxygen decarburization stainless steel slag and its effect on chromium leachability, J. Clean. Prod. 256 (2020) 120377. https://doi.org/10.1016/j.jclepro.2020.120377.
[73] J. Li, B. Liu, Y. Zeng, Z. Wang, Chemosphere Mineralogical determination and geo-chemical modeling of chromium release from AOD slag : Distribution and leachability

aspects, Chemosphere. 167 (2017) 360–366. https://doi.org/10.1016/j.chemosphere.2016.10.020.
[74] J. Li, B. Liu, Y. Zeng, Z. Wang, Z. Gao, Maximum availability and mineralogical control of chromium released from AOD slag, Environ. Monit. Assess. 189 (2017). https://doi.org/10.1007/s10661-017-5843-4.
[75] J.H. Park, S.H. Kim, R.D. Delaune, B.H. Kang, S.W. Kang, J.S. Cho, Y.S. Ok, D.C. Seo, Enhancement of phosphorus removal with near-neutral pH utilizing steel and ferronickel slags for application of constructed wetlands, Ecol. Eng. 95 (2016) 612–621. https://doi.org/10.1016/j.ecoleng.2016.06.052.
[76] H.Y. Wang, K.W. Chen, A study of the engineering properties of CLSM with a new type of slag, Constr. Build. Mater. 102 (2016) 422–427. https://doi.org/10.1016/j.conbuildmat.2015.10.198.
[77] K. Gadja, M. Baune, J. Thoming, Recycling Options for Steel Working Slag and Upcycling Perspectives, Procedia Manuf. 8 (2017) 643–648. https://doi.org/10.1016/j.promfg.2017.02.082.
[78] S.A. Campos, M.F.C. Rafael, A.E.B. Cabral, Evaluation of steel slag of Companhia Siderúrgica do Pecém replacing fine aggregate on mortars, Procedia Struct. Integr. 11 (2018) 145–152. https://doi.org/10.1016/j.prostr.2018.11.020.
[79] J. Setién, D. Hernández, J.J. González, Characterization of ladle furnace basic slag for use as a construction material, Constr. Build. Mater. 23 (2009) 1788–1794. https://doi.org/10.1016/j.conbuildmat.2008.10.003.
[80] A. Radenović, J. Malina, T. Sofilić, Characterization of ladle furnace slag from carbon steel production as a potential adsorbent, Adv. Mater. Sci. Eng. (2013) 6. https://doi.org/10.1155/2013/198240.
[81] T. Herrero, I.J. Vegas, A. Santamaría, J.T. San-José, M. Skaf, Effect of high-alumina ladle furnace slag as cement substitution in masonry mortars, Constr. Build. Mater. 123 (2016) 404–413. https://doi.org/10.1016/j.conbuildmat.2016.07.014.
[82] C. Shi, S. Hu, Cementitious properties of ladle slag fines under autoclave curing conditions, Cem. Concr. Res. 33 (2003) 1851–1856. https://doi.org/10.1016/S0008-8846(03)00211-4.
[83] N.H. Roslan, M. Ismail, Z. Abdul-Majid, S. Ghoreishiamiri, B. Muhammad, Performance of steel slag and steel sludge in concrete, Constr. Build. Mater. 104 (2016) 16–24. https://doi.org/10.1016/j.conbuildmat.2015.12.008.
[84] N.H. Roslan, M. Ismail, N.H.A. Khalid, B. Muhammad, Properties of concrete containing electric arc furnace steel slag and steel sludge, J. Build. Eng. (2019) 25. https://doi.org/10.1016/j.jobe.2019.101060.
[85] A.L.B. Marinho, C.M. Mol Santos, J.M.F. de Carvalho, J.C. Mendes, G.J. Brigolini, R.A.F. Peixoto, Ladle furnace slag as binder for cement-based composites, J. Mater. Civ. Eng. 29 (2017). https://doi.org/10.1061/(ASCE) MT.1943-5533.0002061.
[86] J. Xie, S. Wu, L. Zhang, Y. Xiao, Q. Liu, C. Yang, S. Nie, Material characterization and performance evaluation of asphalt mixture Incorporating basic oxygen furnace slag (BOF) sludge, Constr. Build. Mater. 147 (2017) 362–370. https://doi.org/10.1016/j.conbuildmat.2017.04.131.
[87] IAB, Aço e sustentabilidade, Instituto Aço Brasil, Rio de Janeiro, 2019.
[88] J.L. Calmon, Resíduos Industriais e Agrícolas, in: G.C. Isaia (Ed.), Mater. Construção Civ. e Princípios Ciência e Eng. Mater., 2nd ed., IBRACON, São Paulo, 2010: pp. 1651–87.
[89] C. Shi, Steel slag - Its production, processing, characteristics, and cementitious properties, J. Mater. Civ. Eng. 16 (2004) 230–236. https://doi.org/10.1061/(ASCE)0899-1561(2004)16:3(230).

[90] Q. Wang, P. Yan, Hydration properties of basic oxygen furnace steel slag, Constr. Build. Mater. 24 (2010) 1134–1140. https://doi.org/10.1016/j.conbuildmat.2009.12.028.
[91] T. He, Z. Li, S. Zhao, Z. Zhao, X. Zhao, Effect of reductive component-conditioning materials on the composition, structure, and properties of reconstructed BOF slag, Constr. Build. Mater. 255 (2020) 119269. https://doi.org/10.1016/j.conbuildmat.2020.119269.
[92] R. Palod, S.V. Deo, G.D. Ramtekkar, Effect on mechanical performance, early age shrinkage and electrical resistivity of ternary blended concrete containing blast furnace slag and steel slag, Mater. Today Proc. (2020) 4–9. https://doi.org/10.1016/j.matpr.2020.04.747.
[93] M. Tafesse, H.K. Lee, A.S. Alemu, H.K. Kim, S. Pyo, On the expansive cracking of a cement matrix containing atomized basic oxygen furnace slag with a metallic iron, Constr. Build. Mater. 264 (2020) 119806. https://doi.org/10.1016/j.conbuildmat.2020.119806.
[94] C.A. Cárdenas Balaguera, M.A. Gómez Botero, Characterization of steel slag for the production of chemically bonded phosphate ceramics (CBPC), Constr. Build. Mater. 241 (2020). https://doi.org/10.1016/j.conbuildmat.2020.118138.
[95] Y. Liao, G. Jiang, K. Wang, S. Al, W. Yuan, Effect of steel slag on the hydration and strength development of calcium sulfoaluminate cement, Constr. Build. Mater. 265 (2020) 120301. https://doi.org/10.1016/j.conbuildmat.2020.120301.
[96] J. Liu, B. Yu, Q. Wang, Application of steel slag in cement treated aggregate base course, J. Clean. Prod. 269 (2020) 121733. https://doi.org/10.1016/j.jclepro.2020.121733.
[97] W. Shen, Y. Liu, M. Wu, D. Zhang, X. Du, D. Zhao, G. Xu, B. Zhang, X. Xiong, Ecological carbonated steel slag pervious concrete prepared as a key material of sponge city, J. Clean. Prod. 256 (2020) 120244. https://doi.org/10.1016/j.jclepro.2020.120244.
[98] J. Sun, Z. Zhang, S. Zhuang, W. He, Hydration properties and microstructure characteristics of alkali–activated steel slag, Constr. Build. Mater. 241 (2020). https://doi.org/10.1016/j.conbuildmat.2020.118141.
[99] T. Wen, L. Yang, C. Dang, T. Miki, H. Bai, T. Nagasaka, Effect of basic oxygen furnace slag on succession of the bacterial community and immobilization of various metal ions in acidic contaminated mine soil, J. Hazard. Mater. 388 (2020) 121784. https://doi.org/10.1016/j.jhazmat.2019.121784.
[100] A. Santamaría, V. Ortega-López, M. Skaf, J.A. Chica, J.M. Manso, The study of properties and behavior of self compacting concrete containing Electric Arc Furnace Slag (EAFS) as aggregate, Ain Shams Eng. J. 11 (2020) 231–243. https://doi.org/10.1016/j.asej.2019.10.001.
[101] I. Nikolić, D. Đurović, S. Marković, L. Veselinović, I. Janković-Častvan, V. V. Radmilović, V.R. Radmilović, Alkali activated slag cement doped with Zn-rich electric arc furnace dust, J. Mater. Res. Technol. 9 (2020) 12783–12794. https://doi.org/10.1016/j.jmrt.2020.09.024.
[102] Y. Jiang, M.R. Ahmad, B. Chen, Properties of magnesium phosphate cement containing steel slag powder, Constr. Build. Mater. 195 (2019) 140–147. https://doi.org/10.1016/j.conbuildmat.2018.11.085.
[103] D. Fernández-González, J. Prazuch, I. Ruiz-Bustinza, C. González-Gasca, J. Piñuela-Noval, L.F. Verdeja, The treatment of Basic Oxygen Furnace (BOF) slag with concentrated solar energy, Sol. Energy. 180 (2019) 372–382. https://doi.org/10.1016/j.solener.2019.01.055.
[104] D. Kong, M. Chen, J. Xie, M. Zhao, C. Yang, Geometric characteristics of BOF slag

coarse aggregate and its influence on asphalt concrete, Materials (Basel). 12 (2019). https://doi.org/10.3390/ma12050741.
[105] L. Ma, D. Xu, S. Wang, X. Gu, Expansion inhibition of steel slag in asphalt mixture by a surface water isolation structure, Road Mater. Pavement Des. 0 (2019) 1–15. https://doi.org/10.1080/14680629.2019.1601588.
[106] G. Kang, A.A. Cikmit, T. Tsuchida, H. Honda, Y. sang Kim, Strength development and microstructural characteristics of soft dredged clay stabilized with basic oxygen furnace steel slag, Constr. Build. Mater. 203 (2019) 501–513. https://doi.org/10.1016/j.conbuildmat.2019.01.106.
[107] Z. Wu, Y. Li, J. Zhao, L. Ma, X. Zhang, H. Meng, D. Xu, Thermal effect and kinetic analysis on co-pyrolysis of furnace slag with cellulose from biomass, Energy Procedia. 158 (2019) 440–445. https://doi.org/10.1016/j.egypro.2019.01.129.
[108] M. Ozturk, M.B. Bankir, O.S. Bolukbasi, U.K. Sevim, Alkali activation of electric arc furnace slag: Mechanical properties and micro analyzes, J. Build. Eng. 21 (2019) 97–105. https://doi.org/10.1016/j.jobe.2018.10.005.
[109] B. Pomaro, F. Gramegna, R. Cherubini, V. De Nadal, V. Salomoni, F. Faleschini, Gamma-ray shielding properties of heavyweight concrete with Electric Arc Furnace slag as aggregate: An experimental and numerical study, Constr. Build. Mater. 200 (2019) 188–197. https://doi.org/10.1016/j.conbuildmat.2018.12.098.
[110] H. Guo, S. Yin, Q. Yu, X. Yang, H. Huang, Y. Yang, F. Gao, Iron recovery and active residue production from basic oxygen furnace (BOF) slag for supplementary cementitious materials, Resour. Conserv. Recycl. 129 (2018) 209–218. https://doi.org/10.1016/j.resconrec.2017.10.027.
[111] Y. Wang, L. Wu, Y. Wang, Q. Li, Z. Xiao, Prediction model of long-term chloride diffusion into plain concrete considering the effect of the heterogeneity of materials exposed to marine tidal zone, Constr. Build. Mater. 159 (2018) 297–315. https://doi.org/10.1016/j.conbuildmat.2017.10.083.
[112] J. Liu, R. Guo, Applications of Steel Slag Powder and Steel Slag Aggregate in Ultra-High Performance Concrete, Adv. Civ. Eng. 2018 (2018). https://doi.org/10.1155/2018/1426037.
[113] H.D. Andrade, Carbonatação em Concreto de Escória de Aciaria, Federal University of Ouro Preto (in Portuguese), 2018.
[114] A. Santamaría, A. Orbe, J.T. San José, J.J. González, A study on the durability of structural concrete incorporating electric steelmaking slags, Constr. Build. Mater. 161 (2018) 94–111. https://doi.org/10.1016/j.conbuildmat.2017.11.121.
[115] A. Santamaria, F. Faleschini, G. Giacomello, K. Brunelli, J.-T. San José, C. Pellegrino, M. Pasetto, Dimensional stability of electric arc furnace slag in civil engineering applications, J. Clean. Prod. 205 (2018) 599–609. https://doi.org/10.1016/j.jclepro.2018.09.122.
[116] Y. Biskri, D. Achoura, N. Chelghoum, M. Mouret, Mechanical and durability characteristics of High Performance Concrete containing steel slag and crystalized slag as aggregates, Constr. Build. Mater. 150 (2017) 167–178. https://doi.org/10.1016/j.conbuildmat.2017.05.083.
[117] Y.C. Ding, T.W. Cheng, P.C. Liu, W.H. Lee, Study on the treatment of BOF slag to replace fine aggregate in concrete, Constr. Build. Mater. 146 (2017) 644–651. https://doi.org/10.1016/j.conbuildmat.2017.04.164.
[118] S. Masoudi, S.M. Abtahi, A. Goli, Evaluation of electric arc furnace steel slag coarse aggregate in warm mix asphalt subjected to long-term aging, Constr. Build. Mater. 135 (2017) 260–266. https://doi.org/10.1016/j.conbuildmat.2016.12.177.
[119] M.N.T. Lam, S. Jaritngam, D.H. Le, Roller-compacted concrete pavement made of

Electric Arc Furnace slag aggregate: Mix design and mechanical properties, Constr. Build. Mater. 154 (2017) 482–495. https://doi.org/10.1016/j.conbuildmat.2017.07.240.
[120] H.S. Lee, H.S. Lim, M.A. Ismail, Quantitative evaluation of free CaO in electric furnace slag using the ethylene glycol method, Constr. Build. Mater. 131 (2017) 676–681. https://doi.org/10.1016/j.conbuildmat.2016.11.047.
[121] B.M.C. Silva, A.A. Cunha, J.J. Mendes, R.A.L. Solé, F.L. V. Kruguer, F.G.S. Araújo, Caracterização Tecnológica de Escórias de Aciaria, ABM Week. (2016) 248–255.
[122] L. Qi, J. Liu, Q. Liu, Compound Effect of CaCO3 and CaSO4·2H2O on the Strength of Steel Slag - Cement Binding Materials, Mater. Res. 19 (2016) 269–275. https://doi.org/10.1590/1980-5373-MR-2015-0387.
[123] W. Qiang, S. Mengxiao, Y. Jun, Influence of classified steel slag with particle sizes smaller than 20 μm on the properties of cement and concrete, Constr. Build. Mater. 123 (2016) 601–610. https://doi.org/10.1016/j.conbuildmat.2016.07.042.
[124] B.P. de Souza, W.C. Fontes, J.M.F. de Carvalho, R.M.R. Mol, E.C.P. da Costa, R.A.F. Peixoto, Caracterização físico-química de agregados de escória de aciaria LD pós-processada para concretos sustentáveis, 22º CBECiMat - Congr. Bras. Eng. e Ciência Dos Mater. (2016) 4300–4313. https://doi.org/10.1038/lsa.2017.15.
[125] S. Monosi, M.L. Ruello, D. Sani, Electric arc furnace slag as natural aggregate replacement in concrete production, Cem. Concr. Compos. 66 (2016) 66–72. https://doi.org/10.1016/j.cemconcomp.2015.10.004.
[126] F. Faleschini, K. Brunelli, M.A. Zanini, M. Dabalà, C. Pellegrino, Electric Arc Furnace Slag as Coarse Recycled Aggregate for Concrete Production, J. Sustain. Metall. 2 (2016) 44–50. https://doi.org/10.1007/s40831-015-0029-1.
[127] I.Z. Yildirim, M. Prezzi, Geotechnical properties of fresh and aged basic oxygen furnace steel slag, J. Mater. Civ. Eng. 27 (2015) 1–11. https://doi.org/10.1061/(ASCE)MT.1943-5533.0001310.
[128] I. Arribas, A. Santamaría, E. Ruiz, V. Ortega-López, J.M. Manso, Electric arc furnace slag and its use in hydraulic concrete, Constr. Build. Mater. 90 (2015) 68–79. https://doi.org/10.1016/j.conbuildmat.2015.05.003.
[129] W. Yeih, T.C. Fu, J.J. Chang, R. Huang, Properties of pervious concrete made with air-cooling electric arc furnace slag as aggregates, Constr. Build. Mater. 93 (2015) 737–745. https://doi.org/10.1016/j.conbuildmat.2015.05.104.
[130] M.S. Amin, S.M.A. El-Gamal, S.A. Abo-El-Enein, F.I. El-Hosiny, M. Ramadan, Physico-chemical characteristics of blended cement pastes containing electric arc furnace slag with and without silica fume, HBRC J. 11 (2015) 321–327. https://doi.org/10.1016/j.hbrcj.2014.07.002.
[131] A.V.M. Cardoso, F.M. Dias, A utilização de escória de aciaria para manufatura de Blocos de pavimentação, in: 21º CBECIMAT - Congresso Brasileiro de Engenharia e Ciência dos Materiais, Cuiabá, 2014: pp. 3673–3679.
[132] S. Liu, L. Li, Influence of fineness on the cementitious properties of steel slag, J. Therm. Anal. Calorim. 117 (2014) 629–634. https://doi.org/10.1007/s10973-014-3789-0.
[133] C.J. Tsai, R. Huang, W.T. Lin, H.N. Wang, Mechanical and cementitious characteristics of ground granulated blast furnace slag and basic oxygen furnace slag blended mortar, Mater. Des. 60 (2014) 267–273. https://doi.org/10.1016/j.matdes.2014.04.002.
[134] A. Kavussi, M.J. Qazizadeh, Fatigue characterization of asphalt mixes containing electric arc furnace (EAF) steel slag subjected to long term aging, Constr. Build. Mater. 72 (2014) 158–166. https://doi.org/10.1016/j.conbuildmat.2014.08.052.
[135] D. Mombelli, C. Mapelli, S. Barella, A. Gruttadauria, G. Le Saout, E. Garcia-Diaz, The

efficiency of quartz addition on electric arc furnace (EAF) carbon steel slag stability, J. Hazard. Mater. 279 (2014) 586–596. https://doi.org/10.1016/j.jhazmat.2014.07.045.
[136] Q. Wang, J. Yang, P. Yan, Cementitious properties of super-fine steel slag, Powder Technol. 245 (2013) 35–39. https://doi.org/10.1016/j.powtec.2013.04.016.
[137] Z. Li, S. Zhao, X. Zhao, T. He, Cementitious property modification of basic oxygen furnace steel slag, Constr. Build. Mater. 48 (2013) 575–579. https://doi.org/10.1016/j.conbuildmat.2013.07.068.
[138] J.L. Calmon, F.A. Tristão, M. Giacometti, M. Meneguelli, M. Moratti, J.E.S.L. Teixeira, Effects of BOF steel slag and other cementitious materials on the rheological properties of self-compacting cement pastes, Constr. Build. Mater. 40 (2013) 1046–1053. https://doi.org/10.1016/j.conbuildmat.2012.11.039.
[139] M. Gautier, J. Poirier, F. Bodénan, G. Franceschini, E. Véron, Basic oxygen furnace (BOF) slag cooling: Laboratory characteristics and prediction calculations, Int. J. Miner. Process. 123 (2013) 94–101. https://doi.org/10.1016/j.minpro.2013.05.002.
[140] E.E. Hekal, S.A. Abo-El-Enein, S.A. El-Korashy, G.M. Megahed, T.M. El-Sayed, Hydration characteristics of Portland cement – Electric arc furnace slag blends, HBRC J. 9 (2013) 118–124. https://doi.org/10.1016/j.hbrcj.2013.05.006.
[141] R.I. Iacobescu, Y. Pontikes, D. Koumpouri, G.N. Angelopoulos, Synthesis, characterization and properties of calcium ferroaluminate belite cements produced with electric arc furnace steel slag as raw material, Cem. Concr. Compos. 44 (2013) 1–8. https://doi.org/10.1016/j.cemconcomp.2013.08.002.
[142] J. Xie, S. Wu, J. Lin, J. Cai, Z. Chen, W. Wei, Recycling of basic oxygen furnace slag in asphalt mixture: Material characterization & moisture damage investigation, Constr. Build. Mater. 36 (2012) 467–474. https://doi.org/10.1016/j.conbuildmat.2012.06.023.
[143] E. Belhadj, C. Diliberto, A. Lecomte, Characterization and activation of Basic Oxygen Furnace slag, Cem. Concr. Compos. 34 (2012) 34–40. https://doi.org/10.1016/j.cemconcomp.2011.08.012.
[144] X. Zhu, H. Hou, X. Huang, M. Zhou, W. Wang, Enhance hydration properties of steel slag using grinding aids by mechanochemical effect, Constr. Build. Mater. 29 (2012) 476–481. https://doi.org/10.1016/j.conbuildmat.2011.10.064.
[145] D. Zhang, X. Huang, Y. Zhao, Investigation of the shape, size, angularity and surface texture properties of coarse aggregates, Constr. Build. Mater. 34 (2012) 330–336. https://doi.org/10.1016/j.conbuildmat.2012.02.096.
[146] S.I. Abu-Eishah, A.S. El-Dieb, M.S. Bedir, Performance of concrete mixtures made with electric arc furnace (EAF) steel slag aggregate produced in the Arabian Gulf region, Constr. Build. Mater. 34 (2012) 249–256. https://doi.org/10.1016/j.conbuildmat.2012.02.012.
[147] C.L. Beh, T.G. Chuah, M.N. Nourouzi, T. Choong, Removal of heavy metals from steel making waste water by using electric arc furnace slag, E-Journal Chem. 9 (2012) 2557–2564. https://doi.org/10.1155/2012/128275.
[148] J. Li, Q. Yu, J. Wei, T. Zhang, Structural characteristics and hydration kinetics of modified steel slag, Cem. Concr. Res. 41 (2011) 324–329. https://doi.org/10.1016/j.cemconres.2010.11.018.
[149] M. Uibua, R. Kuusik, L. Andreas, K. Kirsimäe, The CO2-binding by Ca-Mg-silicates in direct aqueous carbonation of oil shale ash and steel slag, Energy Procedia. 4 (2011) 925–932. https://doi.org/10.1016/j.egypro.2011.01.138.
[150] J. Waligora, D. Bulteel, P. Degrugilliers, D. Damidot, J.L. Potdevin, M. Measson, Chemical and mineralogical characterizations of LD converter steel slags: A multi-analytical techniques approach, Mater. Charact. 61 (2010) 39–48. https://doi.org/10.1016/j.matchar.2009.10.004.

[151] M. Etxeberria, C. Pacheco, J.M. Meneses, I. Berridi, Properties of concrete using metallurgical industrial by-products as aggregates, Constr. Build. Mater. 24 (2010) 1594–1600. https://doi.org/10.1016/j.conbuildmat.2010.02.034.
[152] M. Pasetto, N. Baldo, Experimental evaluation of high performance base course and road base asphalt concrete with electric arc furnace steel slags, J. Hazard. Mater. 181 (2010) 938–948. https://doi.org/10.1016/j.jhazmat.2010.05.104.
[153] P.E. Tsakiridis, G.D. Papadimitriou, S. Tsivilis, C. Koroneos, Utilization of steel slag for Portland cement clinker production, J. Hazard. Mater. 152 (2008) 805–811. https://doi.org/10.1016/j.jhazmat.2007.07.093.
[154] L. Cao, W. Shen, J. Huang, Y. Yang, D. Zhang, X. Huang, Z. Lv, X. Ji, Process to utilize crushed steel slag in cement industry directly: Multi-phased clinker sintering technology, J. Clean. Prod. 217 (2019) 520–529. https://doi.org/10.1016/j.jclepro.2019.01.260.
[155] T. Gao, T. Dai, L. Shen, L. Jiang, Benefits of using steel slag in cement clinker production for environmental conservation and economic revenue generation, J. Clean. Prod. 282 (2021) 124538. https://doi.org/10.1016/j.jclepro.2020.124538.
[156] R.I. Iacobescu, D. Koumpouri, Y. Pontikes, R. Saban, G.N. Angelopoulos, Valorisation of electric arc furnace steel slag as raw material for low energy belite cements, J. Hazard. Mater. 196 (2011) 287–294. https://doi.org/10.1016/j.jhazmat.2011.09.024.
[157] J.-M. Kim, S.-H. Cho, E.-G. Kwak, RETRACTED ARTICLE: Experimental evaluation of volume stability of rapidly-cooled steel slag [RCSS] as fine aggregate for concrete, KSCE J. Civ. Eng. 19 (2014) 1548–1548. https://doi.org/10.1007/s12205-014-0328-2.
[158] H. Shen, E. Forssberg, An overview of recovery of metals from slags, Waste Manag. 23 (2003) 933–949. https://doi.org/10.1016/S0956-053X(02)00164-2.
[159] G.C. Wang, Usability criteria for slag use in rigid matrices, Util. Slag Civ. Infrastruct. Constr. (2016) 275–304. https://doi.org/10.1016/b978-0-08-100381-7.00012-4.
[160] G. Wang, Determination of the expansion force of coarse steel slag aggregate, Constr. Build. Mater. 24 (2010) 1961–1966. https://doi.org/10.1016/j.conbuildmat.2010.04.004.
[161] Y. pei Lan, Q. cai Liu, F. Meng, D. liang Niu, H. Zhao, Optimization of magnetic separation process for iron recovery from steel slag, J. Iron Steel Res. Int. 24 (2017) 165–170. https://doi.org/10.1016/S1006-706X(17)30023-7.
[162] C. Kambole, P. Paige-Green, W.K. Kupolati, J.M. Ndambuki, A.O. Adeboje, Basic oxygen furnace slag for road pavements: A review of material characteristics and performance for effective utilisation in southern Africa, Constr. Build. Mater. 148 (2017) 618–631. https://doi.org/10.1016/j.conbuildmat.2017.05.036.
[163] L. Muhmood, S. Vitta, D. Venkateswaran, Cementitious and pozzolanic behavior of electric arc furnace steel slags, Cem. Concr. Res. 39 (2009) 102–109. https://doi.org/10.1016/j.cemconres.2008.11.002.
[164] Y. Guo, J. Xie, W. Zheng, J. Li, Effects of steel slag as fine aggregate on static and impact behaviours of concrete, Constr. Build. Mater. 192 (2018) 194–201. https://doi.org/10.1016/j.conbuildmat.2018.10.129.
[165] S. Wang, C. Wang, Q. Wang, Z. Liu, W. Qian, C.Z. Jin, L. Chen, L. Li, Study on cementitious properties and hydration characteristics of steel slag, Polish J. Environ. Stud. 27 (2018) 357–364. https://doi.org/10.15244/pjoes/74133.
[166] E. Belhadj, C. Diliberto, A. Lecomte, Properties of hydraulic paste of basic oxygen furnace slag, Cem. Concr. Compos. 45 (2014) 15–21. https://doi.org/10.1016/j.cemconcomp.2013.09.016.
[167] L. Lang, C. Song, L. Xue, B. Chen, Effectiveness of waste steel slag powder on the

strength development and associated micro-mechanisms of cement-stabilized dredged sludge, Constr. Build. Mater. 240 (2020) 117975. https://doi.org/10.1016/j.conbuildmat.2019.117975.
[168] C. Shi, J. Qian, High performance cementing materials from industrial slags - A review, Resour. Conserv. Recycl. 29 (2000) 195–207. https://doi.org/10.1016/S0921-3449(99)00060-9.
[169] S. Kourounis, S. Tsivilis, P.E. Tsakiridis, G.D. Papadimitriou, Z. Tsibouki, Properties and hydration of blended cements with steelmaking slag, Cem. Concr. Res. 37 (2007) 815–822. https://doi.org/10.1016/j.cemconres.2007.03.008.
[170] Q. Wang, M. Shi, Z. Zhang, Hydration properties of steel slag under autoclaved condition, J. Therm. Anal. Calorim. 120 (2015) 1241–1248. https://doi.org/10.1007/s10973-015-4397-3.
[171] S.Y. Pan, R. Adhikari, Y.H. Chen, P. Li, P.C. Chiang, Integrated and innovative steel slag utilization for iron reclamation, green material production and CO2 fixation via accelerated carbonation, J. Clean. Prod. 137 (2016) 617–631. https://doi.org/10.1016/j.jclepro.2016.07.112.
[172] L. Gan, H. feng Wang, X. ping Li, Y. hong Qi, C. xia Zhang, Strength activity index of air quenched basic oxygen furnace steel slag, J. Iron Steel Res. Int. 22 (2015) 219–225. https://doi.org/10.1016/S1006-706X(15)60033-4.
[173] F. Engström, Mineralogical influence on leaching behaviour of steelmaking slags, Lulea University of Technology, 2010. http://scholar.google.com/scholar?hl=en&btnG=Search&q=intitle:Mineralogical+Influence+on+Leaching+Behaviour+of+Steelmaking+Slags#7.
[174] F. Han, Z. Zhang, D. Wang, P. Yan, Hydration heat evolution and kinetics of blended cement containing steel slag at different temperatures, Thermochim. Acta. 605 (2015) 43–51. https://doi.org/10.1016/j.tca.2015.02.018.
[175] P.Y. Mahieux, J.E. Aubert, G. Escadeillas, Utilization of weathered basic oxygen furnace slag in the production of hydraulic road binders, Constr. Build. Mater. 23 (2009) 742–747. https://doi.org/10.1016/j.conbuildmat.2008.02.015.
[176] H.Ş. Soykan, Cementitious material production from hot mixing of ironmaking and steelmaking slags, Trans. Institutions Min. Metall. Sect. C Miner. Process. Extr. Metall. 115 (2006) 229–233. https://doi.org/10.1179/174328506X128850.
[177] P. Cui, Y. Xiao, B. Yan, M. Li, S. Wu, Morphological characteristics of aggregates and their influence on the performance of asphalt mixture, Constr. Build. Mater. 186 (2018) 303–312. https://doi.org/10.1016/j.conbuildmat.2018.07.124.
[178] Y. Ye, S. Wu, C. Li, D. Kong, B. Shu, Morphological discrepancy of various basic oxygen furnace steel slags and road performance of corresponding asphalt mixtures, Materials (Basel). 12 (2019). https://doi.org/10.3390/ma12142322.
[179] C. Yang, J. Xie, S. Wu, S. Amirkhanian, X. Zhou, D. Kong, Q. Ye, J. Hu, Revelation and characterization of selective absorption behavior of bitumen to basic oxygen furnace slag, Constr. Build. Mater. 253 (2020) 119210. https://doi.org/10.1016/j.conbuildmat.2020.119210.
[180] C.S.G. Penteado, B.L. Evangelista, G.C. dos S. Ferreira, P.H.A. Borges, R.C.C. Lintz, Use of electric arc furnace slag for producing concrete paving blocks, Ambient. Construído. 19 (2019) 21–32. https://doi.org/10.1590/s1678-86212019000200305.
[181] X. Chen, G. Wang, Q. Dong, X. Zhao, Y. Wang, Microscopic characterizations of pervious concrete using recycled Steel Slag Aggregate, J. Clean. Prod. 254 (2020) 120149. https://doi.org/10.1016/j.jclepro.2020.120149.
[182] Y. Biskri, D. Achoura, N. Chelghoum, M. Mouret, Mechanical and durability characteristics of High Performance Concrete containing steel slag and crystalized slag

as aggregates, Constr. Build. Mater. 150 (2017) 167–178. https://doi.org/10.1016/j.conbuildmat.2017.05.083.
[183] M.R. Hainin, M.A. Aziz, Z. Ali, R.P. Jaya, M.M. El-Sergany, H. Yaacoba, Steel slag as a road construction material, J. Teknol. 73 (2015) 33–38. https://doi.org/10.11113/jt.v73.4282.
[184] M.A. Khalaf, C.C. Ban, M. Ramli, N.M. Ahmed, L.J. Sern, H.A. Khaleel, Physicomechanical and gamma-ray shielding properties of high-strength heavyweight concrete containing steel furnace slag aggregate, J. Build. Eng. 30 (2020) 101306. https://doi.org/10.1016/j.jobe.2020.101306.
[185] M. Alexander, S. Mindess, Aggregates in concrete, 1st Editio, CRC Press, London, 2005.
[186] H. Beshr, A.A. Almusallam, M. Maslehuddin, Effect of coarse aggregate quality on the mechanical properties of high strength concrete, Constr. Build. Mater. 17 (2003) 97–103. https://doi.org/10.1016/S0950-0618(02)00097-1.
[187] A. Kiliç, C.D. Atiş, A. Teymen, O. Karahan, F. Özcan, C. Bilim, M. Özdemir, The influence of aggregate type on the strength and abrasion resistance of high strength concrete, Cem. Concr. Compos. 30 (2008) 290–296. https://doi.org/10.1016/j.cemconcomp.2007.05.011.
[188] H. Qasrawi, The use of steel slag aggregate to enhance the mechanical properties of recycled aggregate concrete and retain the environment, Constr. Build. Mater. 54 (2014) 298–304. https://doi.org/10.1016/j.conbuildmat.2013.12.063.
[189] G. Wang, X. Chen, Q. Dong, J. Yuan, Q. Hong, Mechanical performance study of pervious concrete using steel slag aggregate through laboratory tests and numerical simulation, J. Clean. Prod. 262 (2020) 121208. https://doi.org/10.1016/j.jclepro.2020.121208.
[190] Z. Chen, S. Wu, Y. Xiao, W. Zeng, M. Yi, J. Wan, Effect of hydration and silicone resin on Basic Oxygen Furnace slag and its asphalt mixture, J. Clean. Prod. 112 (2016) 392–400. https://doi.org/10.1016/j.jclepro.2015.09.041.
[191] N. Palankar, A.U. Ravi Shankar, B.M. Mithun, Durability studies on eco-friendly concrete mixes incorporating steel slag as coarse aggregates, J. Clean. Prod. 129 (2016) 437–448. https://doi.org/10.1016/j.jclepro.2016.04.033.
[192] J.M. Franco de Carvalho, W. Schmidt, H.C. Kühne, R.A.F. Peixoto, Influence of high-charge and low-charge PCE-based superplasticizers on Portland cement pastes containing particle-size designed recycled mineral admixtures, J. Build. Eng. 32 (2020) 101515. https://doi.org/10.1016/j.jobe.2020.101515.
[193] J. Zhao, D. Wang, P. Yan, W. Li, Comparison of grinding characteristics of converter steel slag with and without pretreatment and grinding aids, Appl. Sci. 6 (2016) 1–15. https://doi.org/10.3390/app6110237.
[194] Q. Wang, P. Yan, J. Feng, A discussion on improving hydration activity of steel slag by altering its mineral compositions, J. Hazard. Mater. 186 (2011) 1070–1075. https://doi.org/10.1016/j.jhazmat.2010.11.109.
[195] Y.B. Zong, D.Q. Cang, Y.P. Zhen, Y. Li, H. Bai, Component modification of steel slag in air quenching process to improve grindability, Trans. Nonferrous Met. Soc. China (English Ed. 19 (2009) s834–s839. https://doi.org/10.1016/S1003-6326(10)60161-6.
[196] J.M. Franco de Carvalho, W.C. Fontes, C.F. de Azevedo, G.J. Brigolini, W. Schmidt, R.A.F. Peixoto, Enhancing the eco-efficiency of concrete using engineered recycled mineral admixtures and recycled aggregates, J. Clean. Prod. 257 (2020). https://doi.org/10.1016/j.jclepro.2020.120530.
[197] H. Gao, H. Liao, X. Yao, F. Cheng, Insights into the reinforcing mechanism for CO 2 atmosphere in the application process of steel slag ultra-fine powder, Constr. Build.

Mater. 209 (2019) 437–444. https://doi.org/10.1016/j.conbuildmat.2019.03.019.
[198] J. Liu, D. Wang, Influence of steel slag-silica fume composite mineral admixture on the properties of concrete, Powder Technol. 320 (2017) 230–238. https://doi.org/10.1016/j.powtec.2017.07.052.
[199] Q. Wang, D. Wang, S. Zhuang, The soundness of steel slag with different free CaO and MgO contents, Constr. Build. Mater. 151 (2017) 138–146. https://doi.org/10.1016/j.conbuildmat.2017.06.077.
[200] W. Shen, M. Zhou, W. Ma, J. Hu, Z. Cai, Investigation on the application of steel slag-fly ash-phosphogypsum solidified material as road base material, J. Hazard. Mater. 164 (2009) 99–104. https://doi.org/10.1016/j.jhazmat.2008.07.125.
[201] Y. Lun, S. Liu, X. Luo, Mechanical mechanism for expansion and crack of mortars containing basic oxygen furnace slag sand, Mater. Res. Innov. 19 (2015) S5865–S5869. https://doi.org/10.1179/1432891714Z.0000000001209.
[202] P.S. Kandhal, G.L. Hoffman, Evaluation of steel slag fine aggregate in hot-mix asphalt mixtures, Transp. Res. Rec. (1997) 28–36. https://doi.org/10.3141/1583-04.
[203] A.S. Brand, J.R. Roesler, Steel furnace slag aggregate expansion and hardened concrete properties, Cem. Concr. Compos. 60 (2015) 1–9. https://doi.org/10.1016/j.cemconcomp.2015.04.006.
[204] G.C. Wang, Slag processing, Util. Slag Civ. Infrastruct. Constr. (2016) 87–113. https://doi.org/10.1016/b978-0-08-100381-7.00005-7.
[205] J.M. Manso, J.A. Polanco, M. Losañez, J.J. González, Durability of concrete made with EAF slag as aggregate, Cem. Concr. Compos. 28 (2006) 528–534. https://doi.org/10.1016/j.cemconcomp.2006.02.008.
[206] G. Adegoloye, A.L. Beaucour, S. Ortola, A. Noumowe, Mineralogical composition of EAF slag and stabilised AOD slag aggregates and dimensional stability of slag aggregate concretes, Constr. Build. Mater. 115 (2016) 171–178. https://doi.org/10.1016/j.conbuildmat.2016.04.036.
[207] W.C. Wang, Feasibility of stabilizing expanding property of furnace slag by autoclave method, Constr. Build. Mater. 68 (2014) 552–557. https://doi.org/10.1016/j.conbuildmat.2014.06.082.
[208] Z. Ghouleh, R.I.L. Guthrie, Y. Shao, High-strength KOBM steel slag binder activated by carbonation, Constr. Build. Mater. 99 (2015) 175–183. https://doi.org/10.1016/j.conbuildmat.2015.09.028.
[209] D.M. Proctor, K.A. Fehling, E.C. Shay, J.L. Wittenborn, J.J. Green, C. Avent, R.D. Bigham, M. Connolly, B. Lee, T.O. Shepker, M.A. Zak, Physical and chemical characteristics of blast furnace, basic oxygen furnace, and electric arc furnace steel industry slags, Environ. Sci. Technol. 34 (2000) 1576–1582. https://doi.org/10.1021/es9906002.
[210] B. Das, S. Prakash, P.S.R. Reddy, V.N. Misra, An overview of utilization of slag and sludge from steel industries, Resour. Conserv. Recycl. 50 (2007) 40–57. https://doi.org/10.1016/j.resconrec.2006.05.008.
[211] C. Navarro, M. Díaz, M.A. Villa-García, Physico-chemical characterization of steel slag. study of its behavior under simulated environmental conditions, Environ. Sci. Technol. 44 (2010) 5383–5388. https://doi.org/10.1021/es100690b.
[212] P. Chaurand, J. Rose, J. Domas, J.Y. Bottero, Speciation of Cr and V within BOF steel slag reused in road constructions, J. Geochemical Explor. 88 (2006) 10–14. https://doi.org/10.1016/j.gexplo.2005.08.006.
[213] H. Yi, G. Xu, H. Cheng, J. Wang, Y. Wan, H. Chen, An Overview of Utilization of Steel Slag, Procedia Environ. Sci. 16 (2012) 791–801. https://doi.org/10.1016/j.proenv.2012.10.108.

[214] R.M. Santos, D. Ling, A. Sarvaramini, M. Guo, J. Elsen, F. Larachi, G. Beaudoin, B. Blanpain, T. Van Gerven, Stabilization of basic oxygen furnace slag by hot-stage carbonation treatment, Chem. Eng. J. 203 (2012) 239–250. https://doi.org/10.1016/j.cej.2012.06.155.
[215] T.L. DesMarias, M. Costa, Mechanisms of chromium-induced toxicity, Curr. Opin. Toxicol. 14 (2019) 1–7. https://doi.org/10.1016/j.cotox.2019.05.003.
[216] R.R. Moskalyk, A.M. Alfantazi, Processing of vanadium: A review, Miner. Eng. 16 (2003) 793–805. https://doi.org/10.1016/S0892-6875(03)00213-9.
[217] M. Lindvall, S. Rutqvist, G. Ye, Recovery of vanadium from v-bearing bof-slag using an eaf, Proc. 12th Int. Ferroalloys Congr. Sustain. Futur. (2010) 189–195.
[218] I.Z. Yildirim, M. Prezzi, Use of steel slag in subgrade applicatios, 2009. http://oreilly.com/catalog/errata.csp?isbn=9781449340377.
[219] Y. Wang, P. Suraneni, Experimental methods to determine the feasibility of steel slags as supplementary cementitious materials, Constr. Build. Mater. 204 (2019) 458–467. https://doi.org/10.1016/j.conbuildmat.2019.01.196.
[220] J. Zhao, D. Wang, P. Yan, Design and experimental study of a ternary blended cement containing high volume steel slag and blast-furnace slag based on Fuller distribution model, Constr. Build. Mater. 140 (2017) 248–256. https://doi.org/10.1016/j.conbuildmat.2017.02.119.
[221] G. Qian, D.D. Sun, J.H. Tay, Z. Lai, G. Xu, Autoclave properties of kirschsteinite-based steel slag, Cem. Concr. Res. 32 (2002) 1377–1382. https://doi.org/10.1016/S0008-8846(02)00790-1.
[222] D. Wang, H. Wang, Y. Bu, C. Schulze, M. Oeser, Evaluation of aggregate resistance to wear with Micro-Deval test in combination with aggregate imaging techniques, Wear. 338–339 (2015) 288–296. https://doi.org/10.1016/j.wear.2015.07.002.
[223] S. Arasan, E. Yenera, F. Hattatoglu, S. Hinislioglua, S. Akbuluta, Correlation between Shape of Aggregate and Mechanical Properties of Asphalt Concrete, Road Mater. Pavement Des. 12 (2011) 239–262. https://doi.org/10.3166/rmpd.12.239-262.
[224] K. Imamoto, M. Arai, Specific surface area of aggregate and its relation to concrete drying shrinkage, Mater. Struct. Constr. 41 (2008) 323–333. https://doi.org/10.1617/s11527-007-9245-x.
[225] M. Maslehuddin, A.M. Sharif, M. Shameem, M. Ibrahim, M.S. Barry, Comparison of properties of steel slag and crushed limestone aggregate concretes, Constr. Build. Mater. 17 (2003) 105–112. https://doi.org/10.1016/S0950-0618(02)00095-8.
[226] H. Qasrawi, Use of Relatively High Fe2O3 Steel Slag as Coarse Aggregate in Concrete, ACI Mater. J. 109 (2012) 471–478.
[227] A.S. Brand, J. Roesler, Interfacial transition zone of cement composites with recycled concrete aggregate of different moisture states, Adv. Civ. Eng. Mater. 7 (2018) 87–102. https://doi.org/10.1520/ACEM20170090.
[228] H. Qasrawi, Hardened Properties of Green Self-Consolidating Concrete Made with Steel Slag Coarse Aggregates under Hot Conditions, ACI Mater. J. 117 (2020) 107–118.
[229] C. Pellegrino, P. Cavagnis, F. Faleschini, K. Brunelli, Properties of concretes with black/oxidizing electric arc furnace slag aggregate, Cem. Concr. Compos. 37 (2013) 232–240. https://doi.org/10.1016/j.cemconcomp.2012.09.001.
[230] D.R.R. Gonçalves, W.C. Fontes, J.C. Mendes, G.J.B. Silva, R.A.F. Peixoto, Evaluation of the economic feasibility of a processing plant for steelmaking slag, Waste Manag. Res. 34 (2016) 107–112. https://doi.org/10.1177/0734242X15615955.
[231] T. Dyer, Concrete Durability, CRC Press, Boca Raton, 2014.
[232] L. Bertolini, B. Elsener, P. Pedeferri, R.B. Polder, Corrosion of Steel in Concrete,

Weinheim, Wiley, 2004.
[233] ASTM, C1202: Electrical Indication of Chloride's Ability to Resist Chloride, ASTM Standards, Philadelphia, 2005.
[234] F. Han, Z. Zhang, Properties of 5-year-old concrete containing steel slag powder, Powder Technol. 334 (2018) 27–35. https://doi.org/10.1016/j.powtec.2018.04.054.
[235] I. Arribas, I. Vegas, J.T. San-José, J.M. Manso, Durability studies on steelmaking slag concretes, Mater. Des. 63 (2014) 168–176. https://doi.org/10.1016/j.matdes.2014.06.002.
[236] A. Younsi, P. Turcry, A. Aït-Mokhtar, S. Staquet, Accelerated carbonation of concrete with high content of mineral additions: Effect of interactions between hydration and drying, Cem. Concr. Res. 43 (2013) 25–33. https://doi.org/10.1016/j.cemconres.2012.10.008.
[237] X. Zhang, S. Zhao, Z. Liu, F. Wang, Utilization of steel slag in ultra-high performance concrete with enhanced eco-friendliness, Constr. Build. Mater. 214 (2019) 28–36. https://doi.org/10.1016/j.conbuildmat.2019.04.106.
[238] T.V. de Melo, Influência da escória de aciaria LD no desempenho de concretos com baixo consumo de cimento, Federal University of Minas Gerais (in Portuguese), Belo Horizonte, 2020.
[239] G. Xiaolu, S. Huisheng, W. Kai, Effects of strel slag powder on workability and durability of concrete, J. Wuhan Univ. Technol. (2014) 733–739.

CHAPTER 3

Influence of a LAS-based modifying admixture on cement-based composites containing steel slag powder

Abstract

This work presents a study on the influences of a modifying admixture based on Linear Alkyl Benzene Sodium Sulfonate (LAS) in the properties of cement-based composites with partial replacement of the binder by steel slag powder (SSP). A two-level two-factor face-centered composite design (CCD) has been employed with response surface methodology (RSM) for modeling. The effect of the studied parameters (0-1.0% LAS and 0-50% SSP) on the consistency and mechanical strength of mortars was evaluated. The separated and combined effects of SSP and LAS on hydration kinetics and formation of the hydrated product were investigated through ultrasonic pulse velocity (UPV) and X-ray diffraction (XRD). Also, fragments of mortar specimens were observed using scanning electron microscopy (SEM) images. The results obtained through RSM showed that consistency and mechanical strength are linear functions. The increase in SSP and LAS-based admixture levels caused an increase in spread value (22%) and reduced mechanical strength (57%). The SSP was the component that had the greatest impact. In the first ages, both SSP and LAS delayed the hydration kinetics.

Keywords: Linear Alkyl Benzene Sodium Sulfonate (LAS). Steel slag powder (SSP). Modifying admixture. Cement-based composites. Ultrasonic pulse velocity (UPV). Hydration kinetics.

3.1 Introduction

The use of industrial residues and by-products has received increasing attention from researchers. Several studies have attested to the potential of using these materials applied in civil construction, thus contributing to reducing environmental impacts caused by production processes and inadequate disposal and reducing the consumption of natural resources applying the circular economy [1–7]. Examples include recycling of construction and demolition waste [8–11], iron ore tailings [12–15], residue from ornamental stone production [16–18], waste from the paper-pulp industry [19–21], and slag from steel production [1,22–27].

Basic Oxygen Furnace Slag (BOFS), also known as steel slag, converter slag, LD-slag, or BOF-slag, is a by-product of the primary steel refining process in steel mills, carried out in LD oxygen converters (Linz-Donawitz), where liquid pig iron is converted into steel [28–30]. The chemical and mineralogical composition of BOFS depends on several factors, such as the raw material used, the steel production process, the cooling, and the slag curing [31–33]. These parameters are fundamental to determine the slag's potential for hydraulic and cementing activity [30,34]. The chemical constituents commonly found in BOFS are 40-60% CaO, 20-30% Fe_2O_3 (FeO/Fe), 10-20% SiO_2, 1-6% Al_2O_3, and 2-10% MgO, and the remaining minor oxides include MnO, P_2O_5, Na_2O, and SO_3 [35]. Olivine ($(Mg, Fe)_2SiO_4$), merwinite ($Ca_3MgSi_2O_8$), belite (C_2S), alite (C_3S), brownmillerite (C_4AF), ferrite (C_2F), CaO-FeO-MnO-MgO solid solution (RO phase), and free CaO are common minerals found in BOFS, of which C_2S, C_3S and RO phase are the main phases [29,36–38].

The use of steel slag in cementitious composites as supplementary cementing material (SCM) has been studied by several researchers worldwide [1,36,38–41] since the chemical composition of the slag is very similar to that of Portland cement [42]. Moreover, the high demand for fines is an opportunity for using mineral admixtures as cementitious or non-cementitious fillers in partial replacement of cement [41,43]. Usually, cement mixed with steel slag has a longer average hardening time and has less initial strength, and in some cases, has volume expansion due to high oxide contents [37]. The presence of free lime and free magnesia and the oxidation of the metallic fraction raise concerns about the use of steel slag, as these oxides become unstable in the presence of water and can cause expansion problems [44–47]. However, through appropriate treatments such as aging, weathering, and metallic separation, volume expansion can be prevented and these oxides stabilized [2,23,48].

Minerals such as C_2S, C_3S, C_4AF, and C_2F provide the slags hydraulic properties [29,34,49,50]. However, the activity of C_2S and C_3S in steel slag is much lower than those in Portland cement because the rate of cooling process is quite low [34]; thus, steel slag can be considered a low initial resistance hydraulic material [28,37,50–52]. Forms of slag activation have been studied to improve its cementitious activity, such as mechanical activation [1,53], thermal activation [54,55] and chemical activation [56,57]. These activation techniques require additional chemical and energy activators, and the effect of slag modification varies according to their chemical and mineral compositions [37].

The use of admixtures in cement-based composites is growing and widespread worldwide. These components can give considerable physical and economic advantages to cementitious materials, modifying the matrices' properties in the fresh and hardened states [58,59]. Among the various types of admixtures on the market, there are air-entraining agents (AEA), which are surfactants [59,60]. These AEA admixtures confer some advantages to cementitious materials, such as improved workability, reduced water/cement ratio, reduced cement consumption, increased plasticity and improved consistency, reduced exudation and permeability, refined thermal and acoustic performance, in addition to ice and thaw resistance [58–60].

In studies conducted by Mendes et al. [61], a biodegradable surfactant based on Linear Alkyl Benzene Sodium Sulfonate (LAS), present in dishwashing detergents, was used as a plasticizing agent and sustainable air incorporating agent in mortars. Positive results have been achieved from its application, in which the LAS proved to be more efficient than a commercial AEA, considering the volume of incorporated air and the stability of the pore system formed in the matrix. Moreover, it was observed an improvement in the workability and cohesion of mortars in the fresh state.

In this work, the authors explore the use of a LAS-based admixture in cement-based composites containing steel slag powder as supplementary cementitious material, offering new insights into the use of biodegradable and low-cost admixtures and the reduction of cement consumption in eco-friendly composites by reusing a steelmaking by-product towards a circular economy. SSP and LAS-based admixture influence on consistency, hydrated products, setting times, and compressive strength has been discussed. Also, the separated and combined effect of these components on the produced matrices has been compared.

3.2 Material and methods

3.2.1 Materials

A high-early-strength Portland cement (PC) (ASTM Type III equivalent) was used to produce the pastes and mortars. In Brazil, this cement is specified by the standard NBR 16697 [62] and is known as CPV-ARI. The choice for this cement was the almost absence of supplementary cementing material (95-100% clinker). The cement batch's physical, mechanical and chemical properties were obtained from the producer, and they are shown in *Table 3.1*.

Table 3.1 Chemical, physical and mechanical properties of the Portland cement (PC) used.

Parameter	Value
MgO content, %	0.98
SO_3 content, %	3.43
Na_2O content, %	0.07
K_2O content, %	0.86
Na_2Oeq content, %	0.64
Loss on ignition, %	3.97
Insoluble residue, %	1.48
Density, g/cm³	3.12
Specific surface area (Blaine), cm²/g	4372
Hot expandability, mm	0.3
Water for standard cement paste, %	28.8
Initial setting time, min.	105
Final setting time, min.	165
Compressive strength (1/ 3/ 7/ 28 days), MPa	(27.5/ 37.8/ 44.3/ 53.2)

A LAS-based admixture was used as an agent to improve plasticity, cohesion, and incorporation of air microbubbles. It is a biodegradable surfactant present in dishwashing detergents, in a concentration of up to 10% [63].

A river quartz sand with a granulometric range between 0.6 mm (sieve # 30) and 0.15 mm (sieve #100) was used to produce mortars. This sand presented a specific gravity equal to 2.629 g/cm³.

The steel slag powder was obtained from a steel slag generated in an LD oxygen converter from a steel plant located in the city of João Monlevade, Minas Gerais, Brazil. This BOFS has as main chemical components CaO (36.9%), Fe_2O_3 (31.8%), SiO_2 (14.4%), MgO (5.8%) and Al_2O_3 (3.8%), and mineralogical phases such as Larnite (Ca_2SiO_4), Calcite ($CaCO_3$), Brownmillerite [$Ca_2(Al,Fe)_2O_5$], Helvine [$Mn_4Be_3(SiO_4)_3S$], Lime (CaO), and Wuestite (FeO) [64]. This slag was subjected to a weathering procedure to stabilize the oxide expansion process

for five years in an uncovered storage yard at the Laboratory of Civil Construction Materials at the Federal University of Ouro Preto - UFOP, state of Minas Gerais, Brazil. The original material has a dark gray color, particle size between 6.35 mm and 12.5 mm, and a specific gravity of 3.57 g/cm³.

The steel slag went through a comminution process in a jaw crusher to obtain an aggregate with a particle size limited to 4.75mm. The resulting material was comminuted in a ball mill for 360 minutes according to the setup indicated in *Table 3.2*. The steel slag powder (SSP) presented a specific gravity equal to 3.62 g/cm³ and a specific surface area (Blaine) equal to 2,721.3 cm²/g.

Table 3.2 Grinding program and setup parameters.

Parameters	Information
Jar material	Stainless steel
Jar volume (cm³)	15,397
Material produced per cycle (cm³)	2,100 (13.6 %)
Rotation speed (rpm)	200
Balls material	Ceramic
Balls volume (cm³)	2,227 (14.5 %)

Fig. 3.1 shows the particle-size distribution curves of the PC, the SSP and the raw BOFS, determined by sieving and laser diffraction technique (Bettersize2000, distilled water as the dispersing medium). PC has a D90 equal to 41.99 µm, and the SSP has a D90 equal to 179.3 µm. *Fig. 3.2* shows a SEM image of the steel slag powder obtained from a scanning electron microscope JEOL JSM-6010LA (high vacuum, secondary electron images, 10kV). X-ray diffraction (XRD) of SSP is shown in *Fig. 3.3*. Mineralogical phases such as brownmillerite, calcite, lime, larnite and wustite were detected, in agreement with Franco de Carvalho et al. [64].

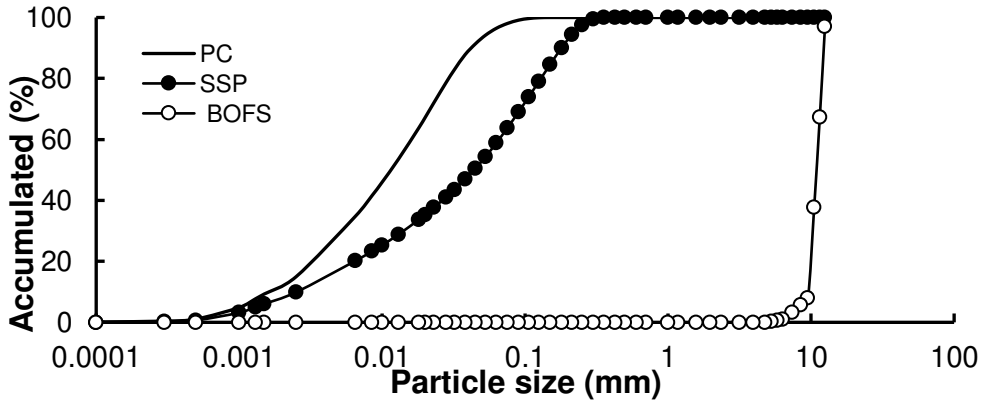

Fig. 3.1 Particle size curve of the materials used

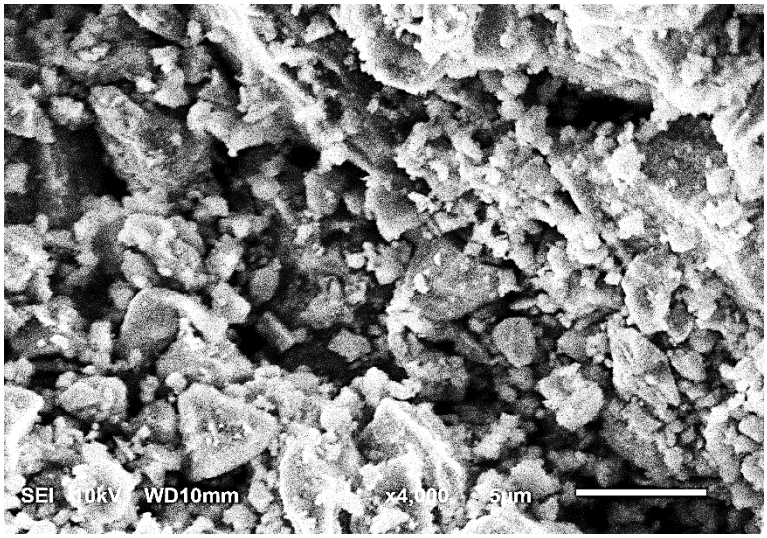

Fig. 3.1 SEM of the SSP sample.

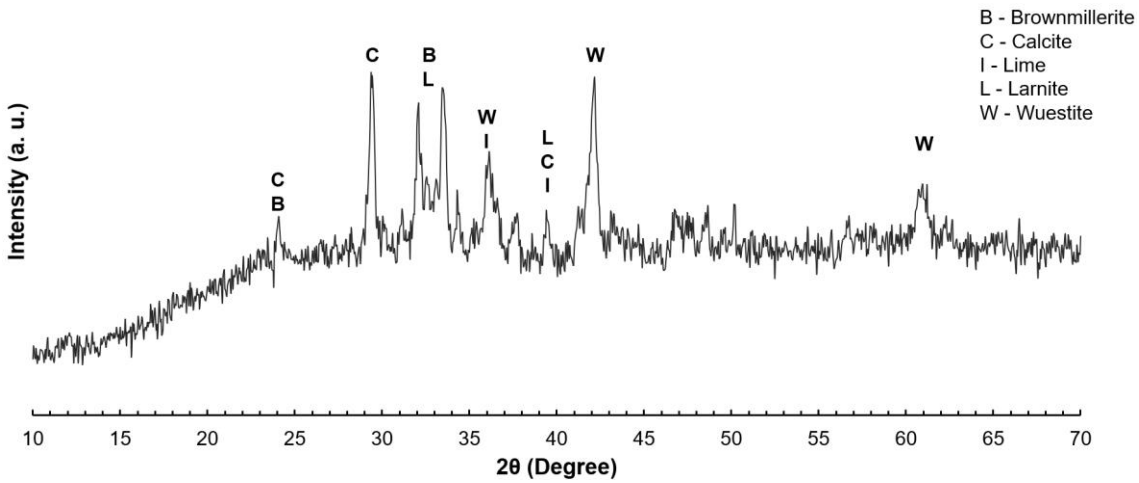

Fig 3.3 XRD of the SSP sample

3.2.2 Design of experiments (DOE)

This study proposed the partial substitution of Portland cement (PC) by steel slag powder (SSP). The water and aggregate contents were kept constant in all the studied mixtures. The replacement of PC by the SSP ranged from 0 to 50%. Accordingly, these mixing variables (cement and SSP) are dependent and complementary to each other.

The central composite face-centered design (CCD) was applied in this present study to determine the influence of SSP and LAS-based admixture by evaluating the effects and statistical significance (p-value) and understanding how the different proportions affect cement-based composites' rheological and mechanical performances. The CCD included nine experimental trials that are listed in *Table 3.3.*

Table 3.3 Central composite face-centered design layout.

Treatment	Coded units		Uncoded units	
	LAS_{cod}	SSP_{cod}	LAS	SSP
1	-1	-1	0.0	00
2	1	-1	1.0	00
3	-1	1	0.0	50
4	1	1	1.0	50
5	-1	0	0.0	25
6	1	0	1.0	25
7	0	-1	0.5	00
8	0	1	0.5	50
9	0	0	0.5	25

The response surface methodology (RSM) was used to statistically specify the effect of important process variables, LAS (0-1.0%) and SSP (0-50%), on the key response process output variables. When two factors, A (LAS) and B (SSP), are presented in quantitative levels, the answer Y is represented by a contour plot in two-dimensional space or by a surface plot in three-dimensional space, originating from a first or second-order model, with or without the double interaction between them. The most commonly used complete Y model is represented by the Eq. (3.1), where Y is the response variable; β_n is the coefficients of regression; a_i and b_j are the coded independent variables.

$$Y = \beta_0 + \beta_1 a_i + \beta_2 a_i^2 + \beta_3 b_j + \beta_4 b_j^2 + \beta_5 a_i b_j + \varepsilon_{ij} \quad (3.1)$$

3.2.3 Evaluation of consistency and mechanical performance in mortars

This study evaluated the influence of SSP and the LAS-based admixture on mortars' consistency and mechanical performance. For this purpose, mortar specimens with a 1:2 volume ratio (PC/SSP: fine river sand) were prepared. A constant water-to-binder weight ratio was used (0.5); hence, the consistency of mortar was not controlled but rather was a response variable. The proportions of SSP and LAS were obtained by CCD. The blends' identifications with the content of binder materials (PC and SSP) and admixture (LAS) used to prepare the cement-based composites are listed in *Table 3.4*. The mixing process was carried out with the aid of a mechanical mixer, following the recommendations of ASTM C305 [65]. Immediately at the end of the mixing, the flow table test was performed for mortars, following the recommendations present in ASTM C230 [66].

Table 3.4 Identification of the blends and proportion of binder and admixture.

Blend	PC (% by volume)	SSP (% by volume)	LAS (% by corresponding PC mass)
100-00-0.0	100	00	0.0
100-00-0.5	100	00	0.5
100-00-1.0	100	00	1.0
75-25-0.0	75	25	0.0
75-25-0.5	75	25	0.5
75-25-1.0	75	25	1.0
50-50-0.0	50	50	0.0
50-50-0.5	50	50	0.5
50-50-1.0	50	50	1.0

The specimens were then molded in reduced cylindrical molds measuring ∅35×35mm, and compressive strength tests were performed at 1, 3, 7, 28, and 63 days. These specimens were demolded and subjected to a curing process in a humid chamber until the test, wrapped in a plastic film to prevent water loss.

3.2.4 Evaluation of the hydration kinetics in pastes

Hydration is a complex physical and chemical reaction between cementitious materials and water, accompanied by a series of mineralogical and microstructural changes, responsible for the binding properties, physical setting, strength gain, and lifetime after the matrix hardening [67,68]. Hydration kinetics tests of the pastes were performed with four different samples (100-00-0.0; 100-00-0.5; 75-25-0.0; 75-25-0.5), whose composition is listed in *Table 3.4*. A constant water-to-binder weight ratio was used (0.5).

Ultrasonic Pulse Velocity (UPV) measurements were performed to monitor the start and end of the cement pastes' setting caused by the selective hydration of the paste components. Lee et al. [69] proposed a method to interpret the ultrasonic pulse velocity variation curves obtained from tests, as shown in *Fig. 3.4*. The curve can be divided into three steps: slow increasing (I), fast increasing (II), and stable (III) [70]. During step I, hydrates are begin formed after the dormant induction period, and the ultrasonic waves propagate through the water-like viscous suspension. Step II begins with an increase in the amount of formed hydration products and UPV; the water-saturated porous solid structure becomes more and more connected as newly formed hydration products fill the pores leading to a rapid increase in stiffness. Step III is characterized by reducing pore volume by filling hydration products; the increase of UPV slows down and approaches the values relative to the solid structure [67–69]. Lee et al. [69] identify

two particular points in the UPV development versus time curves for characterizing the setting process (t_A - the instant the UPV starts to develop, and t_B - the instant the UPV development rate is maximum).

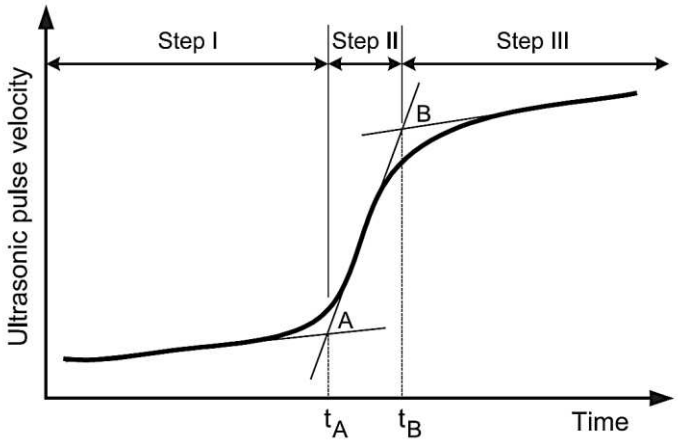

Fig. 3.4 Schematic representation of typical evolution of UPV [67].

In studies conducted by Freitas [71] and Machado [72], UPV tests were performed to determine the initial setting and final setting of cement pastes and reactive powder concrete, respectively. Both studies used a portable ultrasonic pulse monitoring system, "Pundit Lab" from Proceq, and a cubic box made of acrylic with 10 cm edge, as shown in *Fig. 3.5*. The same apparatus used for Machado [72] was also employed in this study (*Fig. 3.6*). The Proceq's "Pundit Lab" equipment connected to the computer and operated by Proceq's Punditlink software were used in these tests. The transducer used operates with a frequency of 54 MHz and a pulse width of 9.3 µs. The frequency of measurements was one reading per minute, taken during the 48-hour interval.

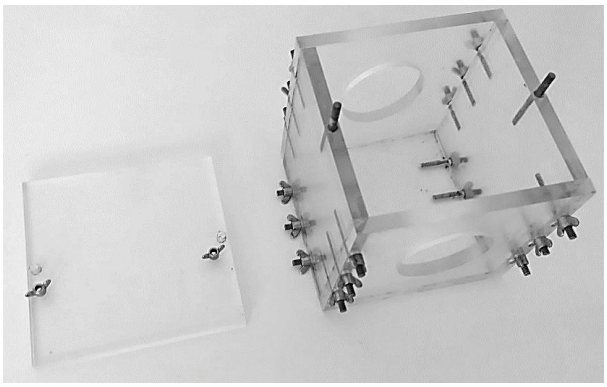

Fig. 3.5 Cubic box made of acrylic for UPV tests [72].

Fig. 3.6 Equipment coupled to the acrylic box.

The monitoring of the evolution of the mineralogical phases at different ages occurred at 1, 3, 7, 28 and 63 days, using the X-ray diffraction (XRD) technique. The equipment used was the D8-Discover diffraction system using Cu Kα radiation (λ=1.789 Å), 2θ range of 5º - 70º, a step of 0.05 °, 1s / step.

3.3 Results and discussion

3.3.1 Hydration kinetics of the pastes

Fig. 3.7 shows the development of UPV through the fresh pastes, measured in the first 48 hours (100-00-0.0; 100-00-0.5; 75-25-0.0, and 75-25-0.5). All UPV curves in Fig. 3.7 are similar to the curve in Fig. 3.4 proposed by Lee et al. [69].

The sample 100-00-0.0 (*Fig. 3.7A*) presented the UPV constant around 900 m/s in the first three hours. In contrast, the sample 100-00-0.5 (*Fig. 3.7B*) maintained a constant UPV of nearly 1,050 m/s for a longer period (almost six hours). The addition of LAS-based admixture to the cement pastes in the sample 100-00-0.5 caused a delay in the initial setting and hydration kinetics. This behavior can be observed by the prolonged period that the UPV remained constant in step I (t_A = 05h42) compared to the reference paste (100-00-0.0). The line drawn in step II for the 100-00-0.5 blend has a higher angulation than the reference paste, showing a slightly shorter t_B time, corresponding to the final setting. In step III, 100-00-0.0 stabilizes at a UPV of 3600 m/s, while 100-00-0.5 reaches 3700 m/s.

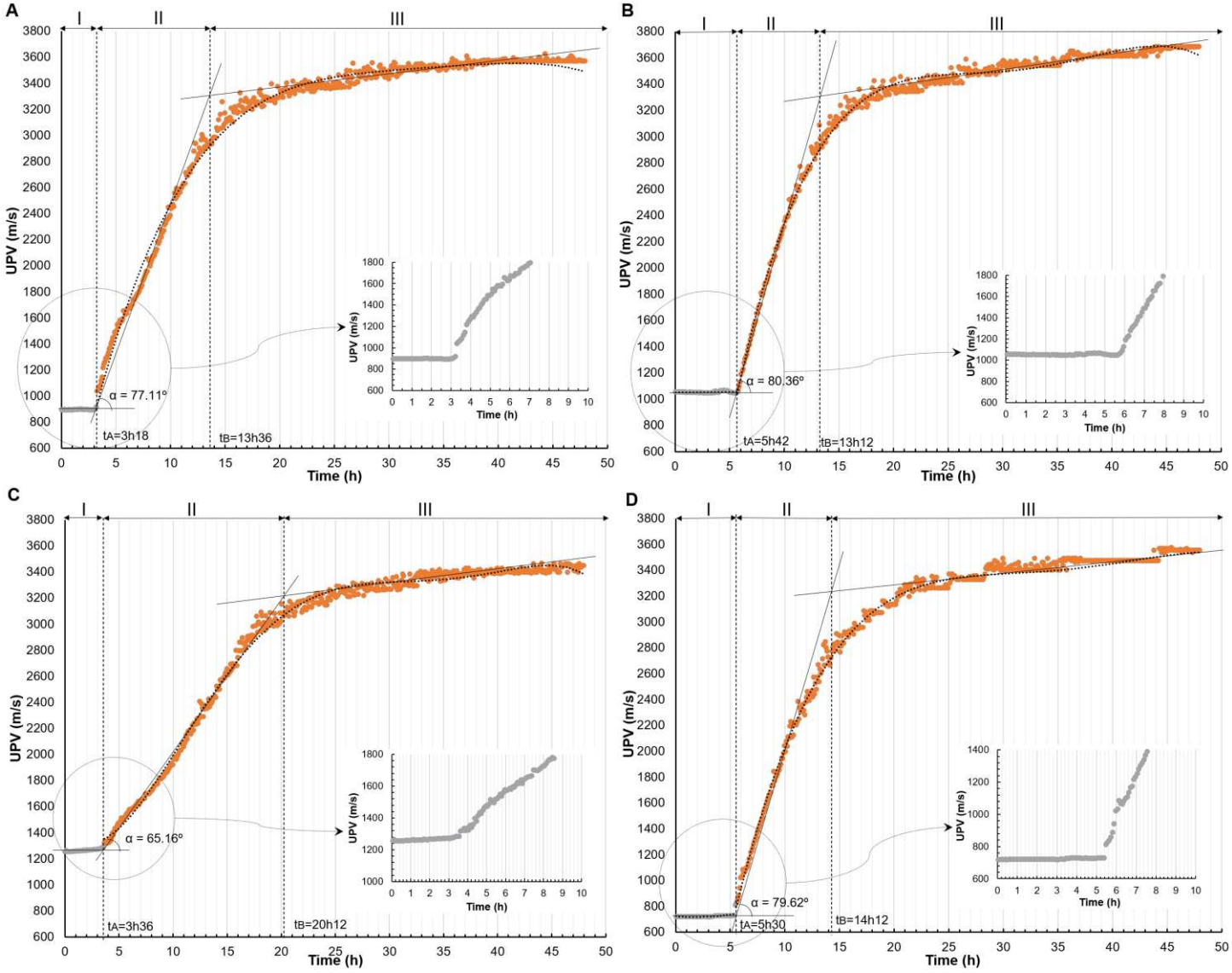

Fig. 3.7 Ultrasonic pulse velocity during the first 48 hours of hydration of the pastes (A) 100-00-0.0; (B) 100-00-0.5; (C) 75-25-0.0; and (D) 75-25-0.5.

The 75-25-0.0 blend (*Fig. 3.7C*) had a UPV around 1,250 m/s at step I of the curve, a higher velocity than observed in the 100-00-0.0 sample. This behavior can be explained by the higher specific gravity and lower fineness of steel slag than Portland cement, which could raise the contact probability between solid particles. Step II, which corresponds to the formation of the hydrated products and hardening of the paste, occurred more slowly (t_B = 20h12) was measured in the sample with greater maintenance). At step III, the curve ended at a lower UPV than the blend without SSP, around 3400 m/s, due to the low pozzolanic reactivity of slag particles [68].

Kourounis et al. [49] investigated the hydration of blended cements with steel slag and found that the addition of steel slag slowed down the hydration of blended cements and showed longer setting time than Portland cement; this is expected as the increase of steel slag content reduces the cement content in the mixture (cement dilution effect). Liao et al. [73] studied the effects of steel slag on the hydration and strength development of calcium sulfoaluminate (CSA) cement and also observed an increase in setting time of CSA cement - steel slag pastes. They explained that steel slag was denser and coarser than the CSA cement, and less steel slag was required for replacing an equal mass of CSA cement particles. Thus the interparticle distances in the freshly mixed pastes increased with the amount of steel slag replacement. The steel slag was also less reactive and took longer to produce sufficient hydration products to fill the interparticle spaces and solidify the pastes, consequently increasing setting time. The dilution effect of cement explains this behavior.

The blend with SSP and LAS-based admixture (75-25-0.5), shown in *Fig. 3.7D*, was the one with the lowest UPV in step I, around 720 m/s during the first five and half hours. Air incorporation caused by LAS in the fresh binder with SSP may account for this low value of UPV [74,75]. Step II presented an acceleration in the setting, as well as the blend 100-00-0.5, both samples containing LAS. Therefore, it can be noticed a trend of LAS to delay the initial and accelerate the final setting in the samples in which it is present, while the SSP delays the initial and final setting time. In studies conducted by Mendes et al. [61], a slight delay was observed at the beginning of the setting with an increase in the LAS-based admixture content in cement pastes. The air-entraining admixtures are surfactants that act at the solid-water interface by binding to the solid and making the surface of the cement particles hydrophobic so that the air can displace the water and remain bound to the solid particles in the form of bubbles [60]. This delay in the initial setting can be explained by the LAS-based admixture's tendency

to hinder the contact of the cement particles with the water molecules, inhibiting the dissolution-precipitation mechanism that is dominant in the early stages of cement hydration.

The XRD studies were carried out on four selected samples (100-00-0.0; 100-00-0.5; 75-25-0.0, and 75-25-0.5). The pastes' hydration kinetics were monitored over time, and the results at 1, 7, and 28 days are presented in *Fig. 3.8*. It could be observed that mineral components of hydration products primarily included ettringite ($3CaO.Al_2O_3.3CaSO_4.32H_2O$), and portlandite ($Ca(OH)_2$), part of larnite ($2CaO.SiO_2$), and alite ($3CaO.SiO_2$) are still not hydrated. Gels are not reflected because of their amorphous structure. Throughout the hydration process, the reduction of the anhydrous phases and the formation of the hydrated phases in the samples is noticeable, although with different proportions from one sample to another. The addition of LAS-based admixture to the samples (100-00-0.5 and 75-25-0.5) caused a delay in the initial setting time and hydration kinetics (Fig. 3.7), and in XRD results with one day it can be observed a lower consumption of alite by these samples (Fig. 3.8A), which can represent an effect of inhibition of hydration by LAS-based admixture.

The sample 75-25-0.0 presented higher peaks of portlandite than the other samples since the first day of testing (Fig. 3.8A-C). This feature is because the weathered slag has free lime in its composition, as shown in Figure 3, and Portlandite could result from CaO hydration. Meanwhile, sample 75-25-0.5 was the one that presented the slowest formation of hydration products, which only at 28 days (Fig. 3.8C) presented peaks with intensity closer to the other samples tested. At 28 days, persistent peaks of ettringite are observed in the blends containing steel slag (75-25-00 and 75-25-0.5). Wang et al. [74] found that the dormant period of a binder containing steel slag is longer than that of cement and extended with an increase in the steel slag addition. The steel slag decreased the early hydration rate of cement; however, it could promote cement hydration in late ages Liao et al. [73] observed that the hydration products of CSA cement - steel slag pastes, ettringite was the main crystalline hydration product, and at 28 days, ettringite peaks remained strong in all pastes.

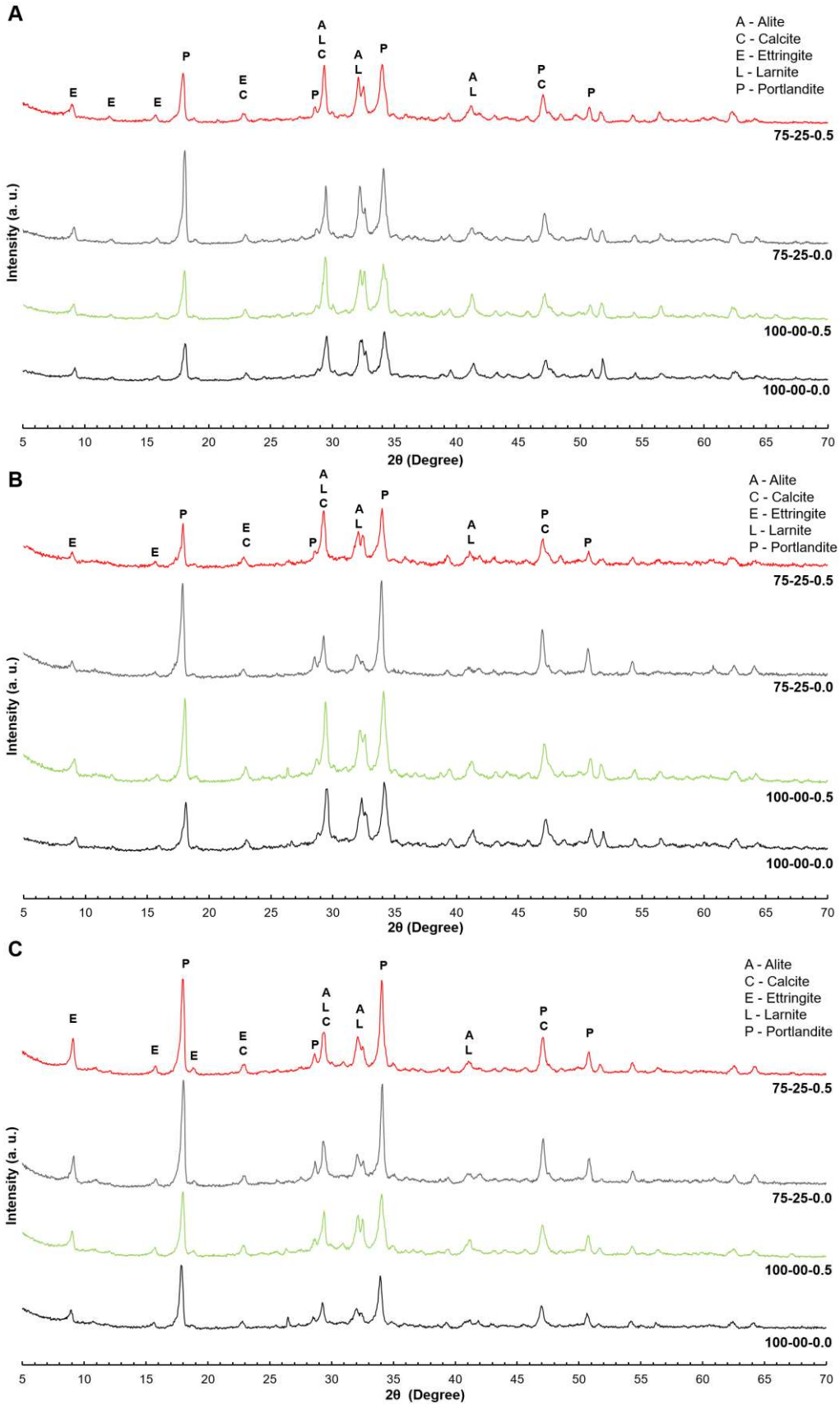

Fig. 3.8 XRD diffractograms of pastes at (A) 1 day; (B) 7 days; and (C) 28 days.

3.3.2 Performance in mortars

3.3.2.1 Consistency of the mixes

The average values (three values for each sample) of the spread diameter measurements in the flow table test are presented in *Fig. 3.9*. A progressive increase in the samples' spread is observed as the content of LAS-based admixture and the rate of SSP increases, reaching almost 10% for the sample 100-00-1.0 compared to the reference (100-00-0.0), and more than 17% for the sample 50-50-0.0. The combined effect of LAS and SSP in its highest levels (50-50-1.0) increases the spread value by more than 22% compared to the reference mortar. The blend with average contents of LAS and SSP (75-25-0.5) showed an increase of about 15% over the reference mortar.

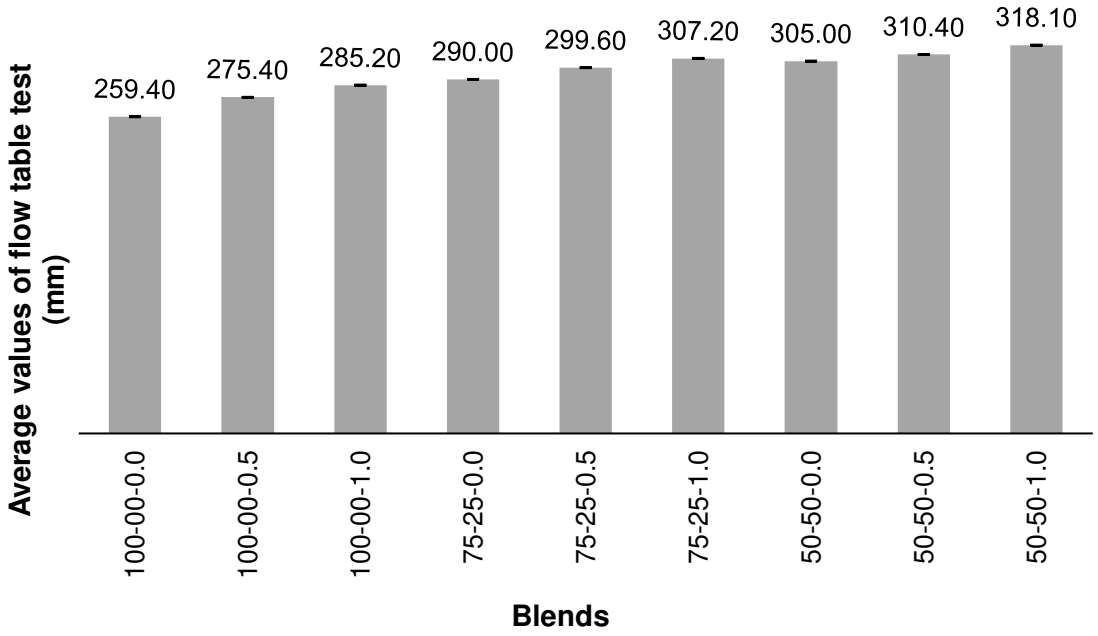

Fig. 3.9 Average spread diameter values from the flow table tests performed in all the mortars evaluated.

The obtained values of the flow table test increased linearly (P-value <0.05) as a function of increases in factors A (LAS) and B (SSP), as can be observed by the regression equation in uncoded units (Eq. 3.2). By the equation, it can be understood that the highest spread value is obtained when the SSP and LAS levels are higher and only linear factors were significant.

$$Y = 266.21 + 18.70^{*} \text{ LAS} + 0.7567^{*} \text{ SSP} \quad (3.2)$$

$$R^2 = 0.95$$

The contour and 3D surface graphs relating the LAS and SSP contents for mortar spread can be seen in *Fig. 3.*10. It is clear from *Fig. 3.10A* that the SSP was the factor that caused the greatest influence on the spread value due to the greater inclination and the number of isolines that intersect the axis. The surface graph (*Fig. 3.10B*) has a linear profile following the linear model fitted.

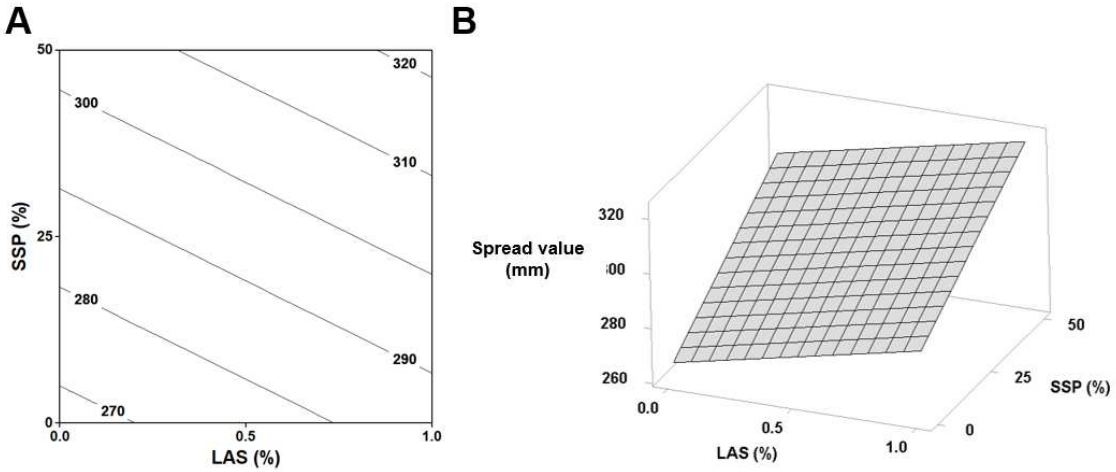

Fig. 3.10 Mortars spread value as a function of SSP and LAS (A) Contour plot (B) Surface plot.

The significant influence of SSP on the spread value of mortars should be attributed to the presence of particles with larger particle sizes than those of Portland cement, as can be seen in *Fig. 3.1*; and also due to the improved shape of its particles with volumetric aspect (*Fig. 3.2*), as it was also observed by Franco de Carvalho et al. [1].

In studies conducted by Calmon et al. [3], the mixture with 100% BOFS required a smaller amount of water to start the flow, although it had a larger Blaine specific surface area than other materials in their study. Some hypotheses were raised to explain this result: (i) the low porosity of BOFS (resulting in a lower amount of water for saturation), (ii) the shape and distribution of the grains, and, mainly (iii) the high specific gravity value of the BOFS when compared to the other cement materials studied. Since the flow table test is subject to a free-flow, the self-weight contributes significantly to the results; thus, the specific mass plays an

important role [3]. In fact, the BOFS particles have a specific mass about 14% higher than the Portland cement used.

Kourounis et al. [50] investigated the water demand of cement pastes with steel slag. They found that the binder with steel slag demanded less water than the reference cement-only paste, improving the mortar workability, and explain that the decrease in water demand is attributed to the delayed hydration of the steel slag due to its mineralogical composition. In studies conducted by Pan et al. [77], superior workability of self-compacting concrete containing steel slag powder was verified. The SSP decreased the water demand to keep the same workability.

The contribution of LAS-based admixture in the increase of mortars' plasticity was also observed by Mendes et al. [61], who compared the proposed LAS-based admixture with a commercial air-entraining admixture (AEA), and both behaved similarly, since they are synthetic anionic detergents. Furthermore, it was observed that the proposed AEA is more efficient as an air entrainer than the commercial AEA for similar dosages [61].

3.3.2.2 Microstructural analysis

The microstructural analysis of the hardened matrix was performed on four samples of mortars (100-00-0.0; 100-00-0.5; 75-25-0.0; and 75-25-0.5) resulting from the compression tests. A digital microscope was used for morphological analysis to capture the samples' images (*Fig. 3.11*). The samples without the LAS-based admixture *(Fig. 3.11A* and *3.11C*) presented a more regular matrix, with few evident pores and smaller dimensions, reinforcing that there are no matrices free of air voids, since these are results of the mixing process and constituent materials, as also observed by Mendes et al. [61]. The samples with 0.5% LAS (*Fig. 3.11B* and 3.*11D*) presented more evident pores, with different sizes well distributed throughout the matrix. These images show that the admixture actually worked as an air-entraining agent into the matrix.

The microstructural analyses were performed by scanning electron microscopy (SEM), and the fractured surfaces of mortar samples are shown in *Fig. 3.12* and *3.13*. The reference sample 100-00-0.0 presented a denser matrix, where it is possible to visualize the paste and small incorporated aggregates (*Fig. 3.12A)*. *Fig. 3.12B* shows a region where there are no apparent pores, and the discontinuity between the paste interface and the aggregate is due to the process of obtaining the fragment that underwent compression strength test. The LAS-based

admixture caused the incorporation of air by forming stable micro-bubbles in the matrix, as shown in *Fig. 3.12C* and 3.*13C*.

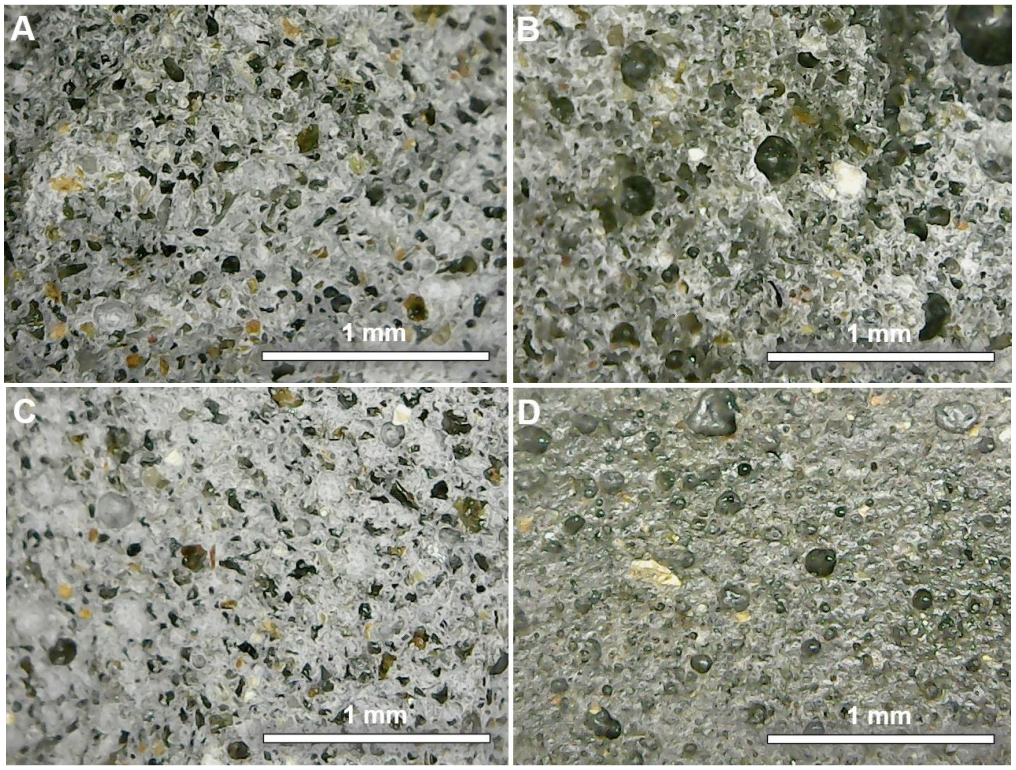

Fig. 3.11 Images of mortar samples (A) 100-00-0.0; (B) 100-00-0.5; (C) 75-25-0.0; and (D) 75-25-0.5.

The blend of cement with steel slag (75-25-0.0) presented a matrix with some small pores and heterogeneous aspects due to the unreacted SSP particles partially replacing PC (*Fig. 3.13A*). *Fig. 3.13B* and 3.*13D* show crystallized needle-shaped ettringite inside pores, and in fact, persistent peaks of ettringite were also observed in XRD patterns at 28 days. A high density of typical plates of $Ca(OH)_2$ and the amorphous structure of the C-S-H gel are also observed in *Fig. 3.12D, 3.13B* and 3.*13D*.

Atahan et al. [78] studied the surface structures of entrained air voids in hardened cement paste. They studied the effect of three different pure anionic surfactants: sodium dodecyl sulfonate (SDS), sodium dodecyl-benzene sulfonate (SDBS), and sodium oleate (SO). At 7-days of hydration, they observed that a number of voids were spotted with the growth of various hydration products, such as $Ca(OH)_2$ and needle-like crystals, that may either be ettringite or a form of calcium silicate hydrate. The crystals' appearance may indicate the existence of a water layer on the void surface during the hydration process. Furthermore, excessive growth of

hydration products within the entrained air voids may also reduce the air void performance during freeze-thaw cycles [78].

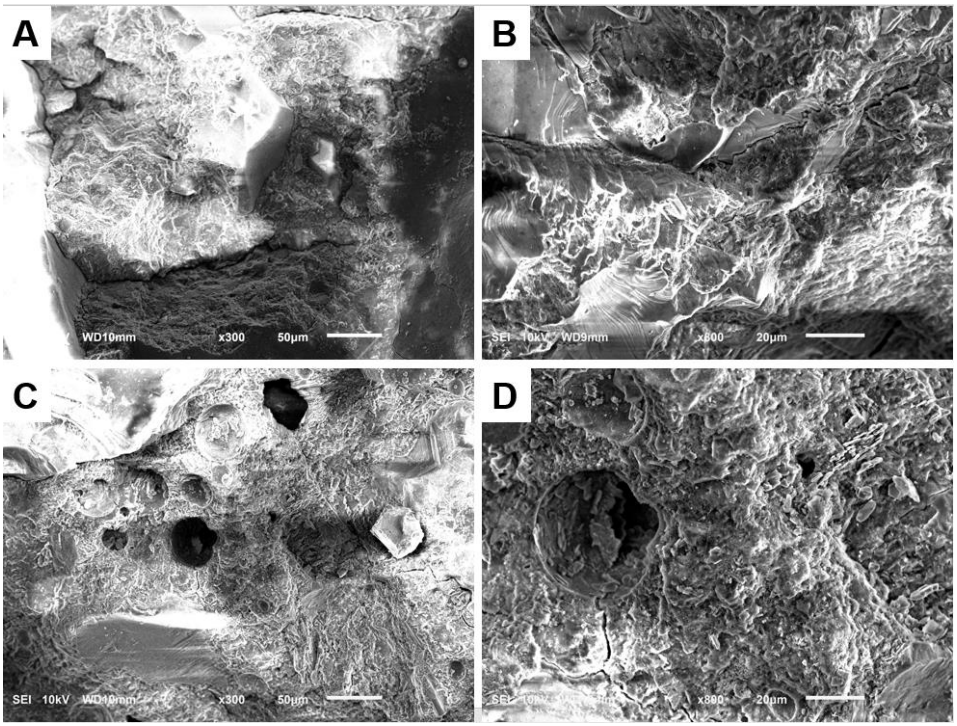

Fig. 3.12 SEM images of the mortar samples (A-B) 100-00-0.0 and (C-D) 100-00-0.5.

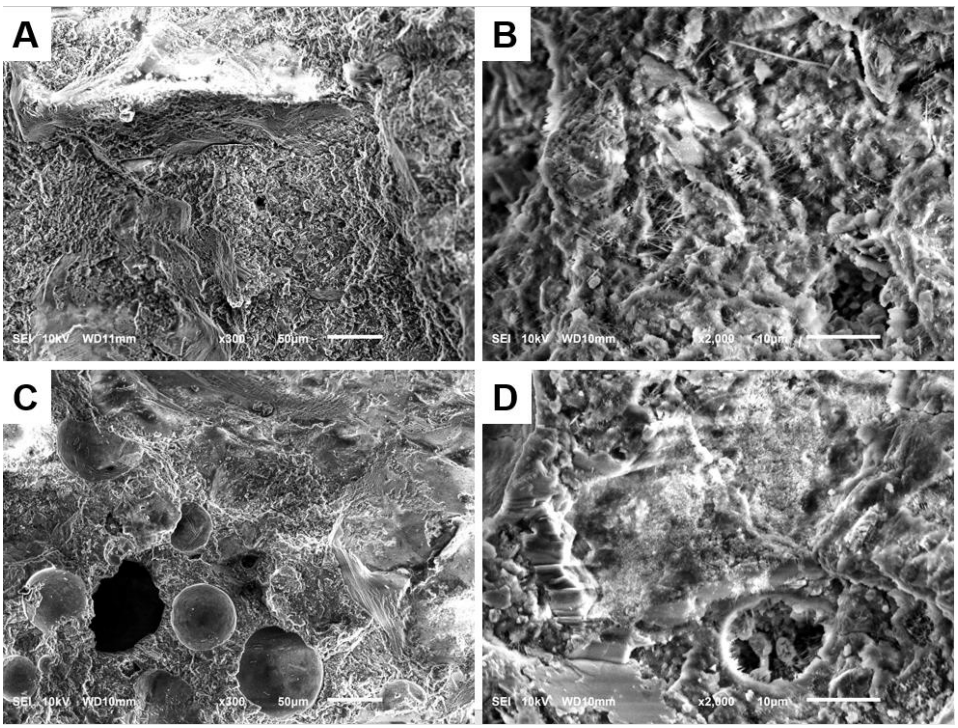

Fig. 3.13 SEM images of the mortar samples (A-B) 75-25-0.0 and (C-D) 75-25-0.5.

Mendes et al. [61] also evaluated the morphological of the hardened matrix with air-entraining agents (LAS and commercial AEA) and noted that the pore content increases with surfactant increase dosing, their average size increased, and they were more spread over the cross-section. The reference matrix and matrices with low AEA content presented small and medium pores, sparse and scattered, and more angular, leaving large matrix areas intact. In turn, the voids from the sections with intermediate AEA content were small and medium-sized, well distributed throughout the matrix and less angular. For similar dosages, LAS resulted in a more stable voids system on the hardened state than the commercial AEA.

3.3.2.3 Compressive strength development

The results of the compressive strength tests on mortars are given in *Fig. 3.14.* Mechanical tests were performed on the nine blends studied at five different test ages (1, 3,7, 28, and 63 days). The strength for all mixes increased with the curing period, although they presented different growth rates; this is mainly due to cement hydration and the accumulation of hydration products, affected by the incorporation of LAS-based admixture and steel slag powder.

It is observed that the 100-00-0.0 sample presented greater initial strength, which was gradually followed by 100-00-0.5 and by 75-25-0.0. For the 25% cement replacement by SSP, good mechanical strength results were obtained, showing a good performance of steel slag powder as supplementary cementing material (SCM) for this dosage. It is noticed that the LAS-based admixture and SSP delayed the beginning of the cement hydration, as seen in the results of UPV (*Fig. 3.7B and 3.7C*, respectively). Nevertheless, in step II of the hydration, the sample 100-0-0.5 followed the reference sample accelerating the final setting, while 75-25-0.0 presented a slower formation of hydration product, as seen in step II of the UPV curve. In addition, the XRD patterns (*Fig. 3.8*) showed the effect of hydration inhibition caused by LAS, with less consumption of the anhydrous phases, and the SSP showed low reactivity and slow formation of hydration products. These factors were the main responsible for the drop in the specimens' mechanical strength (especially in the first ages) by increasing the matrix porosity by the LAS's action and the dilution effect by the partial cement replacement.

As shown in blends with 1.0% of LAS-based admixture, the decrease in compressive strength was 25% in the conventional blend (100% cement), 33% in samples with 25% SSP, and 40% in samples with 50% SSP at 28 days. Since air-entraining surfactants make cement particles hydrophobic, excessive dosage of the admixture can difficult the formation of cement

hydration products, and the mixtures may suffer a corresponding lack of mechanical performance [60]. Furthermore, reduction in compressive strength can also be attributed to the increased porosity of the samples containing LAS due to the incorporation of air microbubbles, as shown in the micrographs (*Fig. 3.12C and 3.12D; and Fig. 3.13C and 3.13D).* Similar results were obtained by Mendes et al. [61] due to the increase of the air-entraining admixture (AEA), and the relationship of mechanical strength and increase in porosity is widely known in the literature. The volume of all the voids influences the compressive strength: trapped air, capillary pores, gel pores, and incorporated air [58].

Besides the effect of LAS, the replacement of 50% of cement by SSP also caused damage in the compressive strength. The mechanical performance of the 50-50-0.0 was 57% lower than the 100-00-0.0 at 28 days. Other authors found similar results. As the amount of SSP replacing PC increases, the compressive strength of the samples decreases, which could be a result of the low hydration activity of the SSP [40,50–52].

At 63-days of hydration, the percentage gain in strength was greater in samples 50-50-1.0, reaching 38% compared to the compressive strength at 28-days. However, the samples containing the high percentage of BOFS continued with the strength well below the reference sample. The mortar 50-50-1.0, for example, presented 30% of the reference mortar's strength.

Mechanical strength at 28 days decreased linearly (P-value <0.05) as a function of increases in factors A (LAS) and B (SSP), as can be observed by the regression equation in uncoded units (Eq. 3.3). By the equation, it can be concluded that both factors cause damage to mechanical strength, being the incorporation of SSP the most prejudicial. Again, only linear factors were significant.

$$Y = 41.39 - 10.20^{*} LAS - 0.4307^{*} SSP \quad (3.3)$$

$$R^2 = 0.943$$

The contour and 3D surface graphs relating the LAS and SSP contents for mortar mechanical strength at 28 days can be seen in *Figure 3.15*. It is clear from *Figure 3.15A* that the SSP was the factor that caused the greatest influence on compressive strength due to the greater inclination and the number of isolines that intersect the SSP axis. The surface graph (*Figure 3.15B*) has a linear profile following the linear model fitted.

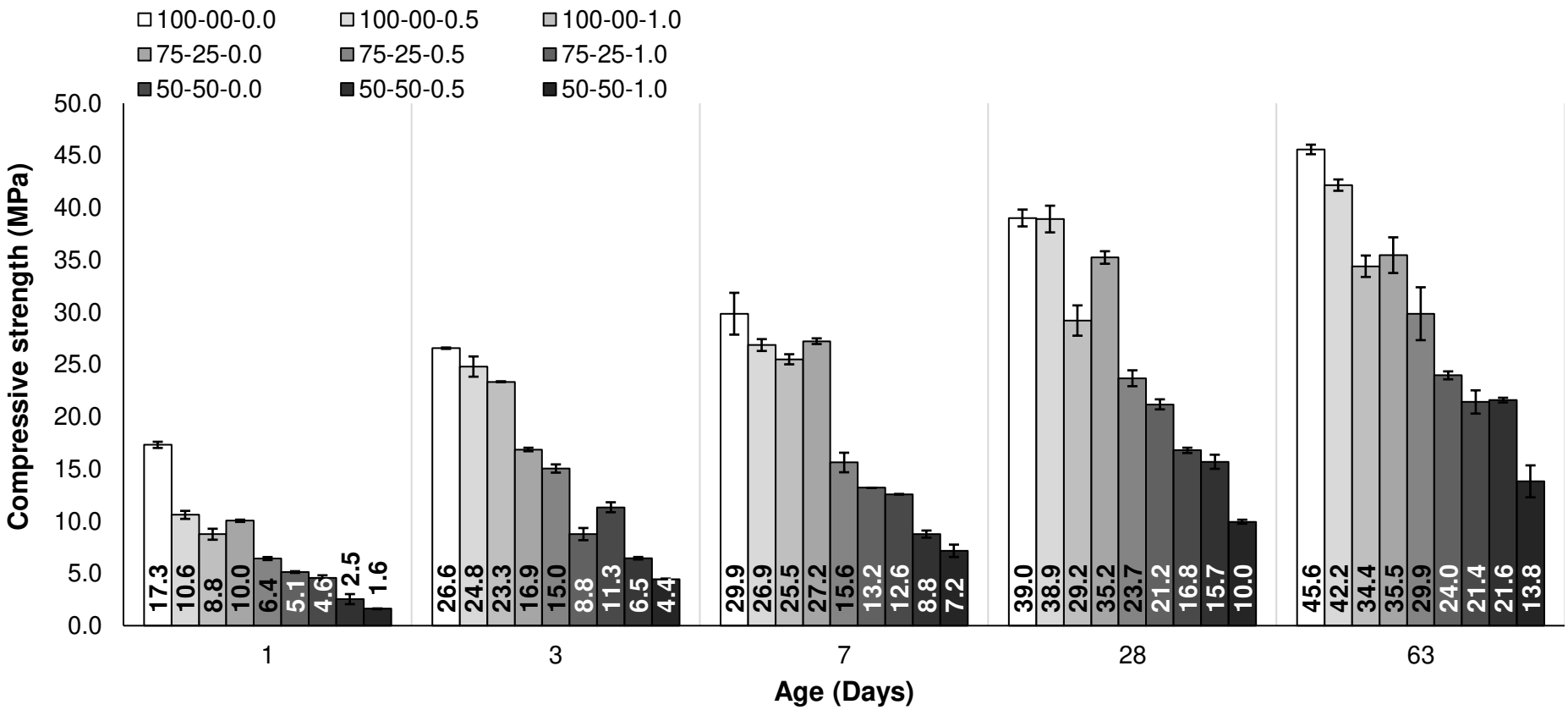

Fig. 3.14 Results of compressive strength of the studied mortars.

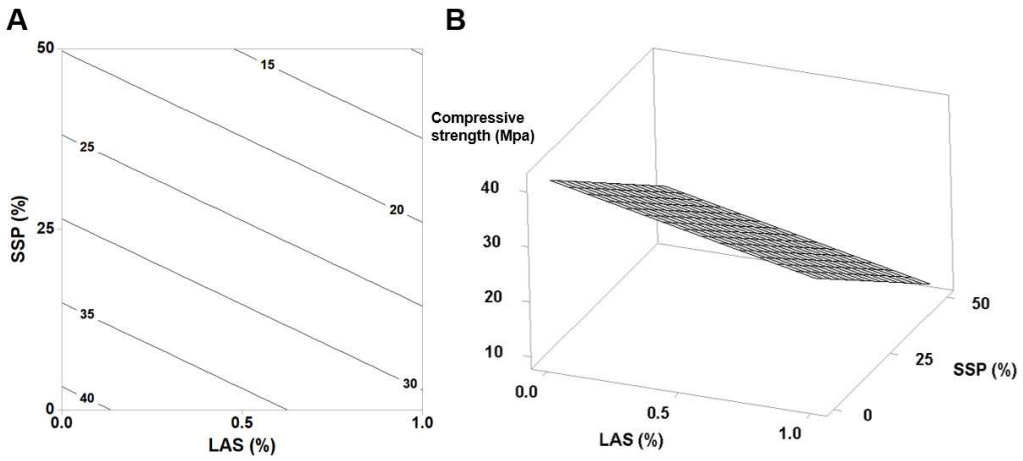

Fig. 3.15 Mortars compressive strength as a function of SSP and LAS (A) Contour plot (B) Surface plot.

3.4 Conclusion

An experimental investigation of the effects of a LAS-based admixture and steel slag powder on the properties of cement-based composites was developed in this work. Based on the results, the following conclusions can be summarized:

- The mortar's spread value in the flow table test is governed by a linear function, in which the increase in LAS and SSP contents caused the increase of the spread value, and SSP was the factor that had the most influence. An increase of more than 22% was achieved by the sample 50-50-1.0 compared to the reference mortar. The significant influence of SSP should be attributed to the improved shape of its particles, with volumetric aspect, and their high specific gravity.
- For the 25% cement replacement by SSP, good mechanical strength results were obtained, showing a good performance of steel slag powder as supplementary cementing material (SCM) for this dosage.
- Both LAS-based admixture and SSP delayed the setting time, influencing the hydration kinetics. The LAS hindered the contact between cement particles and water molecules, inhibiting the hydration mechanism by dissolution-precipitation. Moreover, the SSP caused a dilution effect that interfered directly in the setting time and slowed down the hydration of blended cements, as it was less reactive and took longer to produce sufficient hydration products to solidify the pastes.

- The mortars produced with the LAS-based admixture showed air incorporation evidenced by the appearance of pores with spherical shapes well distributed by the matrix.
- The compressive strength decreased linearly with the increase in LAS and SSP contents. A 57% reduction in mechanical strength was observed in the mortar 50-50-0.0 compared to the reference mortar (100-00-0.0) at 28 days. The low hydration activity of the SSP and the dilution effect of the cement in the blend are the main responsible for this reduction in the mechanical strength. In addition, the LAS-based admixture difficulted the formation of cement hydration products, and the incorporation of air increased porosity and consequently affected the strength.

Acknowledgments

This study was financed in part by the Coordenção de Aperfeiçoamento de Pessoal de Nível Superior – Brasil (CAPES) – Finance code 001. The authors also acknowledge the support provided by the Fundação de Amparo à Pesquisa do Estado de Minas Gerais (FAPEMIG), Conselho Nacional de Desenvolvimento Científico e Tecnológico (CNPq),Universidade Federal de Viçosa (UFV), and Universidade Federal de Ouro Preto (UFOP). Equipment and technical support provided by the Laboratory of Construction Materials, Department of Civil Engineering, UFV; Composite Materials Laboratory, UFV; Laboratory of Construction Materials, Department of Civil Engineering, UFOP; and Physics Department UFV. Thanks are also due to the Brazilian research groups SICon-CNPq/ UFV and RECICLOS-CNPq/UFOP for the infrastructure and collaboration.

References

[1] J.M. Franco de Carvalho, T.V. de Melo, W.C. Fontes, J.O. dos S. Batista, G.J. Brigolini, R.A.F. Peixoto, More eco-efficient concrete: An approach on optimization in the production and use of waste-based supplementary cementing materials, Constr. Build. Mater. 206 (2019) 397–409. https://doi.org/10.1016/j.conbuildmat.2019.02.054.

[2] T. Zhang, Q. Yu, J. Wei, J. Li, P. Zhang, Preparation of high performance blended cements and reclamation of iron concentrate from basic oxygen furnace steel slag, Resour. Conserv. Recycl. 56 (2011) 48–55. https://doi.org/10.1016/j.resconrec.2011.09.003.

[3] J.L. Calmon, F.A. Tristão, M. Giacometti, M. Meneguelli, M. Moratti, J.E.S.L. Teixeira, Effects of BOF steel slag and other cementitious materials on the rheological

properties of self-compacting cement pastes, Constr. Build. Mater. 40 (2013) 1046–1053. https://doi.org/10.1016/j.conbuildmat.2012.11.039.

[4] P. Xue, A. Xu, D. He, Q. Yang, G. Liu, F. Engström, B. Björkman, Research on the sintering process and characteristics of belite sulphoaluminate cement produced by BOF slag, Constr. Build. Mater. 122 (2016) 567–576. https://doi.org/10.1016/j.conbuildmat.2016.06.098.

[5] C.J. Tsai, R. Huang, W.T. Lin, H.N. Wang, Mechanical and cementitious characteristics of ground granulated blast furnace slag and basic oxygen furnace slag blended mortar, Mater. Des. 60 (2014) 267–273. https://doi.org/10.1016/j.matdes.2014.04.002.

[6] J. Lederer, A. Gassner, F. Kleemann, J. Fellner, Potentials for a circular economy of mineral construction materials and demolition waste in urban areas: a case study from Vienna, Resour. Conserv. Recycl. 161 (2020) 104942. https://doi.org/10.1016/j.resconrec.2020.104942.

[7] M.S. Aslam, B. Huang, L. Cui, Review of construction and demolition waste management in China and USA, J. Environ. Manage. 264 (2020) 110445. https://doi.org/10.1016/j.jenvman.2020.110445.

[8] G. Tavakoli Mehrjardi, A. Azizi, A. Haji-Azizi, G. Asdollafardi, Evaluating and improving the construction and demolition waste technical properties to use in road construction, Transp. Geotech. 23 (2020) 100349. https://doi.org/10.1016/j.trgeo.2020.100349.

[9] A.R.G. Azevedo, D. Cecchin, D.F. Carmo, F.C. Silva, C.M.O. Campos, T.G. Shtrucka, M.T. Marvila, S.N. Monteiro, Analysis of the compactness and properties of the hardened state of mortars with recycling of construction and demolition waste (CDW), J. Mater. Res. Technol. 9 (2020) 5942–5952. https://doi.org/10.1016/j.jmrt.2020.03.122.

[10] P. Sormunen, T. Kärki, Recycled construction and demolition waste as a possible source of materials for composite manufacturing, J. Build. Eng. 24 (2019) 100742. https://doi.org/10.1016/j.jobe.2019.100742.

[11] S. Souza, M. Franco, G.G. Silveira, R. Andr, Application of Construction and Demolition Waste in Civil Construction in the Brazilian Amazon — Case Study of the City of Rio Branco, (2021).

[12] B.C. Mendes, L.G. Pedroti, M.P.F. Fontes, J.C.L. Ribeiro, C.M.F. Vieira, A.A. Pacheco, A.R.G. de Azevedo, Technical and environmental assessment of the incorporation of iron ore tailings in construction clay bricks, Constr. Build. Mater. 227 (2019) 116669. https://doi.org/10.1016/j.conbuildmat.2019.08.050.

[13] K. do C. e S. Defáveri, L.F. dos Santos, J.M. Franco de Carvalho, R.A.F. Peixoto, G.J. Brigolini, Iron ore tailing-based geopolymer containing glass wool residue: A study of mechanical and microstructural properties, Constr. Build. Mater. 220 (2019) 375–385. https://doi.org/10.1016/j.conbuildmat.2019.05.181.

[14] W.C. Fontes, J.M. Franco de Carvalho, L.C.R. Andrade, A.M. Segadães, R.A.F. Peixoto, Assessment of the use potential of iron ore tailings in the manufacture of ceramic tiles: From tailings-dams to “brown porcelain,” Constr. Build. Mater. 206 (2019) 111–121. https://doi.org/10.1016/j.conbuildmat.2019.02.052.

[15] W. Zhang, X. Gu, J. Qiu, J. Liu, Y. Zhao, X. Li, Effects of iron ore tailings on the compressive strength and permeability of ultra-high performance concrete, Constr. Build. Mater. 260 (2020) 119917. https://doi.org/10.1016/j.conbuildmat.2020.119917.

[16] G. Fares, M.H. Albaroud, M.I. Khan, Fine limestone dust from ornamental stone factories: A potential filler for a high-performance cementitious matrix, Constr. Build. Mater. 224 (2019) 428–438. https://doi.org/10.1016/j.conbuildmat.2019.07.027.

[17] R. Zulcão, J.L. Calmon, T.A. Rebello, D.R. Vieira, Life cycle assessment of the ornamental stone processing waste use in cement-based building materials, Constr. Build. Mater. 257 (2020). https://doi.org/10.1016/j.conbuildmat.2020.119523.
[18] J. dos S. Vazzoler, G.L. Vieira, C.R. Teles, M.K. Degen, R.A. Teixeira, Investigation of the potential use of waste from ornamental stone processing after heat treatment for the production of cement-based paste, Constr. Build. Mater. 177 (2018) 314–321. https://doi.org/10.1016/j.conbuildmat.2018.05.098.
[19] D.P. Fassoni, R.C. Alvarenga, L. Pedrotti, B. Mendes, Clinker Production from Wastes of Cellulose and Granite Industries, Charact. Miner. Met. Mater. 2016 (2016) 691–696.
[20] A.L. de Oliveira Júnior, L.G. Pedroti, J. de Assis Oliveira, W.E. Hilarino Fernandes, A.G. Fineza, S.N. Monteiro, G.H. Nalon, The influence of partial replacement of natural sand aggregates by grits residues on the mechanical properties of an ecological mortar, J. Build. Eng. 26 (2019) 100912. https://doi.org/10.1016/j.jobe.2019.100912.
[21] M. Saeli, L. Senff, D.M. Tobaldi, J. Carvalheiras, M.P. Seabra, J.A. Labrincha, Unexplored alternative use of calcareous sludge from the paper-pulp industry in green geopolymer construction materials, Constr. Build. Mater. 246 (2020) 118457. https://doi.org/10.1016/j.conbuildmat.2020.118457.
[22] J.M. Franco de Carvalho, P.A.M. Campos, K. Defáveri, G.J. Brigolini, L.G. Pedroti, R.A.F. Peixoto, Low environmental impact cement produced entirely from industrial and mining waste, J. Mater. Civ. Eng. 31 (2019). https://doi.org/10.1061/(ASCE)MT.1943-5533.0002617.
[23] D.H. Diniz, J.M.F. de Carvalho, J.C. Mendes, R.A.F. Peixoto, Blast oxygen furnace slag as chemical soil stabilizer for use in roads, J. Mater. Civ. Eng. 29 (2017) 3–9. https://doi.org/10.1061/(ASCE)MT.1943-5533.0001969.
[24] L.C. Franco, J.C. Mendes, L.C.B. Costa, R.R. Pira, R.A.F. Peixoto, Design and thermal evaluation of a social housing model conceived with bioclimatic principles and recycled aggregates, Sustain. Cities Soc. 51 (2019) 101725. https://doi.org/10.1016/j.scs.2019.101725.
[25] A.L.B. Marinho, C.M. Mol Santos, J.M.F. de Carvalho, J.C. Mendes, G.J. Brigolini, R.A.F. Peixoto, Ladle furnace slag as binder for cement-based composites, J. Mater. Civ. Eng. 29 (2017). https://doi.org/10.1061/(ASCE) MT.1943-5533.0002061.
[26] A. Santamaría, A. Orbe, J.T. San José, J.J. González, A study on the durability of structural concrete incorporating electric steelmaking slags, Constr. Build. Mater. 161 (2018) 94–111. https://doi.org/10.1016/j.conbuildmat.2017.11.121.
[27] S.K. Singh, P. Rekha, M. Surya, Utilization of Linz–Donawitz slag from steel industry for waste minimization, J. Mater. Cycles Waste Manag. 22 (2020) 611–627. https://doi.org/10.1007/s10163-020-00981-z.
[28] D. Wang, J. Chang, W.S. Ansari, The effects of carbonation and hydration on the mineralogy and microstructure of basic oxygen furnace slag products, J. CO2 Util. 34 (2019) 87–98. https://doi.org/10.1016/j.jcou.2019.06.001.
[29] N. Zhang, L. Wu, X. Liu, Y. Zhang, Structural characteristics and cementitious behavior of basic oxygen furnace slag mud and electric arc furnace slag, Constr. Build. Mater. 219 (2019) 11–18. https://doi.org/10.1016/j.conbuildmat.2019.05.156.
[30] J.L. Calmon, Resíduos Industriais e Agrícolas, in: G.C. Isaia (Ed.), Mater. Construção Civ. e Princípios Ciência e Eng. Mater., 2nd ed., IBRACON, São Paulo, 2010: pp. 1651–87.
[31] C. Shi, Steel slag - Its production, processing, characteristics, and cementitious properties, J. Mater. Civ. Eng. 16 (2004) 230–236. https://doi.org/10.1061/(ASCE)0899-1561(2004)16:3(230).
[32] I.Z. Yildirim, M. Prezzi, Chemical, mineralogical, and morphological properties of

steel slag, Adv. Civ. Eng. 2011 (2011). https://doi.org/10.1155/2011/463638.
[33] H. Yi, G. Xu, H. Cheng, J. Wang, Y. Wan, H. Chen, An Overview of Utilization of Steel Slag, Procedia Environ. Sci. 16 (2012) 791–801. https://doi.org/10.1016/j.proenv.2012.10.108.
[34] Q. Wang, P. Yan, Hydration properties of basic oxygen furnace steel slag, Constr. Build. Mater. 24 (2010) 1134–1140. https://doi.org/10.1016/j.conbuildmat.2009.12.028.
[35] Y. Jiang, T.C. Ling, C. Shi, S.Y. Pan, Characteristics of steel slags and their use in cement and concrete—A review, Resour. Conserv. Recycl. 136 (2018) 187–197. https://doi.org/10.1016/j.resconrec.2018.04.023.
[36] S. Wang, C. Wang, Q. Wang, Z. Liu, W. Qian, C.Z. Jin, L. Chen, L. Li, Study on cementitious properties and hydration characteristics of steel slag, Polish J. Environ. Stud. 27 (2018) 357–364. https://doi.org/10.15244/pjoes/74133.
[37] J. Li, Q. Yu, J. Wei, T. Zhang, Structural characteristics and hydration kinetics of modified steel slag, Cem. Concr. Res. 41 (2011) 324–329. https://doi.org/10.1016/j.cemconres.2010.11.018.
[38] Y. Guo, J. Xie, W. Zheng, J. Li, Effects of steel slag as fine aggregate on static and impact behaviours of concrete, Constr. Build. Mater. 192 (2018) 194–201. https://doi.org/10.1016/j.conbuildmat.2018.10.129.
[39] Q. Wang, D. Wang, S. Zhuang, The soundness of steel slag with different free CaO and MgO contents, Constr. Build. Mater. 151 (2017) 138–146. https://doi.org/10.1016/j.conbuildmat.2017.06.077.
[40] X. Han, J. Feng, Y. Shao, R. Hong, Influence of a steel slag powder-ground fly ash composite supplementary cementitious material on the chloride and sulphate resistance of mass concrete, Powder Technol. 370 (2020) 176–183. https://doi.org/10.1016/j.powtec.2020.05.015.
[41] J.M. Franco de Carvalho, W.C. Fontes, C.F. de Azevedo, G.J. Brigolini, W. Schmidt, R.A.F. Peixoto, Enhancing the eco-efficiency of concrete using engineered recycled mineral admixtures and recycled aggregates, J. Clean. Prod. 257 (2020). https://doi.org/10.1016/j.jclepro.2020.120530.
[42] J. Zhao, D. Wang, P. Yan, Design and experimental study of a ternary blended cement containing high volume steel slag and blast-furnace slag based on Fuller distribution model, Constr. Build. Mater. 140 (2017) 248–256. https://doi.org/10.1016/j.conbuildmat.2017.02.119.
[43] J.J. Chen, P.L. Ng, A.K.H. Kwan, L.G. Li, Lowering cement content in mortar by adding superfine zeolite as cement replacement and optimizing mixture proportions, J. Clean. Prod. 210 (2019) 66–76. https://doi.org/10.1016/j.jclepro.2018.11.007.
[44] D. Fernández-González, J. Prazuch, I. Ruiz-Bustinza, C. González-Gasca, J. Piñuela-Noval, L.F. Verdeja, The treatment of Basic Oxygen Furnace (BOF) slag with concentrated solar energy, Sol. Energy. 180 (2019) 372–382. https://doi.org/10.1016/j.solener.2019.01.055.
[45] L. Ma, D. Xu, S. Wang, X. Gu, Expansion inhibition of steel slag in asphalt mixture by a surface water isolation structure, Road Mater. Pavement Des. 0 (2019) 1–15. https://doi.org/10.1080/14680629.2019.1601588.
[46] Y.C. Ding, T.W. Cheng, P.C. Liu, W.H. Lee, Study on the treatment of BOF slag to replace fine aggregate in concrete, Constr. Build. Mater. 146 (2017) 644–651. https://doi.org/10.1016/j.conbuildmat.2017.04.164.
[47] L. V. Fisher, A.R. Barron, The recycling and reuse of steelmaking slags — A review, Resour. Conserv. Recycl. 146 (2019) 244–255. https://doi.org/10.1016/j.resconrec.2019.03.010.

[48] M.J. Da Silva, B.P. De Souza, J.C. Mendes, G.J.S. Brigolini, S.N. Da Silva, R.A.F. Peixoto, Feasibility study of steel slag aggregates in precast concrete pavers, ACI Mater. J. 113 (2016) 439–446. https://doi.org/10.14359/51688986.
[49] C. Shi, J. Qian, High performance cementing materials from industrial slags - A review, Resour. Conserv. Recycl. 29 (2000) 195–207. https://doi.org/10.1016/S0921-3449(99)00060-9.
[50] S. Kourounis, S. Tsivilis, P.E. Tsakiridis, G.D. Papadimitriou, Z. Tsibouki, Properties and hydration of blended cements with steelmaking slag, Cem. Concr. Res. 37 (2007) 815–822. https://doi.org/10.1016/j.cemconres.2007.03.008.
[51] Q. Wang, J. Yang, P. Yan, Cementitious properties of super-fine steel slag, Powder Technol. 245 (2013) 35–39. https://doi.org/10.1016/j.powtec.2013.04.016.
[52] Q. Wang, P. Yan, J. Yang, B. Zhang, Influence of steel slag on mechanical properties and durability of concrete, Constr. Build. Mater. 47 (2013) 1414–1420. https://doi.org/10.1016/j.conbuildmat.2013.06.044.
[53] X. Zhu, H. Hou, X. Huang, M. Zhou, W. Wang, Enhance hydration properties of steel slag using grinding aids by mechanochemical effect, Constr. Build. Mater. 29 (2012) 476–481. https://doi.org/10.1016/j.conbuildmat.2011.10.064.
[54] C. Shi, S. Hu, Cementitious properties of ladle slag fines under autoclave curing conditions, Cem. Concr. Res. 33 (2003) 1851–1856. https://doi.org/10.1016/S0008-8846(03)00211-4.
[55] G. Qian, D.D. Sun, J.H. Tay, Z. Lai, G. Xu, Autoclave properties of kirschsteinite-based steel slag, Cem. Concr. Res. 32 (2002) 1377–1382. https://doi.org/10.1016/S0008-8846(02)00790-1.
[56] Z. Li, S. Zhao, X. Zhao, T. He, Cementitious property modification of basic oxygen furnace steel slag, Constr. Build. Mater. 48 (2013) 575–579. https://doi.org/10.1016/j.conbuildmat.2013.07.068.
[57] L. Qi, J. Liu, Q. Liu, Compound Effect of CaCO3 and CaSO4·2H2O on the Strength of Steel Slag - Cement Binding Materials, Mater. Res. 19 (2016) 269–275. https://doi.org/10.1590/1980-5373-MR-2015-0387.
[58] A.M. Neville, Propriedades do Concreto, 5th ed., Bookman, Porto Alegre, 2016.
[59] H. Hartmann, C.; Jeknavorian, A.; Silva, D.; Benini, Aditivos Químicos para Concretos e Cimentos, in: G.C. Isaia (Ed.), Concreto Ciência e Tecnol., 1st ed., IBRACON, São Paulo, 2011: pp. 347–80.
[60] P.J.M. Mehta, P. K.; Monteiro, Concreto: Microestrutura, Propriedades e Materiais, 2nd ed., IBRACON, São Paulo, 2014.
[61] J.C. Mendes, T.K. Moro, A.S. Figueiredo, K.D. do C. Silva, G.C. Silva, G.J.B. Silva, R.A.F. Peixoto, Mechanical, rheological and morphological analysis of cement-based composites with a new LAS-based air entraining agent, Constr. Build. Mater. 145 (2017) 648–661. https://doi.org/10.1016/j.conbuildmat.2017.04.024.
[62] ABNT, NBR 16697: Cimento Portland - Requisitos, Associação Brasileira de Normas Técnicas, Rio de Janeiro, 2018.
[63] S.A. Bombril, Ficha de informações de segurança de produtos químicos - FISPQ - Detergente Limpol, 2019.
[64] J.M. Franco de Carvalho, K. Defáveri, J.C. Mendes, W. Schmidt, H.C. Kühne, R.A.F. Peixoto, Influence of particle size-designed recycled mineral admixtures on the properties of cement-based composites, Constr. Build. Mater. 272 (2021). https://doi.org/10.1016/j.conbuildmat.2020.121640.
[65] ASTM, ASTM C305: Standard Practice for Mechanical Mixing of Hydraulic Cement Pastes and Mortars of Plastic Consistency, ASTM International, West Conshohocken, 2020.

[66] ASTM, ASTM C230: Standard Specification for Flow Table for Use in Tests of Hydraulic Cement, ASTM International, West Conshohocken, 2021.
[67] J. Zhang, L. Qin, Z. Li, Hydration monitoring of cement-based materials with resistivity and ultrasonic methods, Mater. Struct. Constr. 42 (2009) 15–24. https://doi.org/10.1617/s11527-008-9363-0.
[68] S. Zhang, Y. Zhang, Z. Li, Ultrasonic monitoring of setting and hardening of slag blended cement under different curing temperatures by using embedded piezoelectric transducers, Constr. Build. Mater. 159 (2018) 553–560. https://doi.org/10.1016/j.conbuildmat.2017.10.124.
[69] H.K. Lee, K.M. Lee, Y.H. Kim, H. Yim, D.B. Bae, Ultrasonic in-situ monitoring of setting process of high-performance concrete, Cem. Concr. Res. 34 (2004) 631–640. https://doi.org/10.1016/j.cemconres.2003.10.012.
[70] Y. Lu, H. Ma, Z. Li, Ultrasonic monitoring of the early-age hydration of mineral admixtures incorporated concrete using cement-based piezoelectric composite sensors, J. Intell. Mater. Syst. Struct. 26 (2015) 280–291. https://doi.org/10.1177/1045389X14525488.
[71] J.R. de Freitas, Influência da Substituição Parcial de Cimento Portland por Cinzas do Bagaço de Cana-de-açúcar nos Tempos de Início e Fim de Pega e no Calor de Hidratação de Produtos Cimentícios, Universidade Estadual do Norte Fluminence Darcy Ribeiro, 2013.
[72] F.G.D. Machado, Avaliação das propriedades físicas e mecânicas do concreto de pós reativos utilizando resíduo de granito, no estado fresco e endurecido, Universidade Federal de Viçosa, 2019.
[73] Y. Liao, G. Jiang, K. Wang, S. Al, W. Yuan, Effect of steel slag on the hydration and strength development of calcium sulfoaluminate cement, Constr. Build. Mater. 265 (2020) 120301. https://doi.org/10.1016/j.conbuildmat.2020.120301.
[74] J. Zhu, S.H. Kee, D. Han, Y. Te Tsai, Effects of air voids on ultrasonic wave propagation in early age cement pastes, Cem. Concr. Res. 41 (2011) 872–881. https://doi.org/10.1016/j.cemconres.2011.04.005.
[75] S. Zhang, Y. Zhang, Z. Li, Ultrasonic monitoring of setting and hardening of slag blended cement under different curing temperatures by using embedded piezoelectric transducers, Constr. Build. Mater. 159 (2018) 553–560. https://doi.org/10.1016/j.conbuildmat.2017.10.124.
[76] Q. Wang, P.Y. Yan, S. Han, The influence of steel slag on the hydration of cement during the hydration process of complex binder, Sci. China Technol. Sci. 54 (2011) 388–394. https://doi.org/10.1007/s11431-010-4204-0.
[77] Z. Pan, J. Zhou, X. Jiang, Y. Xu, R. Jin, J. Ma, Y. Zhuang, Z. Diao, S. Zhang, Q. Si, W. Chen, Investigating the effects of steel slag powder on the properties of self-compacting concrete with recycled aggregates, Constr. Build. Mater. 200 (2019) 570–577. https://doi.org/10.1016/j.conbuildmat.2018.12.150.
[78] H.N. Atahan, C. Carlos, S. Chae, P.J.M. Monteiro, J. Bastacky, The morphology of entrained air voids in hardened cement paste generated with different anionic surfactants, Cem. Concr. Compos. 30 (2008) 566–575. https://doi.org/10.1016/j.cemconcomp.2008.02.003.

CHAPTER 4

Use of steel slag and LAS-based modifying admixture in obtaining highly eco-efficient precast concrete products

Abstract

This paper presents a study on improving the eco-efficiency of no-slump concrete for precast elements. Based on a particle packing method, powder and aggregates produced from basic oxygen furnace slag (BOFS) have been provided to obtain mixtures with better particle size distribution and improved packing density. A comprehensive experimental investigation was carried out on mixtures with different cement contents (5%, 10%, and 15% vol.) and three compaction energy levels (6, 10, and 20 blows in a sand rammer). In addition, a modifying admixture based on Linear Alkyl Benzene Sodium Sulfonate (LAS) was used on the steel slag concretes to enhance workability and cohesiveness. The highest compressive strength of 52.1 MPa at 28-days led to a binder intensity (bi) of 7.0 kg/m³/MPa, in a concrete mix with waste consumption of 2,356.57 kg/m³. The concrete containing the highest waste consumption (2,637.82 kg/m³) and the least cement consumption (121.56 kg/m³) achieved a bi of 7.6 kg/m³/MPa. In the steel slag no-slump concretes, the LAS-based admixture did not present effective air incorporation; moreover, it did not cause damage to the physical and mechanical properties.

Keywords: Eco-efficiency. No-slump concrete. Precast concrete. Particle packing. Basic oxygen furnace slag (BOFS).

4.1 Introduction

Solid waste management (SWM) is one of the biggest challenges in the world today that involves many technical, sociocultural, ecological, and political issues [1–3]. Continuous economic development, increase in population, urbanization, and industrialization imply a rapid growth in the amount of solid waste, and the poor management of this waste generates several negative impacts on the environmental, social, economic, and health sectors [1,4–6]. Finding solutions to the current problem of industrial waste management has become a duty of society, given the urgency imposed by environmental and public health issues, in addition to the opportunity provided through the reuse of such materials [2,3,6–8].

The construction industry consumes an enormous amount of natural resources, being responsible for more than 30% of the extraction of natural resources, in addition to being responsible for 25% of the solid waste generated in the world [9,10]. However, these resources have become increasingly scarce, especially in large urban centers, making raw materials more expensive due to the increased costs of transportation from other regions [11–13]. In this way, the construction industry has great potential to reuse considerable amounts of industrial waste, saving natural resources while providing a destination for environmental liabilities in a circular economy framework [14–17].

The steel industry generates residues and by-products in the steel production process [18,19], including steel slag, which is the molten material formed by chemical reactions, responsible for removing impurities and separating them from metal in the production process [19–21]. Basic Oxygen Furnace Slag (BOFS) is generated in the primary refining process, carried out in LD oxygen converters (Linz-Donawitz), resulting from the conversion of liquid pig iron into steel [22–24]. Several studies have been developed with the proposal of using steelmaking slag in cement-based composites as aggregates and binder material [25–30], and its technical and economic viability has been demonstrated.

Precast concrete is increasingly used in current buildings due to its numerous advantages in service and quality, such as reliable performance control, low noise and little pollution on the construction site, improvement of construction quality and reduction of building time [31–34]. Solid industrial wastes should be used as mineral admixtures and aggregates in the cement-based composites to reduce the cost and CO_2 emissions and continue the green development of the precast concrete industry [33–35]. Several studies have evaluated the behavior and influence of steel slag in Portland cement matrices as aggregate and supplementary

cementitious material (SCM), and good results are being achieved, mainly related to mechanical performance [28,36–40]. Also, improvements in concrete eco-efficiency have been observed [27,28,38,41]. Furthermore, steel slag aggregates perform well in prefabricated elements, such as concrete pavers [35,42], concrete blocks [43], and as a cementitious material in prefabricated concrete [32].

The formulation of more eco-efficient cement-based composites becomes a promising strategy to reduce CO_2 emissions and improve cement use efficiency [44]. The combination of strategies as the use of dispersants (superplasticizers) and increasing packing density of the concrete particles aiming the increase in compressive strength (or reduction in cement consumption) has great potential for the production of "green concrete" [44,45]. In this sense, many researchers have been working with mixture designs focused on particle packing methods to mitigate the negative effects of excessive use of Portland cement and natural resources. [27,28,46–49].

This work proposes the application of a mix design method based on particle packing for no-slump eco-efficient concretes to prefabricated elements. For this purpose, steel slag aggregates (SSA) and steel slag powder (SSP) were used in the total replacement of natural aggregates. In addition, the influence of a non-conventional admixture based on Linear Alkyl Benzene Sodium sulfonate (LAS) proposed by Mendes et al.[50] was evaluated.

4.2 Materials and method

4.2.1 Materials

A Portland cement (PC) of high early strength (ASTM Type III) was used. In Brazil, this cement is specified by NBR 16697 [51] with the identification CPV-ARI. Its use is indicated for precast elements due to the need for quick deforms since it demands shorter curing times and presents high mechanical strength at early ages. The properties of the cement used, obtained from the manufacturer, are shown in *Table 4.1*.

The conventional fine aggregates used in the study were natural river quartz sand from the city of Porto Firme, Minas Gerais, Brazil, and gneiss-crushed fine aggregate from São Geraldo, Minas Gerais, Brazil. The materials passed through sieve # 4 (4.8 mm) were used.

Table 4.1 Chemical, physical and mechanical properties of the Portland cement (PC) used in this research.

Parameter	Value
MgO content, %	0.98
SO_3 content, %	3.43
Na_2O content, %	0.07
K_2O content, %	0.86
Na_2Oeq content, %	0.64
Loss on ignition, %	3.97
Insoluble residue, %	1.48
Density, g/cm³	3.12
Specific surface area (Blaine), cm²/g	4,372
Setting time (initial/final), min.	(105 / 165)
Compressive strength (1/ 3/ 7/ 28 days), MPa	(27.5/ 37.8/ 44.3/ 53.2)

Gneiss filler and a gneiss gravel with a 4.75-12.5 mm particle-size range, provided by a producer located in the metropolitan region of Belo Horizonte, in the state of Minas Gerais, was also employed. These aggregates were used in the production of the reference concretes for comparative purposes.

The recycled aggregates used in this study were produced from the crushing of a BOFS sample generated in an oxygen converter through the Linz-Donawitz (LD) process. The samples were obtained from a steelwork located in João Monlevade, Minas Gerais State, Brazil. This slag has as main chemical components CaO (36.9%), Fe_2O_3 (31.8%), SiO_2 (14.4%), MgO (5.8%) and Al_2O_3 (3.8%), and mineralogical phases such as Larnite (Ca_2SiO_4), Calcite ($CaCO_3$), Brownmillerite ($Ca_2(Al,Fe)_2O_5$), Helvine ($Mn_4Be_3(SiO_4)_3S$), Lime (CaO), and Wuestite (FeO) [52].

To stabilize the expansive oxides, the steel slag used in this study was subjected to a weathering process for approximately five years in a storage yard at the Laboratory of Civil Construction Materials at the Federal University of Ouro Preto, Minas Gerais, Brazil. The collected slag had a particle size between 6.35-12.5 mm, and no additional processes were performed to produce the recycled coarse aggregate. The fine aggregates were produced aiming to meet the specifications ASTM C33/C33M-18 [53], for which a comminution procedure in a jaw crusher (Retsch BB 200) was performed until reaching a maximum particle size of 4.75 mm.

The BOFS powder was obtained by grinding from the material passing through the #4 sieve (4.75mm). A laboratory ball mill with the characteristics and setup shown in *Table 4.2* was used. An intermediate particle-size range between the cement and fine aggregates was

aimed. The material obtained, so-called coarse powder, was chosen for economical and technological reasons, as recommended in [28] and [27].

Table 4.2 Grinding program and setup parameters.

Parameters	Information
Jar material	Stainless steel
Jar volume (cm³)	15,397
Material produced per cycle (cm³)	2,100 (13.6 %)
Rotation speed (rpm)	200
Balls material	Ceramic
Balls volume (cm³)	2,227 (14.5 %)

The particle-size distribution curves of the materials used in this research are shown in *Figure 4.1*. *Figures 4.2, 4.3* and 4.*4* show the visual characteristics. The results of the physical characterization are listed in *Table 4.3*. Also, morphological and microstructural aspects of the gneiss filler and BOFS powder were observed using images obtained from a Scanning Electron Microscope (SEM, JEOL JSM-6010LA, high vacuum, secondary electron images, 10 kV) (*Figures 4.5* and 4.*6*).

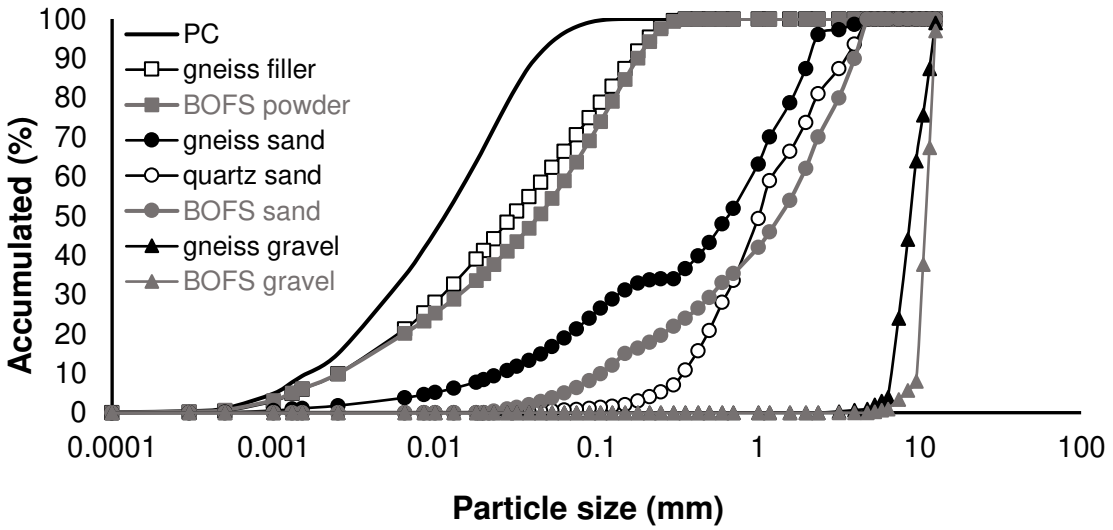

Fig. 4.1 Particle-size distribution curves of the materials used.

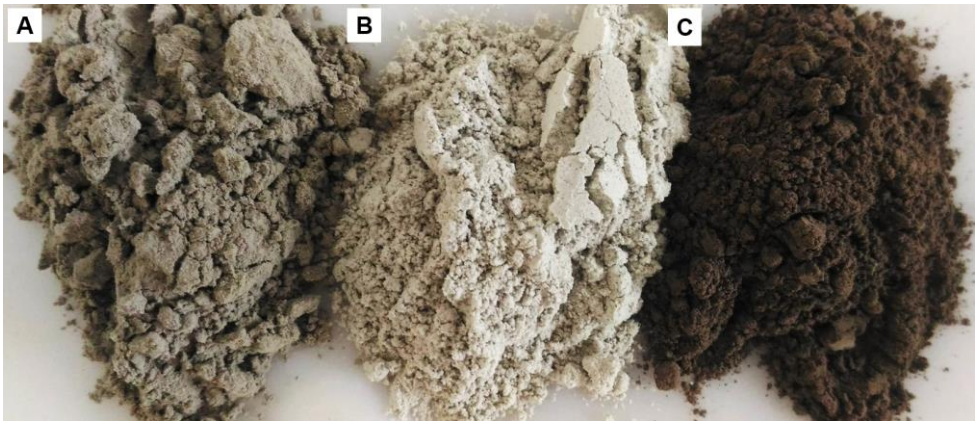

Fig. 4.2 Binders and fillers: (A) PC; (B) gneiss filler; and (C)BOFS powder.

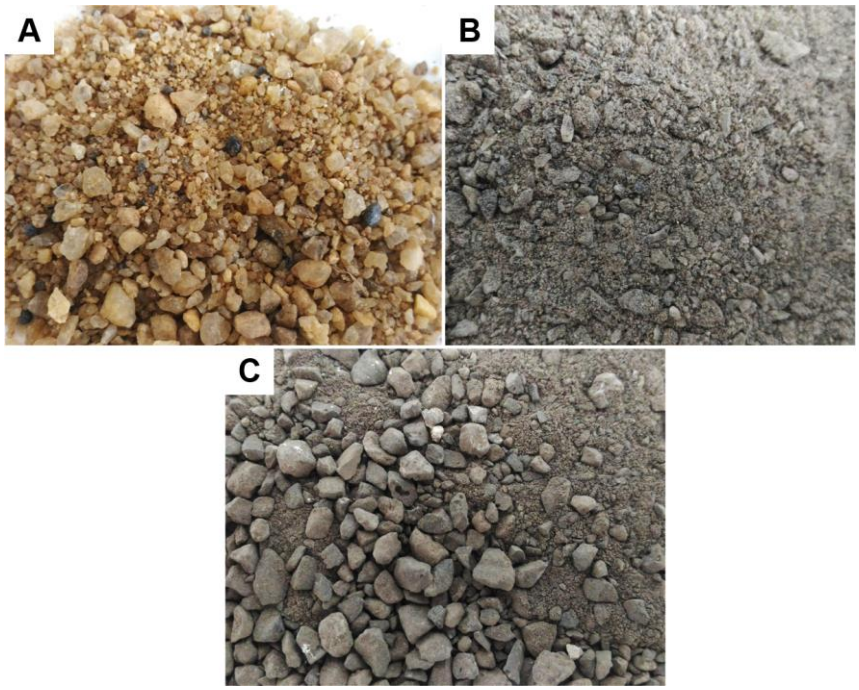

Fig. 4.3 Fine aggregates: (A) quartz sand; (B) gneiss sand; and (C) BOFS sand.

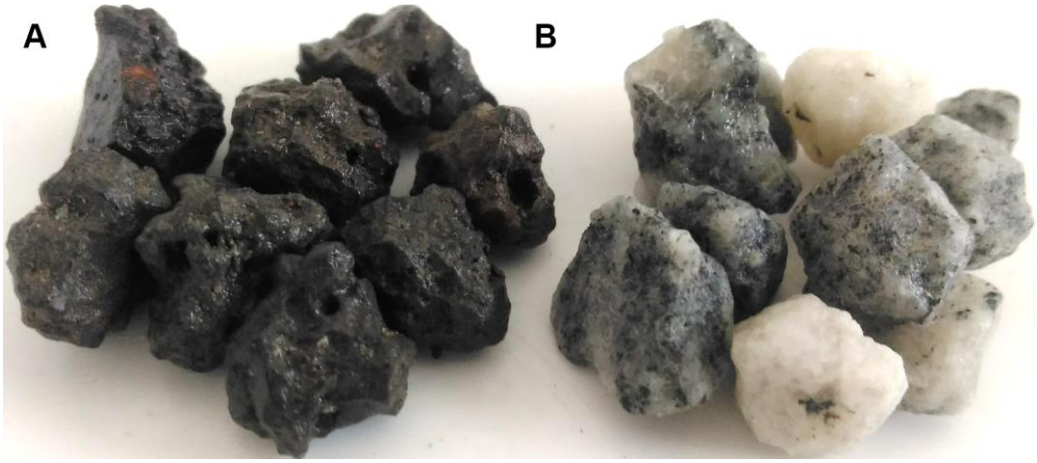

Fig. 4.4 Coarse aggregates: (A) BOFS gravel; and (B) gneiss gravel.

Table 4.3 Physical characterization of the materials used.

Material	Density (g/cm^3)	Specific surface área (cm^2/g)	Standards
BOFS Powder	3.62	2721.3	ASTM C188-18 [54]
Gneiss filler	2.68	3249.5	
Gneiss sand	2.86	-	ASTM C128-15 [55]
Quartz sand	2.63	-	
BOFS sand	3.54	-	
BOFS gravel	3.57	-	ASTM C127-15 [56]
Gneiss gravel	2.68	-	

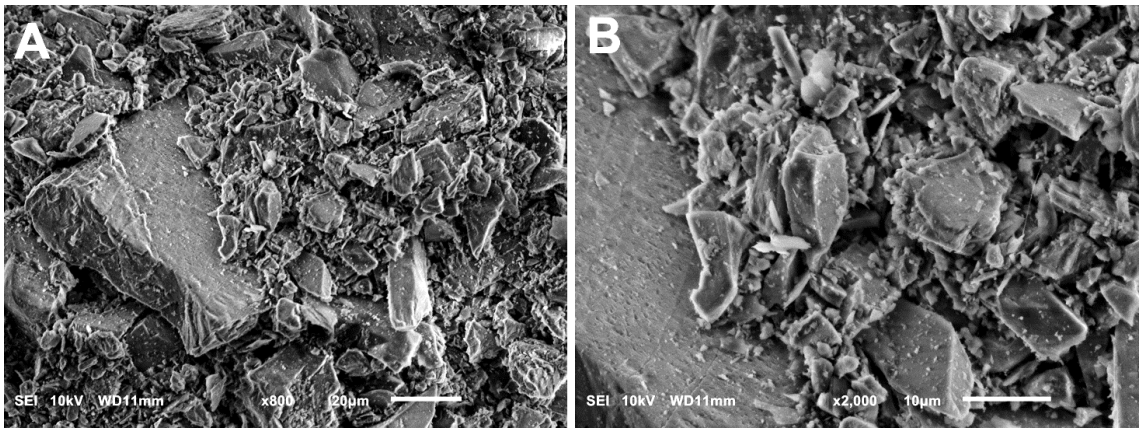

Fig. 4.5 SEM images of the gneiss filler (A)800x magnification; (B)2000x magnification.

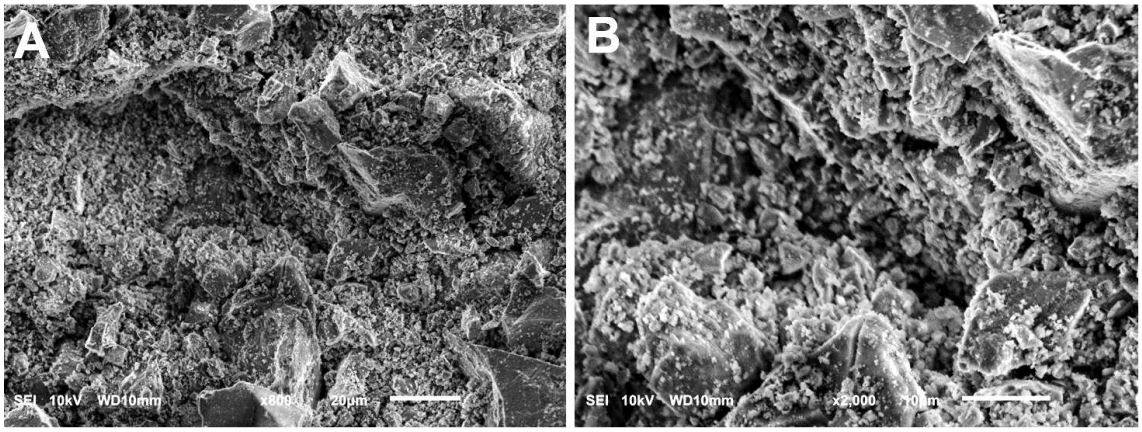

Fig. 4.6 SEM images of the BOFS powder (A)800x magnification; (B)2000x magnification.

Linear Alkyl Benzene Sodium Sulfonate (LAS) was also used as an agent to improve plasticity and cohesion. It is a biodegradable surfactant present in dishwashing detergents, in a concentration of up to 10% [57].

4.2.2 Mixing design of the densely-packed no-slump concrete

The proportion of the dry fraction of the concretes for densely packed mixtures was designed using the modified Andreasen particle size distribution method [58]. Andreasen assumed that the smallest particles would be infinitesimally small, but Funk and Dinger recognized that the finest particles in real materials are finite in size and modified the Andreasen equation considering the minimum particle size in the distribution. The calculations were performed according to Eq. (1) where: CPTF - the accumulated percentage of fines less than "D" in volume; D - particle size; D_S - smaller particle size of the distribution; D_L - larger particle size of the distribution; q - distribution coefficient.

$$CPTF(\%) = 100\left(\frac{D^q - D_S^q}{D_L^q - D_S^q}\right) \quad (4.1)$$

The particle packing dosing methods start from mathematical models in which the particle sizes and a distribution coefficient “q” are considered. Through computer simulations made with the method adopted by Funk and Dinger [58], it was demonstrated that the distribution coefficient should have a value equal to or less than 0.37 to obtain an infinite distribution without porosity. In contrast, for q values above 0.37, residual porosity is always verified [59,60]. For a mixture to show good fluidity, the value of the distribution coefficient must be less than 0.30. Therefore, using “q” values close to 0.30, we have a mixture that needs vibration for its density, while values less than 0.25, the mixture becomes self-compacting. The effect of reducing the value of the distribution coefficient is the increase in the volume of fines in the mixture, which influences the interaction between the particles [59–61]. Thus, after preliminary tests and aiming to obtain a no-slump concrete, the q-value of 0.3 was adopted in this work.

4.2.3 Characterization of concretes

4.2.3.1 Fresh state

The water/binder ratio was obtained through measurements of the concretes dry densities in the fresh state to evaluate the packing density based on the test of optimum moisture content using compaction energy with the aid of a sand rammer. Different moisture contents were tested for each mix and each compaction energy. The cylindrical specimens in the fresh state used for the proposed mixtures' packing measurements were molded using three different

compaction energies (6, 10, and 20 blows). For this, the material was previously weighed and molded in two layers of approximately 70 mL each. After this process, the specimen was demolded, and the final height and weight were measured. The principles of geotechnical engineering attest that greater compaction energy increases mechanical strength and stiffness and reduces permeability.

The compaction curve (*Figure 4.7*) is the relationship between moisture content and dry density (γ_d), obtained from Eq. (4.2), where w_c is water content. The water content corresponding to the maximum dry density is called the optimum moisture content (OMC). Each compaction energy has its own OMC. As the compaction energy increases, the maximum dry density generally increases, and the OMC decreases.

$$\gamma_d = \frac{\gamma}{1 + w_c} \tag{4.2}$$

The zero air voids curve or saturation line represents the fully saturated condition (S = 100%), theoretical dry density is given by Eq. (4.3), where γ_w is the specific weight of water, and G_s is the density of solid particles.

$$\gamma_d = \frac{\gamma_w G_S}{1 + w_c * G_S} \tag{4.3}$$

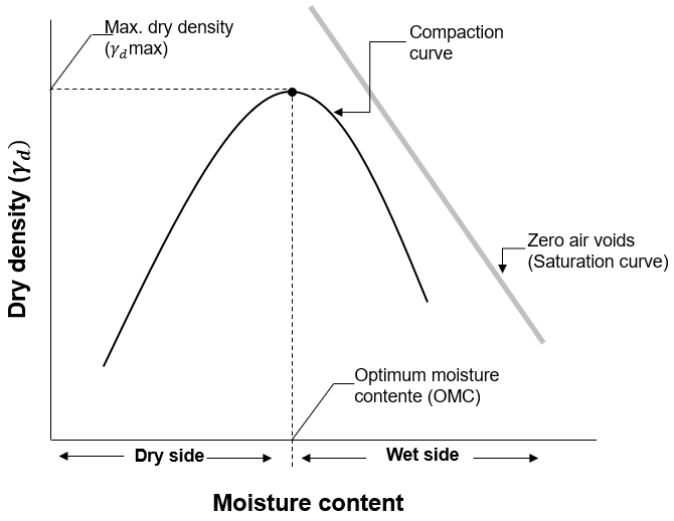

Fig. 4.7 Moisture content and dry density relationship (adapted from [62]).

4.2.3.2 Hardened state

The cylindrical specimens for testing in the hardened state were produced by applying the same procedure as the fresh state test for optimum moisture content determined in each mixture. These specimens were tested for compression following the method ASTM C39/C39M-21 [63] at the ages of 1, 7, 28, and 63 days. For each designed mixture and each compaction energy, 12 specimens were molded. After demolded (24-hour), these specimens were subjected to curing submerged in water saturated with lime. Besides, additional specimens were molded for non-destructive tests of dynamic elastic modulus through the ultrasonic pulse velocity and absorption, void index and specific gravity measurements.

The absorption, voids, and specific gravity measurements were performed at 28 days, based on the method ASTM C642-13 [64]. These parameters are obtained through the following procedure: weighing the oven-dried specimens (105 ± 5 ºC, 168 h); this results in their dry mass - m_s. Then they are weighed on a hydrostatic balance - m_i, and then their surfaces are wiped with a damp cloth, and the saturated surface-dry masses are obtained - m_{sat} (168 h immersion in room temperature water and additional 5 h immersion in boiling water). Thus, the samples' volume, including their internal pores, are given by (m_{sat} - m_i). The water absorption (W.A.), the void index (V. I.), and specific gravity (γ) are calculated by the equations (Eq.4.4 - 4.6):

$$\text{W. A.} = \frac{m_{sat} - m_s}{m_s} \text{ x } 100 \tag{4.4}$$

$$\text{V. I.} = \frac{m_{sat} - m_s}{m_{sat} - m_i} \text{ x } 100 \tag{4.5}$$

$$\gamma = \frac{m_s}{m_{sat} - m_i} \tag{4.6}$$

Ultrasonic pulse velocity measurements were performed in the same oven-dried specimens (105 ± 5 ºC, 168 h), following the requirements of the standard ASTM 597-16 [65] for cylindrical concrete specimens. The upper and lower faces were polished and covered with contact gel. A portable ultrasonic pulse monitoring system (Proceq's Pundit Lab) was used, connected to the computer and operated by Proceq's Punditlink software. The transducer used operates with a frequency of 54 MHz and a pulse width of 9.3 μs. The frequency of measurements was one reading per second, taken during 100 seconds, and the result was obtained by averaging these measurements.

Finally, to evaluate the no-slump concrete's microstructural characteristics, samples were subjected to a micromorphology analysis through scanning electron microscopy (SEM) using a JEOLJSM-6010LA microscope. The mixtures containing 15 vol.% cement and compaction energy equal to 20 blows in the sand rammer were selected for this SEM investigation (They are identified by the codes C 15-03-00; E 15-00-03, and L 15-00-03, as shown afterward in *Table 4.4*). They were chosen to represent the integrity of the matrix and microstructural behavior of representative samples, considering the physical and mechanical performance.

4.2.4 Eco-efficiency evaluation

The binder intensity (*bi*) index measures the amount of binder (kg m^{-3}) necessary to develop 1 MPa of mechanical strength and consequently expresses the efficiency of using binder materials [44]. The waste consumption and *bi* were used in the no-slump concrete eco-efficiency evaluation. Eq. (4.7) was used for *bi* calculation, where *b* is the total consumption of binder materials (kg m^{-3}) and *p* is the performance achieved. In this case, *p* is the compressive strength (MPa) at 28 days.

$$bi = \frac{b}{p} \tag{4.7}$$

4.3 Results and discussion

4.3.1 Characterization of densely-packed no-slump concrete

Three different cement levels (5 vol.%, 10 vol.%, and 15 vol.%) were evaluated for all mixtures designed. Firstly, three reference mixtures containing filler and natural aggregates were adjusted and proposed. Based on those reference mixtures, three mixtures replacing 100% of the conventional filler and aggregates by the BOFS powder and BOFS aggregates were proposed. Finally, three mixtures of the BOFS-concretes containing fixed levels of the LAS-based admixture were considered. *Table 4.4* shows the no-slump concrete mixtures with the proportions in volume. These compositions of the concretes' dry fractions were designed from Eq. (4.1) and reached the closest fit with the Modified Andreasen curve [58].

The proximity and good fit of all mixtures with the Andreasen curve can be highlighted, both in concrete with conventional aggregates and with aggregates produced with steel slag,

reaching the goal of the mix-design stage (*Figure 4.8*). The similarity achieved by the different mixtures can be explained by the proximity in the particle size distribution of the materials used. It can be seen from *Figure 4.1* that the gneiss filler and BOFS powder were very close in particle size, as well the gneiss gravel and BOFS gravel. The BOFS sand also presented an intermediate fine fraction compared to the gneiss sand and quartz sand.

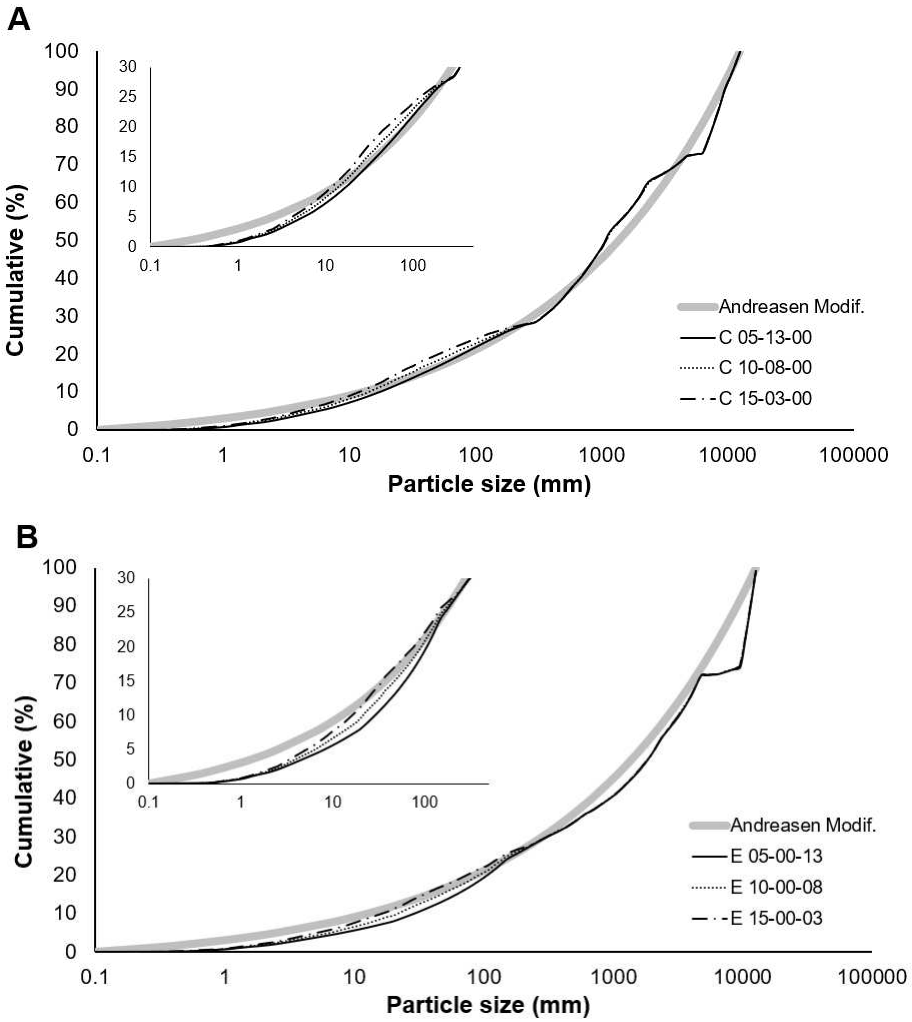

Fig. 4.8 Andreasen Modified curve and particle-size distribution curves of the mixtures obtained: (A) conventional no-slump concrete (B) BOFS no-slump concrete.

According to Zheng et al. [66], the particle shape does not directly appear in the improved equations as a parameter. However, the derivation of the improved equations is based on a packing model, which is suitable for particles with any shape insofar as small particles fill the voids between larger particles. Normally, the shape factor affects the pore fraction (ø) since spherical particles have a smaller ø value and the highest packing efficiency for random particle packing, and randomly arranged fiber-shaped particles and flakes have a higher ø [66].

Table 4.4 Identification of the no-slump concretes designed, constituent materials and volumetric proportions of the dry mixtures.

Blend	Fines fraction % total volume (% fines volume)			Aggregates fraction % total volume					Admixture % by the fine fraction
	Portland cement	Gneiss filler	BOFS powder	Gneiss sand	Quartz Sand	BOFS sand	Gneiss gravel	BOFS gravel	LAS
C 05-13-00	5.0 (27.78)	13.0 (72.22)	0.0 (0)	25.0	29.0	0.0	28.0	0.0	0.0
C 10-08-00	10.0 (55.56)	8.0 (44.44)	0.0 (0)	25.0	29.0	0.0	28.0	0.0	0.0
C 15-03-00	15.0 (83.33)	3.0 (16.67)	0.0 (0)	25.0	29.0	0.0	28.0	0.0	0.0
E 05-00-13	5.0 (27.78)	0.0 (0)	13.0 (72.22)	0.0	0.0	54.0	0.0	28.0	0.0
E 10-00-08	10.0 (55.56)	0.0 (0)	8.0 (44.44)	0.0	0.0	54.0	0.0	28.0	0.0
E 15-00-03	15.0 (83.33)	0.0 (0)	3.0 (16.67)	0.0	0.0	54.0	0.0	28.0	0.0
L 05-00-13	5.0 (27.78)	0.0 (0)	13.0 (72.22)	0.0	0.0	54.0	0.0	28.0	0.5
L 10-00-08	10.0 (55.56)	0.0 (0)	8.0 (44.44)	0.0	0.0	54.0	0.0	28.0	0.5
L 15-00-03	15.0 (83.33)	0.0 (0)	3.0 (16.67)	0.0	0.0	54.0	0.0	28.0	0.5

4.3.2 Dry density and moisture content relationship

Compaction tests were performed to determine the OMC for each mixture and each energy applied, thus establishing a relationship with the dry density. The curves indicate great sensitivity of the dry density in relation to the variations in the concrete analyzed moisture content, as shown in *Figures 4.9-4.11*.

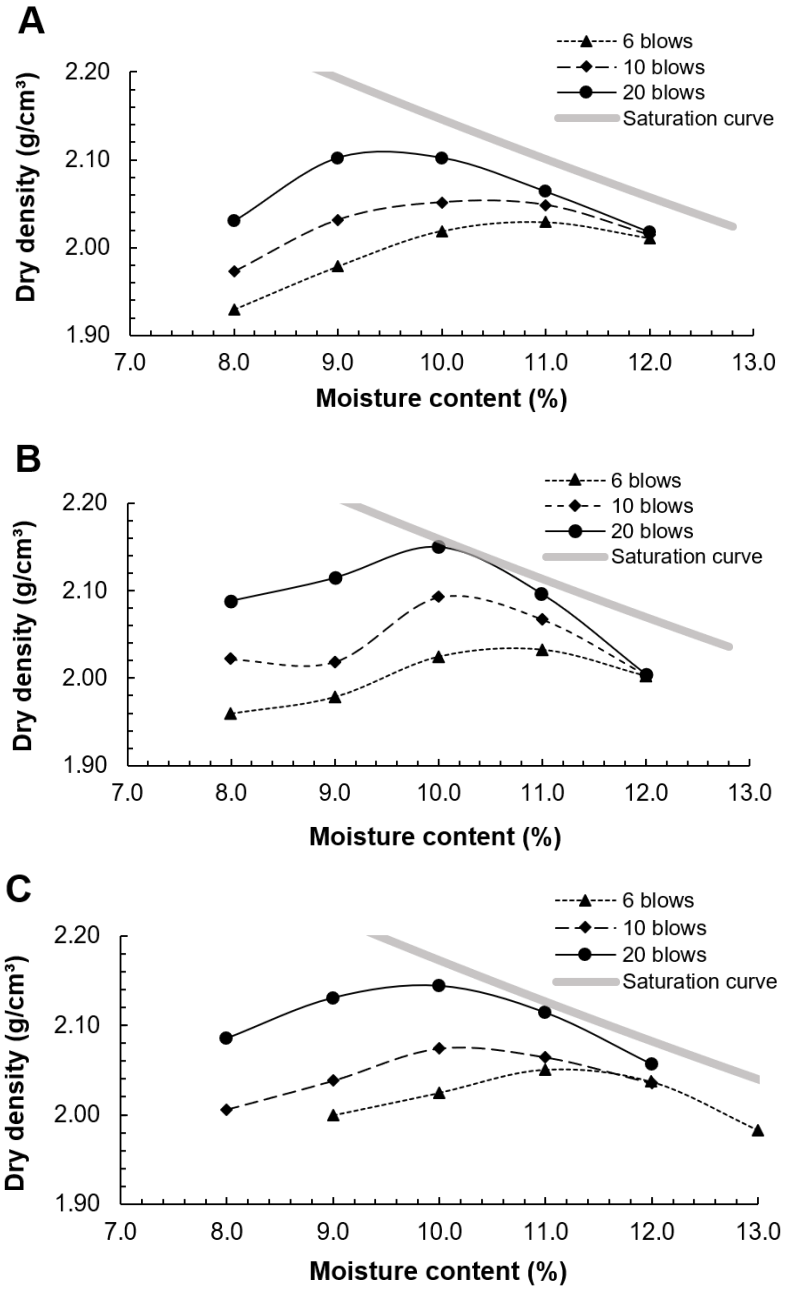

Fig. 4.9 Moisture contents of the conventional no-slump concretes: (A) C 05-13-00; (B) C 10-08-00; and (C) C 15-03-00.

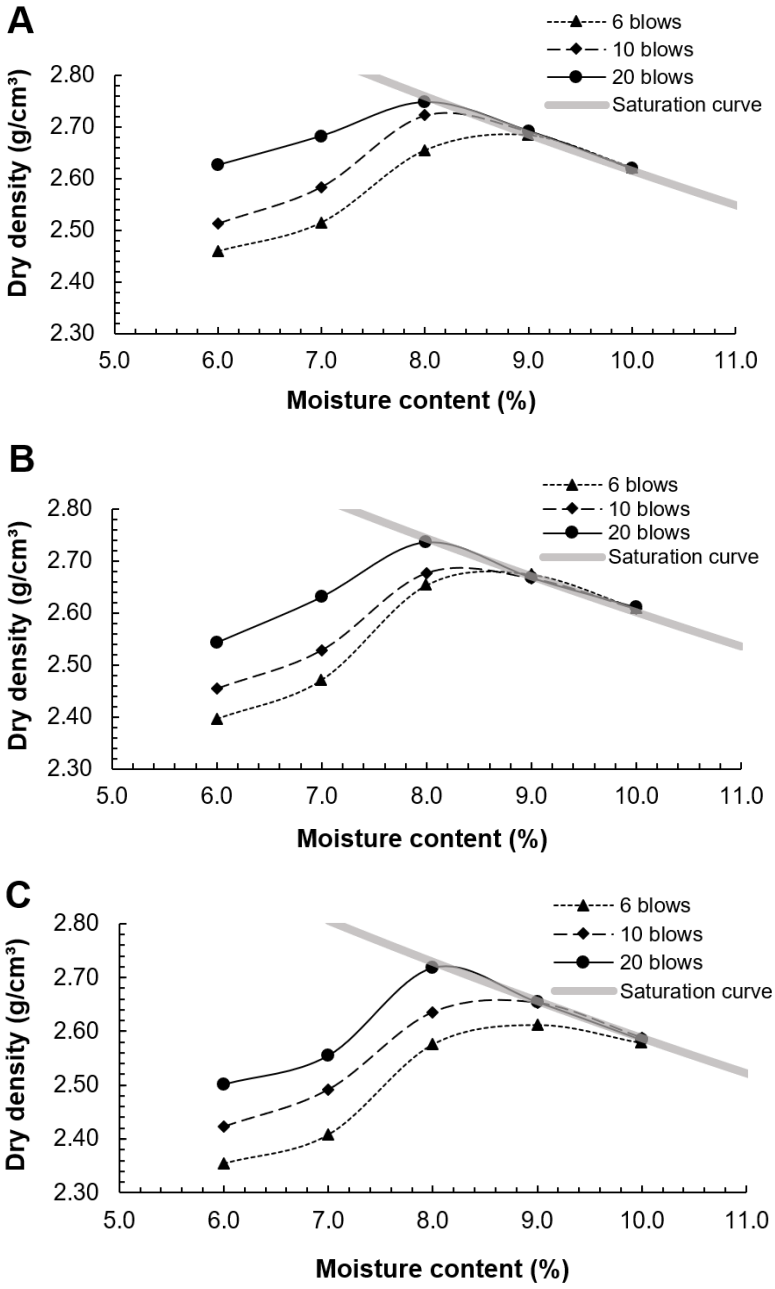

Fig. 4.10 Moisture contents of the steel slag no-slump concretes: (A) E 05-00-13; (B) E 10-00-08; and (C) E 15-00-03.

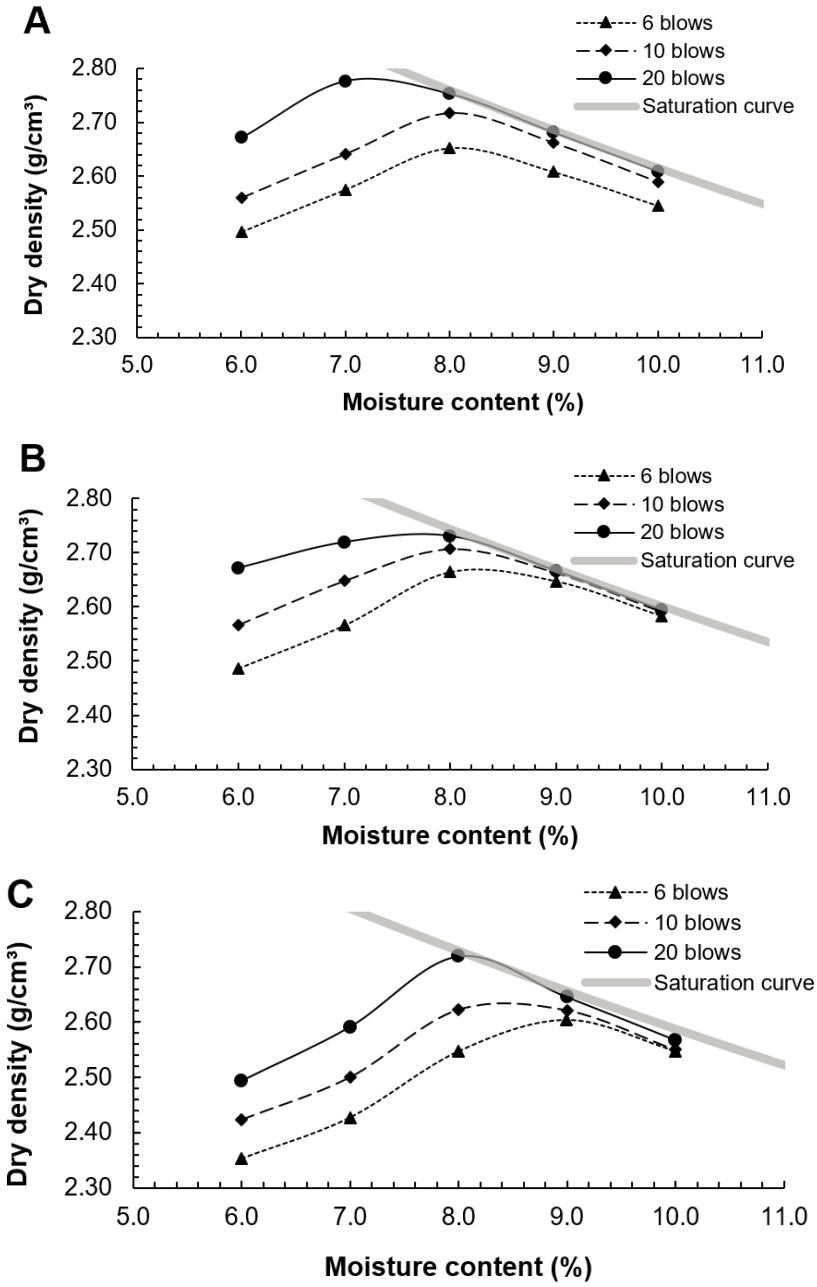

Fig. 4.11 Moisture contents of the steel slag + LAS no-slump concretes: (A) L 05-00-13; (B) L 10-00-08; and (C) L 15-00-03.

It is observed that the dry density increases with an increase in moisture content till the maximum density is attained. With further increase in moisture content, the dry density decreases. According to geotechnical engineering principles, a higher dry density is usually accompanied by a lower OMC [67], and this definition is in agreement with the obtained results.

It is evident from the compaction curves that both materials differ in their compaction behavior to a large extend. BOFS concrete presents less water required to obtain the OMC, and it can be seen from *Figures 4.10* and *4.11* that the compaction curves have reached the

saturation curve, characterized by the complete saturation of the voids (S = 100%). This behavior can be related to the difference in particle shape of the applied fines fraction. BOFS powder and BOFS sand are mainly composed of volumetric particles compared to the angular and elongated particles of gneiss filler and gneiss sand.

Similar results were obtained by Hüsken and Brouwers [46], who studied the influence of fly ash and quartz flour on zero-slump concrete's compaction behavior and achieved better results with fly ash due to the spherical particles in comparison to the angular particles of the quartz flour. The more spherical shape of the fly ash particles and the resulting ball-bearing effect positively influences the compaction behavior and the final packing fractions obtained. In contrast to this, the quartz flour's angular shape increases the internal friction of the mix, and lower values of the packing fraction were obtained for comparable compaction energy and moisture content [46].

Table 4.5 presents a summary with the principal data of each mixture studied and the respective compaction energy, making a correlation with *Figures 4.9-4.11*. Lower values of OMC were achieved by the samples with steel slag when the LAS-based admixture was used. The mixtures achieved this reduction with lower cement contents (5% and 10%). It can be explained by the presence of some air entrainment caused by the admixture. The performance of these microbubbles in the system may have improved the lubricating effect of the particles. The mixtures with higher compaction energy (20 blows) obtained the best packing performances, demonstrating that the increase in energy provided greater accommodation of the particles in all the mixtures studied. Furthermore, both concrete with conventional aggregates and BOFS aggregates showed a range very close to packing density (0.76 - 0.80). Although gneiss filler and gneiss sand have angular and elongated particles, the gneiss gravel has a more volumetric aspect, as well as the BOFS gravel (Figure 4.4), which may have improved the particle packing of conventional concrete mixtures.

Table 4.5 Characteristics of the fresh no-slump concrete mixtures.

Blend	Compacting energy (blows)	OMC (%)	Dry density (g/cm³)	Cement consumption (kg/m³)	water/binder (by mass)	Packing density
C 05-13-00	6	10.80	2.027	120.45	0.585	0.77
	10	10.40	2.050	121.48	0.563	0.78
	20	9.40	2.102	124.12	0.509	**0.80**
C 10-08-00	6	10.70	2.030	240.98	0.560	0.77
	10	10.30	2.085	243.05	0.539	0.78
	20	9.90	2.147	245.15	0.518	**0.79**
C 15-03-00	6	11.20	2.048	356.99	0.567	0.76
	10	10.20	2.072	364.72	0.516	0.78
	20	9.80	2.142	367.90	0.496	**0.79**
E 05-00-13	6	8.80	2.679	118.94	0.497	0.76
	10	8.20	2.716	120.90	0.463	0.77
	20	8.00	2.747	121.56	0.452	**0.78**
E 10-00-08	6	8.60	2.666	239.57	0.502	0.77
	10	8.30	2.674	241.52	0.485	0.77
	20	8.05	2.715	243.17	0.470	**0.78**
E 15-00-03	6	9.00	2.612	356.14	0.545	0.76
	10	8.60	2.646	359.94	0.521	0.77
	20	8.10	2.680	364.84	0.490	**0.78**
L 05-00-13	6	8.05	2.650	121.40	0.455	0.78
	10	8.00	2.717	121.56	0.452	0.78
	20	7.20	2.753	124.31	0.407	**0.80**
L 10-00-08	6	8.20	2.661	242.19	0.479	0.78
	10	8.00	2.707	243.51	0.467	0.78
	20	7.80	2.731	244.85	0.456	**0.78**
L 15-00-03	6	9.00	2.604	356.14	0.545	0.76
	10	8.40	2.622	361.88	0.509	0.77
	20	8.10	2.690	364.84	0.490	**0.78**

4.3.3 Microstructural evaluation

Microstructural analysis of the hardened matrix was performed on three samples of 28-day no-slump concrete (C 15-03-00; E 15-00-03; and L 15-00-03) with the compaction energy of 20 blows resulting from the compression tests. SEM images of the concretes are shown in *Figure 4.12*.

It can be observed the presence of irregular pores filled with hydration products, markedly needle-like crystals (ettringite) in the samples containing no LAS-based admixture (*Figures 4.12A-D*). In the sample containing the LAS-based admixtures (*Figures 4.12E-F*), it is also observed the presence of Portlandite [$Ca(OH)_2$]. According to the results of the hydration kinetics evaluations of cement pastes containing SSP and LAS, discussed in Chapter 3, the

presence of persistent ettringite was evident at 28-days aged samples, as observed in XRD patterns (*Figure 3.7*) and SEM images (3.12).

In the sample containing the LAS-based admixture (*Figures 4.12E-F)*, there is no evidence of air incorporation in the concrete matrix, in contrast to the mortars samples containing LAS studied in Chapter 3, whose digital microscopy (*Figures 3.10B* and *3.10D*) and scanning electron microscopy (*Figures 3.11C*-D and *Figures 3.12C-D*) images demonstrated the incorporation of microbubbles in the matrices.

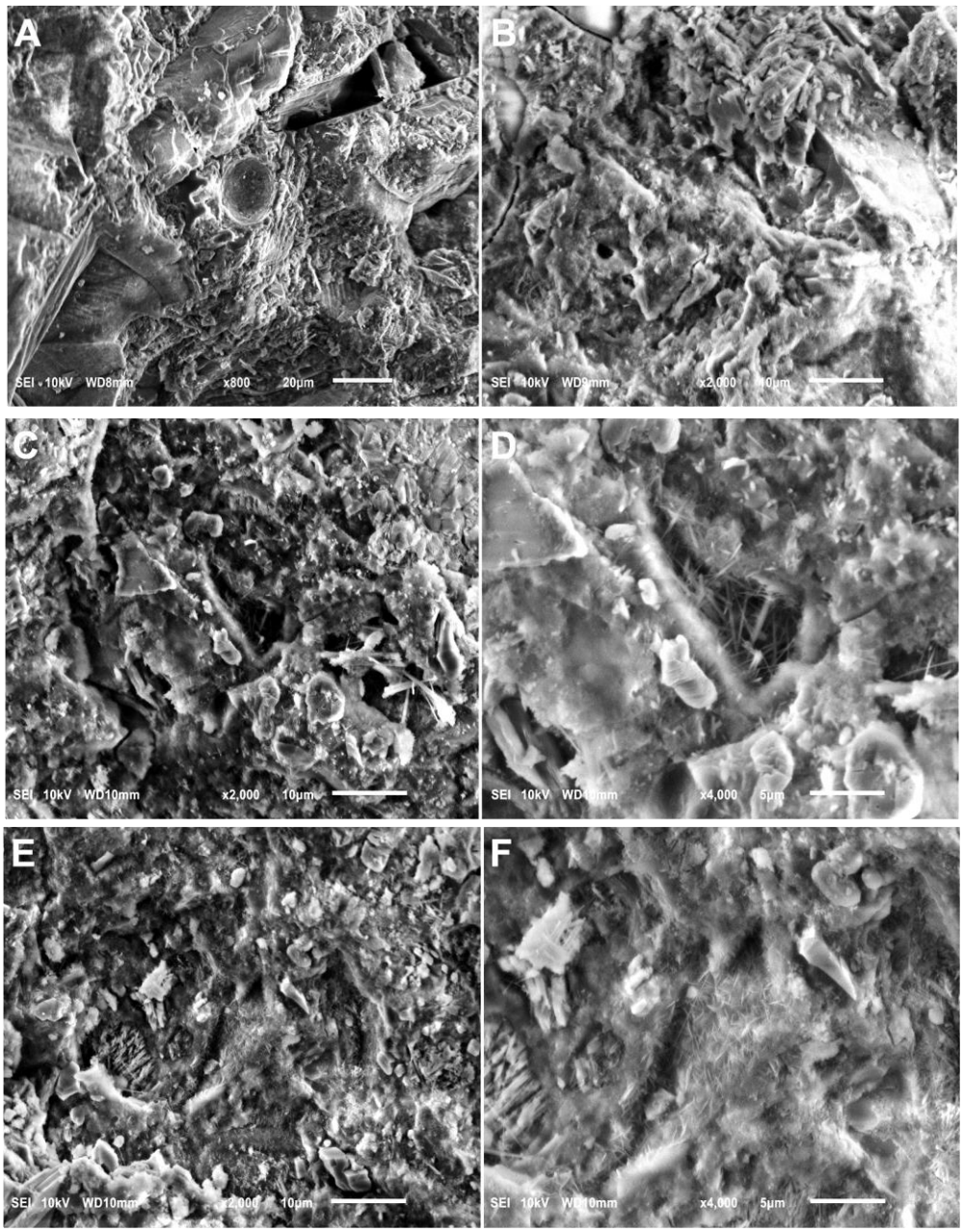

Fig. 4.12 SEM images of no-slump concretes: (A-B) C 15-03-00; (C-D) E 15-00-03; and (E-F) L 15-00-03.

4.3.4 Physical and mechanical performance of the concretes

The physical characterization of the hardened no-slump concretes comprised density, absorption, void index, and ultrasonic pulse velocity. These tests were performed in 28-day-old cylindrical specimens (Ø50 mm), and the results are shown in *Figures 4.13A, 4.13B, 4.13C,* and *4.13D,* respectively. The steel slag no-slump concretes presented the highest densities *(Figure 4.13A)*, both with and without the LAS-based admixture, about 37.0% denser than the reference conventional concrete produced. This result was expected given the higher densities of the steel slag aggregates compared to the natural ones. The results of physical tests showed the relationship between the different parameters, as expected.

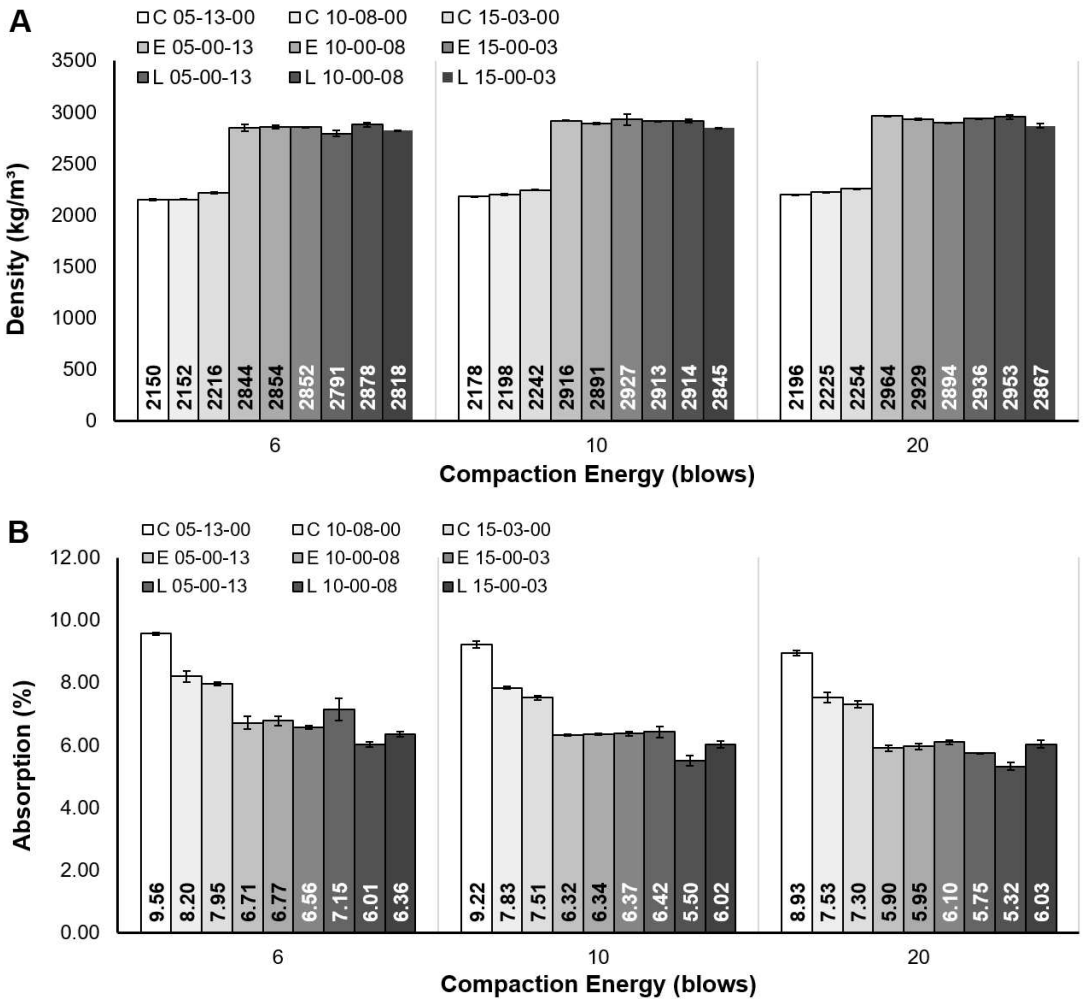

Fig. 4.13 Results of the physical characterization of no-slump concretes: (A) density; (B) absorption; (C) void index; and (D) ultrasonic pulse velocity.

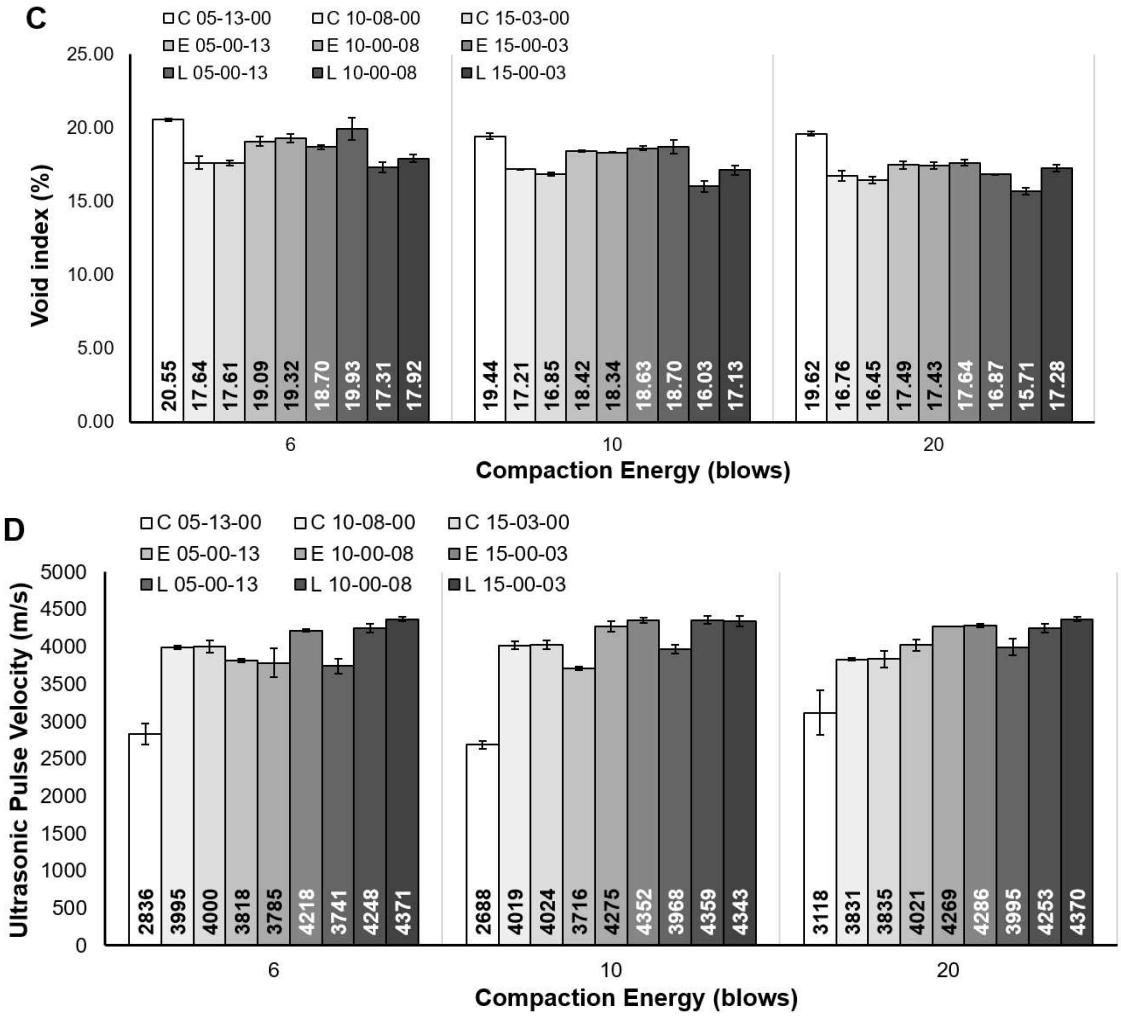

Fig. 4.13 Results of the physical characterization of no-slump concretes: (A) density; (B) absorption; (C) void index; and (D) ultrasonic pulse velocity (continued).

The ultrasonic pulse velocity measurements (*Figure 4.13D*) have been used to assess the uniformity and relative quality of concrete and the porosity (*Figure 4.13C*) and showed consistent results in this study. Samples with lower UPV values tend to be more porous, with the presence of cracks and other imperfections and, consequently, have higher water absorption rates *(Figure 4.13B)*. In the region of imperfections, the ultrasonic pulse is diffracted around the periphery of the defect and takes more time to reach the receiving transducer [68]. In comparison, higher ultrasonic pulse velocity is obtained when the concrete presents quality regarding its homogeneity, uniformity, and lack of imperfections [68]. The mixture C 05-13-00 showed the highest void index and absorption, allied to a lower UPV. Samples with steel slag, with and without the LAS-based admixture, presented close results, being the best results of UPV, absorption, and void index shown by E 15-00-03, L 10-00-08 and L 15-00-03.

Other authors observed similar results that relate UPV to voids and cracks. Saxena and Tembhurkar [68] performed ultrasonic pulse velocity tests studying the durability of concrete with partial replacement of coarse aggregate by steel slag. Higher pulse velocities were obtained for all concrete mixtures containing steel slag aggregate replacements of steel slag aggregates. Anastasiou et al. [69] evaluated UPV to detect voids in self-compacting concrete mixtures using ladle furnace slag as filler and steel fibers. The velocity decreased when increased fiber content was used, which could be attributed to the presence of voids in the fiber-paste transition zone. Franco de Carvalho et al. [28] observed good agreements between UPV and porosity in hardened sand-concretes made with different waste-based supplementary cementing materials. The sand-concretes presented lower void indices and showed higher ultrasonic pulse velocities as a result of dense and sound matrices.

Another relevant aspect of the results is that concretes with LAS-based admixture showed low porosity and water absorption, and consequently high ultrasonic pulse velocity, in accordance with the SEM images taken from the concrete samples (*Figure 4.12C*) in which there is no significant presence of pores in the matrices evidencing significant air incorporation effect.

An ultrasonic pulse velocity range was provided by BIS 13,311- Part 1 [70]. The quality of concrete is considered medium, good and excellent if the pulse velocity falls into 3,000-3,500 m/s, 3,500-4,500 m/s and more than 4,500 m/s, respectively. The pulse velocity <3,000 m/s is considered as having doubtful quality. Most of the studied mixtures fell into the range of good quality. According to this criterion, only C 05-13-00 showed doubtful quality with 6 and 10 blows, and medium quality with 20 blows.

The no-slump concrete's compressive strength tests were performed at four different ages (1, 7, 28, and 63 days). The results are shown in *Figure 4.14* and were separated by compaction energy: 6 blows (*Figure 4.14A*), 10 blows (*Figure 4.14B*), and 20 blows (*Figure 4.14C*). An improvement in the mechanical strength with the increase of the compaction energy can be observed in all the mixtures. In some of them, this increase is more evident than the others.

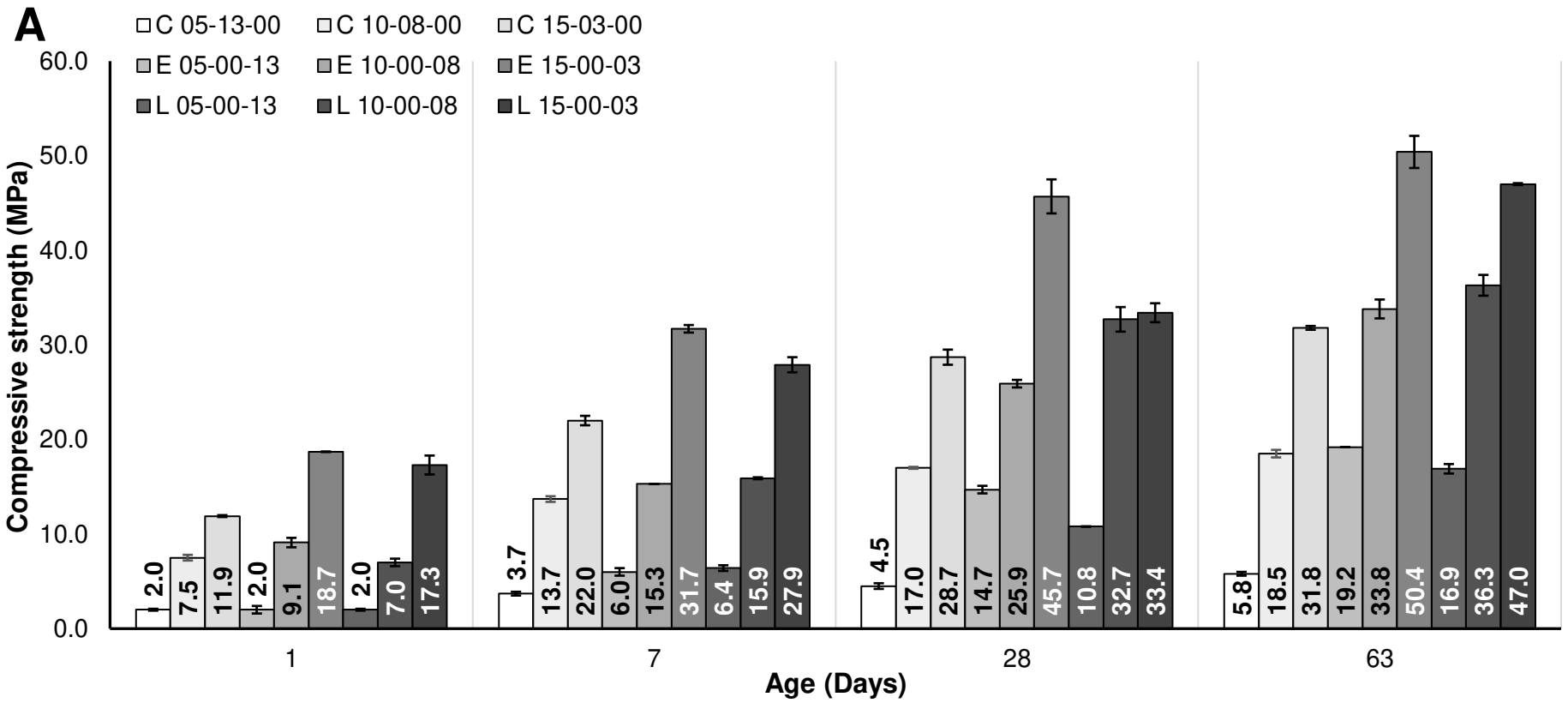

Fig. 4.14 Results of mechanical performance of the no-slump concretes: (A) 6 blows; (B) 10 blows; and (C) 20 blows.

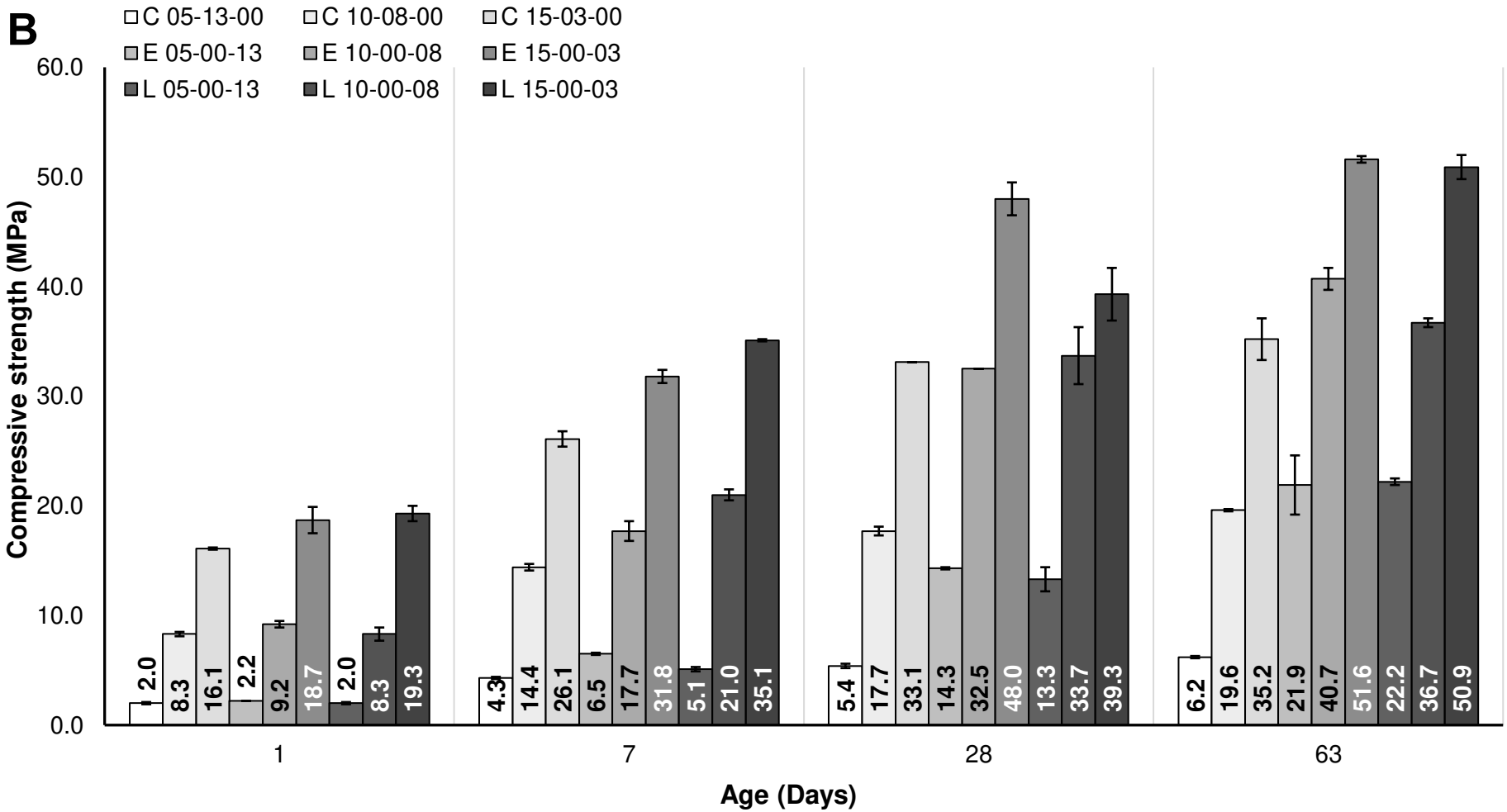

Fig. 4.14 Results of mechanical performance of the no-slump concretes: (A) 6 blows; (B) 10 blows; and (C) 20 blows (continued).

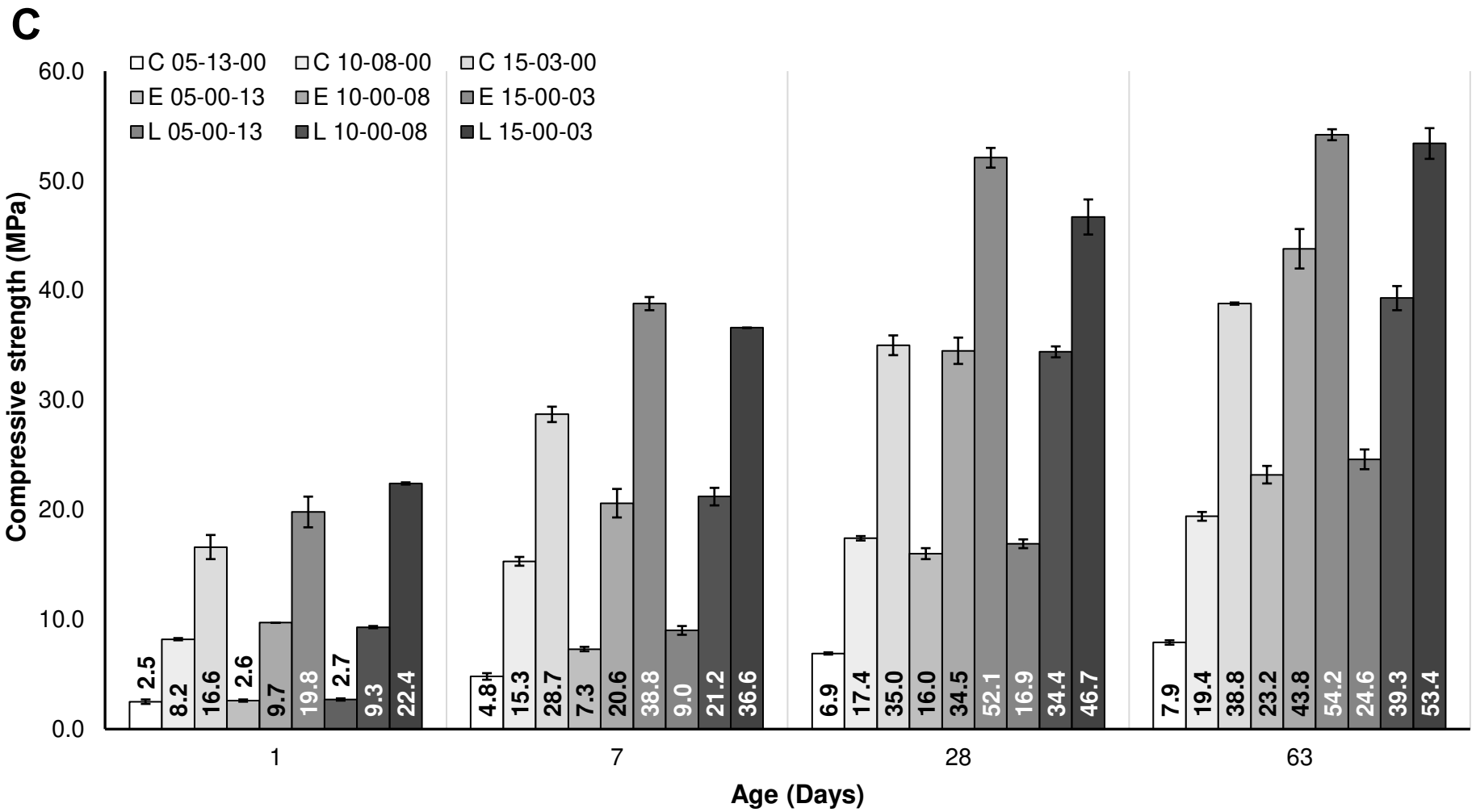

Fig. 4.14 Results of mechanical performance of the no-slump concretes: (A) 6 blows; (B) 10 blows; and (C) 20 blows (continued).

The concretes produced with steel slag aggregates showed better mechanical performances than the samples with conventional materials, comparing the results for the same cement contents (5%, 10%, and 15%) and the same compaction energies (6 blows, 10 blows, and 20 blows). The highest compressive strength at 28-days for all the compaction energies was obtained by the E 15-00-03 mixture, exceeding 50.0 MPa with 20 blows. At 63-days, there was a small increase in mechanical strength of the conventional concretes, considering the three levels of compaction energy. However, the steel slag concrete with and without LAS-based admixture presented a more expressive strength gain at 63-days. This behavior is due to the fact that steel slags present slower hydration with a longer dormant period compared to cement, but this could promote cement hydration at later ages [71]. The steel slag concrete E 15-00-03 continued to present the best mechanical performance than the others, reaching 54.2 MPa with 20 blows, and the steel slag + LAS concrete L 15-00-03 presented a very close strength, with 53.4 MPa.

Improvements in mechanical performances of concretes containing steel slags were also observed by other authors [28,41,72,73], who attributed this trend to the morphology of BOFS aggregates, which enhances the interaction between the aggregate and the cementitious matrix. In this study, the BOFS particles are predominantly volumetric, rough and have some pores (*Figure 4.4A*). The concretes with steel slag + LAS presented compressive strength values very close to the steel slag concretes without the LAS-based admixture. This behavior is explained by the fact that the LAS did not increase the porosity and air entrainment into the matrices, as seen in the results of porosity, UPV (*Figures 4.13C and 4.13D*) and SEM images (*Figures 4.12E and 4.12F*). Thus, there was no significant loss in mechanical strength.

Mixtures containing 5% in volume of cement showed low compressive strength, both in conventional concrete and in steel slag concretes for the three compaction energy levels studied. That resulted from the dilution effect since a high cement content was replaced by the gneiss filler or BOFS powder, which reduced the amount of cement to less than 30% in volume of the fines fraction (paste). Thus, it is noted by statistical tests that the most significant factor in the influence of mechanical strength was the cement content and not the compaction energy (P-value <0.05).

4.3.5 Eco-efficiency evaluation

Studies conducted by Damineli et al. [44] searched a database with 1,585 registers related to compressive strength and binder consumption to measure cement use efficiency. As

a result, they observed that the *bi* in most data obtained was in the range of 5-20 kg/m³/MPa. The conventional no-slump concrete presented a cement consumption varying from 120.45 kg/m³ to 367.90 kg/m³ and compressive strength from 4.5 MPa to 35.0 MPa, which implies a *bi* of 26.77 to 10.51 kg/m³/MPa. Thus, for the mixtures containing 5% in volume of cement, the binder intensity (*bi*) was higher than the limit evaluated by Damineli et al. [44] due to the low mechanical strength achieved by the mixtures with low cement consumption (below 250 kg/m³).

Table 4.6 shows that all no-slump concrete with a blend of cement + BOFS powder and natural aggregates replacement by BOFS aggregates achieved better eco-efficiency results compared to the conventional concretes. The best result of *bi* was observed in the mixture E 15-00-03 for 20 blows, with cement consumption of 364.84 kg/m³, binder intensity of 7.0 kg/m³/MPa and waste consumption of 2,356.57 kg/m³, but the mixture E 05-00-13 for 20 blows, consumed more waste (2,637.82 kg/m³) with less cement consumption (121.56 kg/m³) and achieved a close value of *bi* (7.6 kg/m³/MPa). This way, E 05-00-13 presented the best eco-efficiency performance in both criteria: binder intensity and waste consumption. The eco-efficiency indicator *bi* is related to the cement consumption of the mixture. According to the statistical analysis results for the factorial experiment 3^2, the compaction energy factor was not significant in this case, only the cement content (P-value <0.05).

Pelisser et al. [74] investigate self-compacting concrete (SCC) with low cement consumption added metakaolin and fly ash, a minimum compressive strength of 28.6 MPa and low cement consumption (240 kg/m³) achieved a binder intensity of 10.2 kg/m³/MPa, while for a high compressive strength of 67.2 MPa, the *bi* achieved was 7.8 kg/m³/MPa for a cement consumption of 472 kg/m³. Those results were due to the dense grain packing achieved in the mix design and fly ash and metakaolin contributions in the SCC's properties.

Franco de Carvalho et al. [28] achieved better results in sand-concretes with BOFS, a *bi* of 3.62 kg/m³/MPa for a cement consumption of 317.9 kg/m³ and waste consumption of 519.5 kg/m³. The finer-than-cement powders proposed by the authors were effective in improving the mechanical performance and the binder intensity with high waste consumption. However, the coarse powders played an important role in waste consumption.

Table 4.6 Eco-efficiency indicators: Cement consumption, compressive strength, binder intensity and waste consumption.

No-slump concrete	Compacting energy	Cement consumption (kg/m³)	Compressive strength at 28 days (MPa)	Binder intensity - bi (kg/m³/MPa)	Waste consumption (kg/m³)
C 05-13-00	6	120.45	4.50	26.77	0.0
	10	121.48	5.40	22.50	0.0
	20	124.12	6.90	17.99	0.0
C 10-08-00	6	240.98	17.00	14.18	0.0
	10	243.05	17.70	13.73	0.0
	20	245.15	17.40	14.09	0.0
C 15-03-00	6	356.99	28.70	12.44	0.0
	10	364.72	33.10	11.02	0.0
	20	367.90	35.00	10.51	0.0
E 05-00-13	6	118.94	14.70	8.09	2,580.35
	10	120.90	14.30	8.45	2,623.34
	20	121.56	16.00	**7.60**	2,637.82
E 10-00-08	6	239.57	25.90	9.25	2,459.61
	10	241.52	32.50	7.43	2,480.21
	20	243.17	34.50	**7.05**	2,497.19
E 15-00-03	6	356.14	45.70	7.79	2,299.72
	10	359.94	48.00	7.50	2,324.93
	20	364.84	52.10	**7.00**	2,356.57
L 05-00-13	6	121.40	10.80	11.24	2,633.68
	10	121.56	13.10	9.28	2,637.82
	20	124.31	16.60	7.49	2,697.39
L 10-00-08	6	242.19	32.80	**7.38**	2,486.46
	10	243.51	33.00	**7.38**	2,500.62
	20	244.85	33.70	**7.27**	2,514.42
L 15-00-03	6	356.14	33.40	10.66	2,299.72
	10	361.88	39.30	9.21	2,337.48
	20	364.84	46.70	7.81	2,356.57

4.4 Conclusion

In this research, a comprehensive investigation on steel slag no-slump concretes has been provided. Experimental tests were performed to evaluate some relevant physical and microstructural properties. The following results could be drawn from this investigation:

- The proposed densely-packed no-slump concrete dry mixtures presented a good fit with the modified Andreasen curve for the study's conditions for all the mixtures, for both

conventional and steel slag concrete, as a result of the compatibility of the particle sizes of the conventional materials and the recycled BOFS powder and aggregates.

- Steel slag concrete required less water to achieve the optimum moisture content (OMC) in the compaction curves compared to the conventional concrete. That is related to the better particle shape of the BOFS powder and aggregates, mainly composed of volumetric particles compared to the angular and elongated particles of the gneiss filler and gneiss aggregates.
- Conventional concrete C 05-13-00 was the one with the lowest ultrasonic pulse velocity and, consequently, the highest void index and water absorption compared to the other samples. Samples containing steel slag with and without the LAS-based admixture presented close results, with the best results of UPV, absorption, and void index shown by E 15-00-03, L 10-00-08 and L 15-00-03.
- Concrete produced with steel slag aggregates showed better mechanical performance than samples with conventional materials. The steel slag concrete E 15-00-03 achieved 54.2 MPa at 63-days, with 20 blows, and the steel slag + LAS concrete L 15-00-03 presented a very close strength, with 53.4 MPa, showing that LAS-based admixture did not impair the concrete strength.
- All the steel slag concretes presented high ecoefficiency performances. BOFS powder and BOFS aggregates effectively improved the no-slump concretes' compressive strength and reduced the binder intensities while increased the waste consumption.

The results emphasize the great potential to obtain highly eco-efficient no-slump concretes with the total replacement of conventional aggregates by BOFS, exploring its potential to obtain cement-based composites with improved physical and mechanical performances. Moreover, the consumption of considerable volumes of waste amplifies the relevance by contributing to reduce CO_2 emissions and consumption of natural resources.

Acknowledgments

The authors acknowledge the financial support provided by the Coordenação de Aperfeiçoamento de Pessoal de Nível Superior – Brasil (CAPES) - Finance Code 001, Universidade Federal de Viçosa (UFV), and Universidade Federal de Ouro Preto (UFOP). Equipment and technical support provided by the Laboratory of Construction Materials,

Department of Civil Engineering, UFV; Laboratory of Composite Materials, UFV; Laboratory of Construction Materials, UFOP; and Department of Physics UFV. Thanks are also due to the Research Group on Sustainable and Innovative Construction SICon-CNPq and Research Group on Solid Wastes RECICLOS-CNPq for infrastructure use and collaboration.

References

[1] T.D. Bui, F.M. Tsai, M.L. Tseng, M.D.H. Ali, Identifying sustainable solid waste management barriers in practice using the fuzzy Delphi method, Resour. Conserv. Recycl. 154 (2020) 104625. https://doi.org/10.1016/j.resconrec.2019.104625.

[2] S. Das, S.H. Lee, P. Kumar, K.H. Kim, S.S. Lee, S.S. Bhattacharya, Solid waste management: Scope and the challenge of sustainability, J. Clean. Prod. 228 (2019) 658–678. https://doi.org/10.1016/j.jclepro.2019.04.323.

[3] Y. Fu, R.A.W. Kok, B. Dankbaar, P.E.M. Ligthart, A.C.R. van Riel, Factors affecting sustainable process technology adoption: A systematic literature review, J. Clean. Prod. 205 (2018) 226–251. https://doi.org/10.1016/j.jclepro.2018.08.268.

[4] G.D. Meyers, G. McLeod, M.A. Anbarci, An international waste convention: Measures for achieving sustainable development, Waste Manag. Res. 24 (2006) 505–513. https://doi.org/10.1177/0734242X06069474.

[5] A. Taşkin, N. Demir, Life cycle environmental and energy impact assessment of sustainable urban municipal solid waste collection and transportation strategies, Sustain. Cities Soc. (2020) 102339. https://doi.org/10.1016/j.scs.2020.102339.

[6] A. Yousefloo, R. Babazadeh, Designing an integrated municipal solid waste management network: A case study, J. Clean. Prod. (in press) (2020). https://doi.org/10.1016/j.jclepro.2019.118824.

[7] R.E. Marshall, K. Farahbakhsh, Systems approaches to integrated solid waste management in developing countries, Waste Manag. 33 (2013) 988–1003. https://doi.org/10.1016/j.wasman.2012.12.023.

[8] W. Wang, D. Jiang, D. Chen, Z. Chen, W. Zhou, B. Zhu, A Material Flow Analysis (MFA)-based potential analysis of eco-efficiency indicators of China's cement and cement-based materials industry, J. Clean. Prod. 112 (2016) 787–796. https://doi.org/10.1016/j.jclepro.2015.06.103.

[9] G.L.F. Benachio, M. do C.D. Freitas, S.F. Tavares, Circular economy in the construction industry: A systematic literature review, J. Clean. Prod. 260 (2020) 121046. https://doi.org/10.1016/j.jclepro.2020.121046.

[10] M. Yeheyis, K. Hewage, M.S. Alam, C. Eskicioglu, R. Sadiq, An overview of construction and demolition waste management in Canada: A lifecycle analysis approach to sustainability, Clean Technol. Environ. Policy. 15 (2013) 81–91. https://doi.org/10.1007/s10098-012-0481-6.

[11] Y. Kulaif, SUMÁRIO MINERAL - Departamento Nacional de Produção Mineral, Sumário Miner. 35 (2015) 135.

[12] OECD, Material Resources, Productivity and the Environment, OECD Green, OECD Publishing, Paris, 2015. https://doi.org/10.1787/9789264190504-en.

[13] UNEP, Worldwide Extraction of Materials Triples in Four Decades, Intensifying Climate Change and Air Pollution, 20 July 2016. (2016). https://www.unenvironment.org/news-and-stories/press-release/worldwide-extraction-

materials-triples-four-decades-intensifying (accessed November 8, 2019).
[14] J.M. Franco de Carvalho, P.A.M. Campos, K. Defáveri, G.J. Brigolini, L.G. Pedroti, R.A.F. Peixoto, Low environmental impact cement produced entirely from industrial and mining waste, J. Mater. Civ. Eng. 31 (2019). https://doi.org/10.1061/(ASCE)MT.1943-5533.0002617.
[15] D.R.R. Gonçalves, W.C. Fontes, J.C. Mendes, G.J.B. Silva, R.A.F. Peixoto, Evaluation of the economic feasibility of a processing plant for steelmaking slag, Waste Manag. Res. 34 (2016) 107–112. https://doi.org/10.1177/0734242X15615955.
[16] S.H. Ghaffar, M. Burman, N. Braimah, Pathways to circular construction: An integrated management of construction and demolition waste for resource recovery, J. Clean. Prod. 244 (2020) 118710. https://doi.org/10.1016/j.jclepro.2019.118710.
[17] Z. Zhao, F. Xiao, S. Amirkhanian, Recent applications of waste solid materials in pavement engineering, Waste Manag. 108 (2020) 78–105. https://doi.org/10.1016/j.wasman.2020.04.024.
[18] WorldSteel, Steel industry co-products, World Steel Association, 2020. https://doi.org/10.1201/9781420003840.sec2.
[19] IAB, Aço e sustentabilidade, Instituto Aço Brasil, Rio de Janeiro, 2019.
[20] C.S. Neto, Agregados Naturais, Britados e Artificiais para Concreto, in: G.C. Isaia (Ed.), Concreto Ciência e Tecnol., 1st ed., IBRACON, São Paulo, 2011: pp. 233–60.
[21] WorldSteel, About Steel, (2019). https://www.worldsteel.org/about-steel.html (accessed November 8, 2019).
[22] N. Zhang, L. Wu, X. Liu, Y. Zhang, Structural characteristics and cementitious behavior of basic oxygen furnace slag mud and electric arc furnace slag, Constr. Build. Mater. 219 (2019) 11–18. https://doi.org/10.1016/j.conbuildmat.2019.05.156.
[23] L. V. Fisher, A.R. Barron, The recycling and reuse of steelmaking slags — A review, Resour. Conserv. Recycl. 146 (2019) 244–255. https://doi.org/10.1016/j.resconrec.2019.03.010.
[24] D. Wang, J. Chang, W.S. Ansari, The effects of carbonation and hydration on the mineralogy and microstructure of basic oxygen furnace slag products, J. CO2 Util. 34 (2019) 87–98. https://doi.org/10.1016/j.jcou.2019.06.001.
[25] E. Belhadj, C. Diliberto, A. Lecomte, Properties of hydraulic paste of basic oxygen furnace slag, Cem. Concr. Compos. 45 (2014) 15–21. https://doi.org/10.1016/j.cemconcomp.2013.09.016.
[26] Z. Pan, J. Zhou, X. Jiang, Y. Xu, R. Jin, J. Ma, Y. Zhuang, Z. Diao, S. Zhang, Q. Si, W. Chen, Investigating the effects of steel slag powder on the properties of self-compacting concrete with recycled aggregates, Constr. Build. Mater. 200 (2019) 570–577. https://doi.org/10.1016/j.conbuildmat.2018.12.150.
[27] J.M. Franco de Carvalho, W.C. Fontes, C.F. de Azevedo, G.J. Brigolini, W. Schmidt, R.A.F. Peixoto, Enhancing the eco-efficiency of concrete using engineered recycled mineral admixtures and recycled aggregates, J. Clean. Prod. 257 (2020). https://doi.org/10.1016/j.jclepro.2020.120530.
[28] J.M. Franco de Carvalho, T.V. de Melo, W.C. Fontes, J.O. dos S. Batista, G.J. Brigolini, R.A.F. Peixoto, More eco-efficient concrete: An approach on optimization in the production and use of waste-based supplementary cementing materials, Constr. Build. Mater. 206 (2019) 397–409. https://doi.org/10.1016/j.conbuildmat.2019.02.054.
[29] Y. Jiang, T.C. Ling, Production of artificial aggregates from steel-making slag: Influences of accelerated carbonation during granulation and/or post-curing, J. CO2 Util. 36 (2020) 135–144. https://doi.org/10.1016/j.jcou.2019.11.009.
[30] A. Abdelbary, A.R. Mohamed, Investigating abrasion resistance of interlocking blocks incorporating steel slag aggregate, ACI Mater. J. 115 (2018) 47–54.

https://doi.org/10.14359/51700898.
[31] Q. Wang, M. Li, B. Zhang, Influence of pre-curing time on the hydration of binder and the properties of concrete under steam curing condition, J. Therm. Anal. Calorim. 118 (2014) 1505–1512. https://doi.org/10.1007/s10973-014-4053-3.
[32] C. Xu, W. Ni, K. Li, S. Zhang, Y. Li, D. Xu, Hydration mechanism and orthogonal optimisation of mix proportion for steel slag–slag-based clinker-free prefabricated concrete, Constr. Build. Mater. 228 (2019) 117036. https://doi.org/10.1016/j.conbuildmat.2019.117036.
[33] M. VanGeem, Achieving sustainability with precast concrete, PCI J. 51 (2006). https://doi.org/10.15554/pcij.01012006.42.61.
[34] F. Han, S. Song, J. Liu, S. Huang, Properties of steam-cured precast concrete containing iron tailing powder, Powder Technol. 345 (2019) 292–299. https://doi.org/10.1016/j.powtec.2019.01.007.
[35] M.J. Da Silva, B.P. De Souza, J.C. Mendes, G.J.S. Brigolini, S.N. Da Silva, R.A.F. Peixoto, Feasibility study of steel slag aggregates in precast concrete pavers, ACI Mater. J. 113 (2016) 439–446. https://doi.org/10.14359/51688986.
[36] Y. Biskri, D. Achoura, N. Chelghoum, M. Mouret, Mechanical and durability characteristics of High Performance Concrete containing steel slag and crystalized slag as aggregates, Constr. Build. Mater. 150 (2017) 167–178. https://doi.org/10.1016/j.conbuildmat.2017.05.083.
[37] J. Liu, R. Guo, Applications of Steel Slag Powder and Steel Slag Aggregate in Ultra-High Performance Concrete, Adv. Civ. Eng. 2018 (2018). https://doi.org/10.1155/2018/1426037.
[38] N. Palankar, A.U. Ravi Shankar, B.M. Mithun, Durability studies on eco-friendly concrete mixes incorporating steel slag as coarse aggregates, J. Clean. Prod. 129 (2016) 437–448. https://doi.org/10.1016/j.jclepro.2016.04.033.
[39] L. Mo, F. Zhang, M. Deng, F. Jin, A. Al-Tabbaa, A. Wang, Accelerated carbonation and performance of concrete made with steel slag as binding materials and aggregates, Cem. Concr. Compos. 83 (2017) 138–145. https://doi.org/10.1016/j.cemconcomp.2017.07.018.
[40] M. Maslehuddin, A.M. Sharif, M. Shameem, M. Ibrahim, M.S. Barry, Comparison of properties of steel slag and crushed limestone aggregate concretes, Constr. Build. Mater. 17 (2003) 105–112. https://doi.org/10.1016/S0950-0618(02)00095-8.
[41] H. Qasrawi, The use of steel slag aggregate to enhance the mechanical properties of recycled aggregate concrete and retain the environment, Constr. Build. Mater. 54 (2014) 298–304. https://doi.org/10.1016/j.conbuildmat.2013.12.063.
[42] A.V.M. Cardoso, F.M. Dias, A utilização de escória de aciaria para manufatura de Blocos de pavimentação, in: 21º CBECIMAT - Congresso Brasileiro de Engenharia e Ciência dos Materiais, Cuiabá, 2014: pp. 3673–3679.
[43] L.C. Franco, J.C. Mendes, L.C.B. Costa, R.R. Pira, R.A.F. Peixoto, Design and thermal evaluation of a social housing model conceived with bioclimatic principles and recycled aggregates, Sustain. Cities Soc. 51 (2019) 101725. https://doi.org/10.1016/j.scs.2019.101725.
[44] B.L. Damineli, F.M. Kemeid, P.S. Aguiar, V.M. John, Measuring the eco-efficiency of cement use, Cem. Concr. Compos. 32 (2010) 555–562. https://doi.org/10.1016/j.cemconcomp.2010.07.009.
[45] J.S. Damtoft, J. Lukasik, D. Herfort, D. Sorrentino, E.M. Gartner, Sustainable development and climate change initiatives, Cem. Concr. Res. 38 (2008) 115–127. https://doi.org/10.1016/j.cemconres.2007.09.008.
[46] G. Hüsken, H.J.H. Brouwers, On the early-age behavior of zero-slump concrete, Cem.

Concr. Res. 42 (2012) 501–510. https://doi.org/10.1016/j.cemconres.2011.11.007.
[47] M. Najimi, J. Sobhani, A.R. Pourkhorshidi, A comprehensive study on no-slump concrete: From laboratory towards manufactory, Constr. Build. Mater. 30 (2012) 529–536. https://doi.org/10.1016/j.conbuildmat.2011.12.012.
[48] W. Zuo, J. Liu, Q. Tian, W. Xu, W. She, P. Feng, C. Miao, Optimum design of low-binder Self-Compacting Concrete based on particle packing theories, Constr. Build. Mater. 163 (2018) 938–948. https://doi.org/10.1016/j.conbuildmat.2017.12.167.
[49] O.A. Mayhoub, E.S.A.R. Nasr, Y.A. Ali, M. Kohail, The influence of ingredients on the properties of reactive powder concrete: A review, Ain Shams Eng. J. (2020). https://doi.org/10.1016/j.asej.2020.07.016.
[50] J.C. Mendes, T.K. Moro, A.S. Figueiredo, K.D. do C. Silva, G.C. Silva, G.J.B. Silva, R.A.F. Peixoto, Mechanical, rheological and morphological analysis of cement-based composites with a new LAS-based air entraining agent, Constr. Build. Mater. 145 (2017) 648–661. https://doi.org/10.1016/j.conbuildmat.2017.04.024.
[51] ABNT, NBR 16697: Cimento Portland - Requisitos, Associação Brasileira de Normas Técnicas, Rio de Janeiro, 2018.
[52] J.M. Franco de Carvalho, K. Defáveri, J.C. Mendes, W. Schmidt, H.C. Kühne, R.A.F. Peixoto, Influence of particle size-designed recycled mineral admixtures on the properties of cement-based composites, Constr. Build. Mater. 272 (2021). https://doi.org/10.1016/j.conbuildmat.2020.121640.
[53] ASTM, ASTM C33/C33M-18: Standard Specification for Concrete Aggregates, ASTM International, West Conshohocken, 2018. https://doi.org/10.1520/C0033.
[54] ASTM, ASTM C188-17: Standard Test Method for Density of Hydraulic Cement, ASTM International, West Conshohocken, 2017. https://doi.org/10.1520/C0188-17.2.
[55] ASTM, ASTM C128-15: Standard Test Method for Relative Density (Specific Gravity) and Absorption of Fine Aggregates, ASTM International, West Conshohocken, 2015. https://doi.org/10.1520/C0128-15.2.
[56] ASTM, ASTM C127-15: Standard Test Method for Relative Density (Specific Gravity) and Absorption of Coarse Aggregate, ASTM International, West Conshohocken, 2015. https://doi.org/10.1520/C0127-15.2.
[57] S.A. Bombril, Ficha de informações de segurança de produtos químicos - FISPQ - Detergente Limpol, 2019.
[58] D.A. FUNK, J. E.; DINGER, Particle size control for high-solids castable refractories, Am. Ceram. Soc. Bull. 73(10) (1994) 66–69.
[59] A.L. Castro, V.C. Pandolfelli, Revisão: Conceitos de dispersão e empacotamento de partículas para a produção de concretos especiais aplicados na construção civil, Cerâmica. 55 (2009) 18–32. https://doi.org/10.5414/VDX00749.
[60] R. Vanderlei, Análise experimental do concreto de pós reativos: dosagem e proprieda-des mecânicas, (2006) 115–148196.
[61] S. V. Kumar, M. Santhanam, Particle packing theories and their application in concrete mixture proportioning: A review, Indian Concr. J. 77 (2003) 1324–1331.
[62] H.P. Caputo, Mecânica dos Solos e suas Aplicações, LCT - Livros Técnicos e Científicos Editora S.A., Rio de Janeiro, 1988. https://engenhariacivilfsp.files.wordpress.com/2015/05/mecanica-solos-fundamentos-vol1-6ed-caputo.pdf.
[63] ASTM, ASTM C39/C39M-21: Standard Test Method for Compressive Strength of Cylindrical Concrete Specimens, ASTM International, West Conshohocken, 2021. https://doi.org/10.1520/C0039.
[64] ASTM, ASTM C642-13: Standard Test Method for Density, Absorption, and Voids in Hardened Concrete, ASTM International, West Conshohocken, 2013.

https://doi.org/10.1520/C0642-13.5.
[65] ASTM, ASTM C597-16: Standard Test Method for Pulse Velocity Through Concrete, ASTM International, West Conshohocken, 2016. https://doi.org/10.1520/C0597-16.2.
[66] J. Zheng, P.F. Johnson, J.S. Reed, Improved Equation of the Continuous Particle Size Distribution for Dense Packing, Z J. Am. Ceram. Soc. 73 (1990) 1392–1398. https://doi.org/10.1111/j.1151-2916.1990.tb05210.x.
[67] B.M. Das, N. Sivakugan, Fundamentals of Geotechnical Engineering, Fifth Edit, Cengage Learning, 2015.
[68] S. Saxena, A.R. Tembhurkar, Impact of use of steel slag as coarse aggregate and wastewater on fresh and hardened properties of concrete, Constr. Build. Mater. 165 (2018) 126–137. https://doi.org/10.1016/j.conbuildmat.2018.01.030.
[69] E.K. Anastasiou, I. Papayianni, M. Papachristoforou, Behavior of self compacting concrete containing ladle furnace slag and steel fiber reinforcement, Mater. Des. 59 (2014) 454–460. https://doi.org/10.1016/j.matdes.2014.03.030.
[70] BIS, IS 13311-1: Method of Non-destructive testing of concret, Part 1: Ultrasonic pulse velocity, Bureau of Indian Satandards, New Delhi, 1992.
[71] Q. Wang, P.Y. Yan, S. Han, The influence of steel slag on the hydration of cement during the hydration process of complex binder, Sci. China Technol. Sci. 54 (2011) 388–394. https://doi.org/10.1007/s11431-010-4204-0.
[72] H. Qasrawi, Use of Relatively High Fe2O3 Steel Slag as Coarse Aggregate in Concrete, ACI Mater. J. 109 (2012) 471–478.
[73] B. Pang, Z. Zhou, H. Xu, Utilization of carbonated and granulated steel slag aggregate in concrete, Constr. Build. Mater. 84 (2015) 454–467. https://doi.org/10.1016/j.conbuildmat.2015.03.008.
[74] F. Pelisser, A. Vieira, A.M. Bernardin, Efficient self-compacting concrete with low cement consumption, J. Clean. Prod. 175 (2018) 324–332. https://doi.org/10.1016/j.jclepro.2017.12.084.

CHAPTER 5

Final consideration

Abstract

This study was dedicated to using steel slag in the production of eco-efficient concrete for the precast industry as recycled aggregates and complementary cementitious materials. In this chapter, a general conclusion to the research is presented, as well as proposals for future work.

5.1 General conclusions

This study comprised an extensive literature review of steel slag over the past 20 years and experimental investigations of the effects of a LAS-based admixture and steel slag powder (SSP) and steel slag aggregates on the properties of cement-based composites.

The main constituents of steel slag are CaO (25.08-57.44%), Fe/Fe_2O_3 (0.48-38.5%), SiO_2 (7.75-36.33%), Al_2O_3 (0.33-12.2%), and MgO (1.93-10.46%). Due to the high content of dense oxides, the specific gravity of steel slag is higher than natural aggregates by around 30%. Typically, steel slag aggregates have a greater specific surface, with high angularity and rough surface texture, that can positively contribute to the performance of cementitious matrices, implying greater durability. The grindability of the non-active components (e.g., RO-phase and Fe_3O_4) of steel slag is very difficult because of the high metallic iron. Steel slag powder can significantly improve the samples' mechanical strength because of their cementing properties, improvement in the particle size distribution obtained, and a reduction in the water/cement ratio for the same fluidity.

Both LAS and SSP increased the mortars' spread value in the flow table test compared to the reference mortar. The significant influence of SSP should be attributed to the improved shape of its particles, with volumetric aspect, and their high specific gravity. For the 25% cement replacement by SSP, good mechanical strength results were obtained, showing a good performance of steel slag powder as supplementary cementing material (SCM) for this dosage. Substitutions of 50% cement by SSP, on the other hand, caused a considerable drop in mechanical strength due to the low hydration activity of SSP and the dilution effect of cement in the mixture. In addition, the LAS-based mixture hindered the formation of cement hydration products, and the incorporation of air increased porosity and consequently affected the compressive strength.

Recycled aggregates and mineral admixtures obtained from steel slag optimized the eco-efficiency of no-slump concrete produced. Steel slag presented good particle shape, with volumetric aspect, and improved physical and mechanical properties of densely-packed no-slump concrete. Steel slag concrete presented good quality into the ultrasonic pulse velocity range of 3,500 - 4,500 m/s, with lower void index and water absorption than conventional concrete. An increase of 49% and 40% in compressive strength was observed at 28 and 63 days, respectively, compared to conventional concrete. Highly eco-efficient precast concrete with total replacement of conventional aggregates by BOFS materials was obtained. Experimental

results indicated compressive strength of 52.1 MPa in steel slag concrete at 28-days, binder intensity (bi) of 7.0 kg/m³/MPa and waste consumption of 2,356.57 kg/m³. A bi of 7.6 kg/m³/MPa with a waste consumption of 2,637.82 kg/m³ and less cement consumption of 121.56 kg/m³ was also achieved and showed better eco-efficiency due to the high consumption of waste. The consumption of considerable volumes of waste amplifies the relevance of obtaining products of better performance and more sustainable, aiming at reducing consumption of natural resources.

5.2 Proposals for future works

During the development of this research, it was observed that the concepts explored are susceptible to variations in several aspects. In addition, many opportunities for further investigation have been identified. Some proposals for future work follow:

- Evaluation of more efficient grinding methods with lower energy consumption for steel slag powder production;
- Development of durability and performance studies of different types of concrete (no-slump concrete, self-compacting concrete and reactive powder concrete) produced entirely with aggregates and steel slag powder for application in civil construction;
- Evaluation of the influence of different types of curing on the hydration kinetics and hardened state properties of concretes with steel slag;
- Expansion of high packing density dosage proposals using other theories and experimental approaches.